

Smooth Muscle Molecular Mechanics in the Latch-State

Horia Nicolae Roman

Doctor of Philosophy

Department of Biomedical Engineering

McGill University

Montréal, Québec, Canada

November 2013

A thesis submitted to McGill University in partial fulfillment of the requirements of
the degree of Doctor of Philosophy

©Copyright 2013 All rights reserved.

To Maria and Ioana

ABSTRACT

The latch-state is the capacity of smooth muscle to maintain force for long periods of time with low energy consumption. The prevalent theory to explain the latch-state suggests that if myosin gets deactivated (dephosphorylated) while attached to actin, it remains attached and maintains force. Other theories suggest that dephosphorylated and detached myosin can bind to actin to maintain force and that actin regulatory proteins participate in the force maintenance. All theories of the latch-state were based on measurements performed at the whole muscle level and were never confirmed at the molecular level. Verifying the latch-state theories at the molecular level was the main goal of this thesis.

To further our understanding of the latch-state, the role of calponin in the binding of unphosphorylated myosin to actin was determined. The laser trap assay was used to measure the average force of unbinding (F_{unb}) in the absence and presence of calponin. Calponin enhanced the F_{unb} . Phosphorylation of calponin with Ca^{2+} -calmodulin dependant protein kinase II, which detaches calponin from actin, decreased the F_{unb} to the unregulated actin level. Performing the measurements at high ionic strength, which detaches calponin from myosin, had the same effect on the F_{unb} . These later two measurements demonstrate that calponin enhances the F_{unb} of unphosphorylated myosin to actin by crosslinking them together.

Next, the effect of caldesmon on the F_{unb} was studied; caldesmon enhanced the F_{unb} . Because tropomyosin is known to potentiate biochemical and mechanical effects of caldesmon, its action on the F_{unb} in combination with caldesmon was also measured. Tropomyosin enhanced the F_{unb} on its own but had no synergistic effect with caldesmon. Phosphorylation of caldesmon with

the extracellular signal-regulated kinase (ERK) decreased the F_{unb} below the unregulated actin level. Because ERK phosphorylation of caldesmon occurs late in the contraction, this last result suggests a relaxation mechanism from the latch-state. Examination of the force traces revealed a visco-elastic behavior of myosin in the presence of ERK phosphorylated caldesmon which either prevents binding or promotes detachment from actin, thus leading to muscle relaxation.

Finally, the ultimate molecular level demonstration of the latch-state requires dephosphorylation of myosin during molecular force measurements with a laser trap assay. However, addition of myosin light chain phosphatase cannot be done without disturbing the single molecule level mechanics measurements. Thus, a microfluidic device was designed and developed to allow the addition of chemicals to a molecular mechanics flow-through chamber without creating any bulk flow. A micro-channel chamber was created by standard photolithography on silicon wafers with the patterns transferred to polymethylsiloxane (PDMS). The chamber was then bound to a polycarbonate membrane which itself was bound to the molecular mechanics chamber. The micro-channels assured rapid distribution of the chemicals whereas the membrane assured efficient delivery but prevented bulk flow. The device was tested by injection of adenosine triphosphate to initiate the propulsion of actin by myosin. The proof of principle of this microfluidic device concludes this thesis.

ABRÉGÉ

Le muscle lisse possède la capacité unique de maintenir une force élevée tout en consommant peu d'adénosine triphosphate (ATP); cette propriété est appelée 'latch-state'. La théorie la mieux connue pour expliquer cet état suggère que si la myosine est désactivée (déphosphorylation de sa chaîne légère) pendant qu'elle est attachée à l'actine, elle reste attachée et maintient la force. D'autres théories suggèrent que la myosine désactivée et détachée peut s'attacher à l'actine pour maintenir la force et que les protéines régulatrices de l'actine participent aussi à cet effort. Toutes les théories sur l'état 'latch' ont été extrapolées à partir de mesures réalisées sur la totalité du muscle sans jamais être confirmées au niveau moléculaire. Le but principal de cette thèse était de vérifier les théories de l'état 'latch' au niveau moléculaire.

Afin de mieux comprendre l'état 'latch', le rôle de la calponine, dans l'attachement de la myosine non-phosphorylée à l'actine, a été déterminé. Des pinces optiques ont été utilisées pour mesurer la force moyenne de leur détachement (F_{umb}) en l'absence et en présence de la calponine. La calponine a augmenté la F_{umb} . La phosphorylation de la calponine avec l'enzyme protéine kinase II (Ca^{2+} -calmoduline dépendante), qui a pour effet de détacher la calponine de l'actine, a diminué la F_{umb} jusqu'au niveau de l'actine non-réglée. De plus, des mesures de force ont été réalisées à haute force ionique, détachant cette fois-ci la calponine de la myosine. Ceci a aussi diminué la F_{umb} jusqu'au niveau de l'actine non-réglée. Ces résultats montrent que la calponine augmente la F_{umb} de la myosine non-phosphorylée à l'actine par liaison croisée (myosine-calponine-actine).

Ensuite, l'effet de la caldesmone sur la F_{unb} a été étudié; la caldesmone augmente aussi la F_{unb} . Puisque la tropomyosine est connue pour promouvoir les actions biochimiques et mécaniques de la caldesmone, son action sur la F_{unb} en combinaison avec la caldesmone a aussi été mesurée. La tropomyosine augmente la F_{unb} lorsqu'elle est seule mais n'a pas d'effet synergétique avec la caldesmone. La phosphorylation de la caldesmone avec la kinase régulatrice des signaux extracellulaires (ERK) a diminué la F_{unb} en dessous du niveau de l'actine non-régulée. Ce dernier résultat suggère un mécanisme de relaxation à partir de l'état 'latch' étant donné que la phosphorylation de la caldesmone par ERK se produit tard dans la contraction. D'autre part, l'examen des traces de force a révélé un comportement viscoélastique de la myosine en présence de la caldesmone phosphorylée, ce qui semble soit prévenir l'attachement, soit promouvoir le détachement de l'actine, menant ainsi à la relaxation du muscle à partir de l'état 'latch'.

Enfin, la démonstration ultime de l'état 'latch' au niveau moléculaire requiert la déphosphorylation de la myosine pendant les mesures de forces moléculaires faites à l'aide de pinces optiques. Cependant l'addition de la phosphatase de la chaîne légère de myosine ne peut se faire sans perturber les mesures de mécanique au niveau moléculaire. A cet effet, un appareil micro-fluidique a été conçu et développé pour permettre l'ajout de solutions biochimiques à la chambre de mesure de micromécanique sans créer de débit net. Des micro-canaux ont été créés par photolithographie sur substrats de silicium suivie d'un transfert des formes sur polyméthylsiloxane (PDMS). La chambre des micro-canaux a ensuite été collée à une membrane de polycarbonate qui elle a ensuite été collée à la chambre de micromécanique. Les micro-canaux assurent la livraison rapide et uniforme tandis que la membrane assure le transfert efficace des produits biochimiques tout en empêchant un débit net. Le fonctionnement de l'appareil a été

vérifié en injectant de l'ATP en présence d'actine et de myosine phosphorylée. La propulsion de l'actine par la myosine a été observée validant ainsi le principe de l'appareil microfluidique.

ACKNOWLEDGEMENTS

First of all, I wish to express my appreciation and gratitude to my supervisor, Dr. Anne-Marie Lauzon for her constant mentoring and support. She provided not only guidance, but also an excellent research environment, in regard to both technical, but most importantly human resources. She taught me to let my research be conducted by passion and enthusiasm and to never stop believing in myself. Above all, she made me realize why is always better to offer help than to receive it. I wish to also thank her for the opportunity to present my work at so many conferences and enjoy the presence of my peers. My only regret is that despite all her sustained efforts I didn't learn how to be concise and precise.

I will always be obliged to Dr. David Juncker for opening me the door of his laboratory. His guidance, advice and novel approach to research have constantly challenged and pushed me to fulfill my potential. I am grateful to the other members of my advisory committee, Drs. D. Rassier and S. Prakash for their continuous encouragement and suggestions.

I have always appreciated the Meakins-Christie environment and I like to address many thanks to Drs. J.G. Martin and Q. Hamid for their leadership and support; also all supporting staff: Maria, Bill, Normand, Angela, Nicky and Angie were there for me when I needed their help. I cannot forget the help provided by the McGill's Biomedical Engineering department, especially Ms. Pina Sorrini, Ms. Lina Vuch and Ms. Nancy Abate.

I would like to acknowledge the funding sources that assisted my research: Fonds Québécois de la Recherche de la Nature et des Technologies (FQRNT), the Research Institute of McGill University Health Centre, Meakins-Christie (Costello) and McGill (GREAT Awards).

When I started my adventure in Dr. Lauzon's laboratory, Dr. Nedjma Zitouni, Linda Kachmar and Genevieve Bates were there to welcome me. I want to thank them for so many years of enjoyable and fruitful collaboration and for teaching me so many things. The climate was always friendly and it was a pleasure to work aside Isabelle, Rob, Paul-Andre, Ellen, Sharon, Jack, Frederic, Jenna, Shivy, Stefanie and Zsombor. Some of this work concluded in published results and I take the opportunity to thank Dr. Saba Al Heialy, Dr. Oleg Matusovsky and Lennart Hilbert for collaborating with me. My special appreciation goes to Dr. Gijs IJpma, who not only helped me in my work but also became a close friend. I wish to mention also the people in Dr. D. Juncker's laboratory: Sebastien, Mohammad, Roozbeh, Parnaz, Adiel, Mohsen, Ali, Kate, Ayo, Tohid for offering me their suggestions and insightful comments.

Last but not least, this thesis is dedicated to my family: to my wife, Florentina who until the last minute before handing this thesis was helping and supporting me; to my brother, Radu for convincing me that I am capable to do it; to my parents for teaching me to be humble and grateful and most of all, to my daughters for smiling at their frustrated father.

TABLE OF CONTENTS

TITLE	Page #
ABSTRACT.....	iii
ABRÉGÉ	v
ACKNOWLEDGEMENTS.....	viii
TABLE OF CONTENTS.....	x
LIST OF FIGURES.....	xiv
LIST OF TABLES.....	xv
PREFACE (CONTRIBUTION OF AUTHORS)	xvi

CHAPTER

1. INTRODUCTION.....	2
1.1. MUSCLE CONTRACTION.....	3
1.2 LITERATURE REVIEW	6
1.2.1. MUSCLE TYPE AND ROLE.....	6
1.2.2. MYOSIN	7
1.2.3. ACTIN.....	10
1.2.3.1. Actin regulatory proteins.....	12
1.2.3.2. Tropomyosin.....	13
1.2.3.3. Caldesmon	14
1.2.3.4. Calponin	15
1.2.4. MUSCLE MOLECULAR MECHANICS.....	16

1.2.5. LATCH-STATE.....	21
1.2.6. METHODS TO STUDY MUSCLE MOLECULAR MECHANICS.....	23
1.2.6.1. In vitro motility assay.....	23
1.2.6.2. Laser trap assay.....	26
1.2.7. MICROFLUIDICS	30
1.3. THE GOAL OF THIS THESIS.....	31
1.4. REFERENCES.....	32
2. UNPHOSPHORYLATED CALPONIN ENHANCES THE BINDING FORCE OF UNPHOSPHORYLATED MYOSIN TO ACTIN	44
2.1. PREFACE	45
2.2. ABSTRACT.....	46
2.3. INTRODUCTION	47
2.4. MATERIALS AND METHODS.....	48
2.4.1. Proteins.....	48
2.4.2. Buffers	49
2.4.3. In vitro motility assay.....	49
2.4.4. Laser trap assay.....	51
2.4.5. Microsphere displacement analysis software	54
2.4.6. Western Blot analysis of purified calponin	56
2.4.7. Co-sedimentation assay.....	57
2.4.8. Statistical analysis.....	58
2.5. RESULTS.....	58

2.5.1. Maximal velocity of actin propulsion.....	58
2.5.2. Cross-linking of unphosphorylated myosin to actin	59
2.5.3. Control measurements in the absence of myosin.....	61
2.5.4. Co-sedimentation assay	61
2.6. DISCUSSION.....	63
2.7. CONCLUSION.....	68
2.8. ACKNOWLEDGEMENTS.....	69
2.9. REFERENCES.....	70
3. THE ROLE OF CALDESMON AND ITS PHOSPHORYLATION BY ERK ON THE BINDING FORCE OF UNPHOSPHORYLATED MYOSIN TO ACTIN.....	77
3.1. PREFACE.....	78
3.2. ABSTRACT.....	79
3.3. INTRODUCTION.....	80
3.4. MATERIALS AND METHODS.....	82
3.4.1. Proteins.....	82
3.4.2. Buffers.....	83
3.4.3. In vitro motility assay.....	83
3.4.4. Laser trap assay	85
3.4.5. Microsphere displacement analysis software.....	87
3.4.6. Statistical analysis.....	88
3.5. RESULTS.....	89
3.6. DISCUSSION.....	96

3.7. CONCLUSION.....	101
3.8. ACKNOWLEDGEMENTS.....	102
3.9. REFERENCES.....	103
4. A MICROFLUIDIC CHAMBER TO STUDY THE DYNAMICS OF MUSCLE	
CONTRACTION.....	111
4.1. PREFACE.....	112
4.2. ABSTRACT.....	113
4.3. INTRODUCTION.....	114
4.4. METHODS.....	119
4.4.1. Microfabrication of the micro-channel chamber.....	119
4.4.2. Membrane.....	120
4.4.3. Molecular mechanics chamber.....	120
4.4.4. Protein preparation.....	121
4.4.5. Buffers.....	121
4.4.6. In vitro motility assay.....	122
4.5. RESULTS.....	123
4.6. DISCUSSION.....	128
4.7. CONCLUSION.....	131
4.8. REFERENCES.....	132
5. CONCLUSIONS.....	135
5.1 CONCLUSIONS AND FUTURE DIRECTIONS.....	136
5.2. SUMMARY (ORIGINAL CONTRIBUTION TO THE FIELD).....	139

LIST OF FIGURES

Nr.	TITLE	Page #
1.1.	Striated muscle structure	4
1.2.	Myofibril micrographs	5
1.3.	Myosin molecules	9
1.4.	ATP hydrolysis cycle	19
1.5.	Latch-bridge cycle	22
1.6.	In vitro motility assay.....	25
1.7.	Three-bead laser trap assay.....	29
2.1.	A single beam laser trap assay.....	51
2.2.	Video analysis for the calculation of microsphere displacement	55
2.3.	Velocity of actin filament.....	58
2.4.	Unbinding force (F_{unb}) of unphosphorylated myosin to actin	60
2.5.	Co-sedimentation assay	62
3.1.	F_{unb} in presence of caldesmon and tropomyosin	90
3.2.	Total F_{unb}/l in the absence or presence of unphosphorylated myosin.....	91

3.3. v_{\max} in presence of caldesmon and tropomyosin.....	92
3.4. F_{unb} in presence of phosphorylated caldesmon.....	94
3.5. Sample traces of the unbinding force	95
3.6. v_{\max} in presence of phosphorylated caldesmon	96
4.1. Traditional molecular mechanics assays	115
4.2. Microfluidic chamber prototype	118
4.3. Channel architecture design	124
4.4. Channel filling time	125
4.5. Biocompatibility test.....	126
4.6. Microfluidic device test	127

LIST OF TABLES

<i>Table 1. Acto-myosin attachment time scale.....</i>	20
--	----

PREFACE (CONTRIBUTION OF AUTHORS)

Following McGill University “Guidelines for Thesis Preparation, Submission and Examination”: “... A thesis can be written and organized either in the traditional, monograph style or ‘manuscript (article)-based’ style”, this thesis is submitted as a collection of manuscripts elaborated by the candidate with the contribution of the co-authors. This thesis comprises five chapters. Chapter 1 includes the introduction, the literature review and the objectives of this thesis. The following three chapters are in the form of manuscripts. Each manuscript includes an introduction, the relevant methodology, the results and a discussion. Chapter 2 is already published in *Biochimica et Biophysica Acta*, General Subjects, Roman HN, Zitouni NB, Kachmar L, IJpma G, Hilbert L, Matusovsky O, Benedetti A, Sobieszek A & Lauzon AM 1830: 4634-4641, 2013. Chapter 3 will be submitted to the *Biophysical Journal* after adding a mathematical model that aims at further explaining the observations made. (The model is still in development by collaborators in the Lauzon laboratory). Chapter 4 is a technological manuscript that will be submitted to the Journal *Lab on a Chip*, after a more extensive data collection. A proof of concept is presented in 4. Chapter 5 contains the conclusions and contributions to original knowledge. The manuscripts report original work based on experimental data that I collected at the Meakins Christie Laboratories, using either established techniques or techniques that I modified. Drs. A-M. Lauzon and D. Juncker appear as co-authors to reflect their supervisory role during the data collection and their involvement in the preparation and editing of the manuscripts. Dr. N. Zitouni was involved in protein preparations and analysis. Dr. A. Sobieszek is an external collaborator who also provided proteins used in the experiments. Dr. A. Benedetti provided support for the statistical analysis of the data. Dr. O. Matusovsky and L. Kachmar helped with the co-

sedimentation assay in chapter 2. Dr. G. IJpma contributed by automating the image analysis for the laser trap assay and L. Hilbert designed the automated filament analysis for the motility assay. Some further technical contributions are listed in the acknowledgements of the chapters concerned.

CHAPTER 1

INTRODUCTION

CHAPTER 1

1.1. MUSCLE CONTRACTION

The muscular system is responsible for body posture and displacement. Muscles are also effectors of several internal organ functions. In order to fulfill their assignment, muscles transform the chemical energy into force and movement (Lohman, 1934). There are three types of mammalian muscle: skeletal, cardiac and smooth. They differ, not only in their function, but also structurally and in their regulatory mechanisms. The skeletal muscle contraction is usually under voluntary control in contrast with the cardiac and smooth muscle contraction that are under involuntary control. Under the microscope the striated muscle is seen to have a very regular structure whereas smooth muscle shows a more disorganized or smooth appearance, thus its name. Despite these differences, all three muscles generate force via the interaction between myosin, a molecular motor protein and actin. Myosin hydrolyses MgATP to inorganic phosphate (Pi) and MgADP, binds to actin, and undergoes a conformational change that leads to force generation and movement of the actin filament. Myosin and actin are considered to be the main proteins participating in muscle contraction as they account for more than 80% of the total proteins in muscular tissue (Galpin, et al., 2012). Even before being able to visualize them it was believed that myosin and actin were bundled in filaments and that muscle contraction occurred due to the folding (Astbury & Bell, 1941) or shortening of filaments of either actin or myosin (Astbury, 1945; W. A. Engelhardt, 1942; Varga, 1946). It is only in 1963, after Hugh E. Huxley and his team (H. E. Huxley, 1963) used X-ray diffraction combined with electron microscopy to

investigate muscular structure at the molecular level, that it was determined that myosin and actin filaments kept the same length during contraction, invalidating the initial hypotheses for muscle contraction. Thus, Huxley suggested that actin and myosin filaments interact by sliding next to each other, leading to the shortening of repeating patterns of the myofibrils (basic tubular unit of the skeletal muscle cell). The repeating pattern structure of a myofibril is called sarcomere and is shown in figures 1.1 and 1.2.

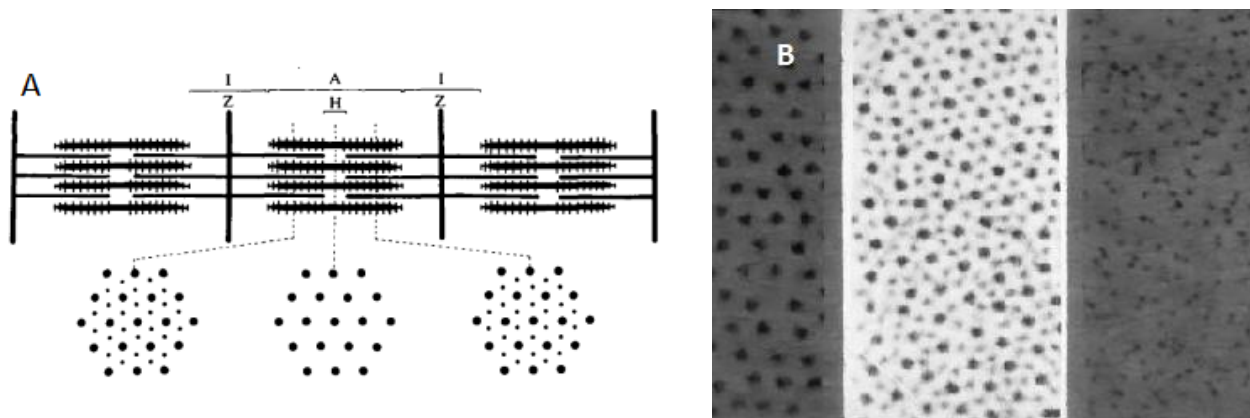


Fig. 1.1. Striated muscle structure. *A) Schematic of a myofibril showing the layout of thick (myosin) and thin (actin) filaments and the repeating sarcomeres in the relaxed skeletal muscle. B) Electron micrograph of a cross-section of the frog Sartorius muscle through (left to right) the H region (actin filaments do not superimpose the myosin filaments), the A region (the thick and thin filaments overlap) and the I region (myosin filaments do not superimpose the actin filaments). The actin filaments are bound to Z-lines, formed of α -actinin; the Z-lines limit the sarcomeres; adapted from (H. E. Huxley, 2004)*

In order for the muscle to lengthen or shorten, the overlap of myosin filaments with the actin filaments has to decrease or to increase, respectively. The actin filaments are connected to the Z-bands which leads to muscle shortening when the overlap increases. Due to its disorganized structure, similar observations cannot be made in smooth muscle but the same molecular mechanism is believed to occur (Draeger, Amos, Ikebe, & Small, 1990). As there are no Z bands in smooth muscle, it is believed that the actin filaments attach to Z-bands equivalent structural units specific to smooth muscle called the dense bodies (Draeger, et al., 1990). However, recent data in the literature have challenged this view (Zhang, Herrera, Pare, & Seow, 2010).

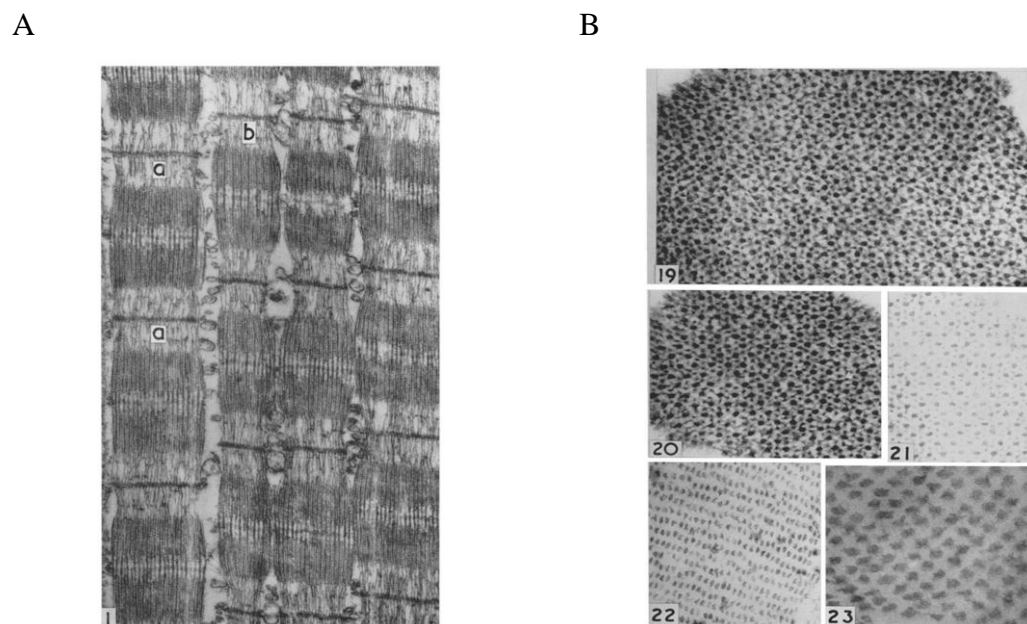


Fig. 1.2. Electron micrographs of myofibrils. A) Longitudinal section, 60.000x magnification. B) Cross-section through: 19-21: A-region, 150,000 x magnification; 22-23: H-region, 22: 100,000 x magnification and 23: 200,000 x magnification. Adapted from (H. E. Huxley, 1957)

In striated and smooth muscles, contraction is initiated by calcium ions entering the cell (Weber, 1959). Activation of the myosin-actin interaction is done at the actin (thin) filament level in skeletal muscle (Ebashi, 1967), whereas in smooth muscle, the activation is done at the myosin thick filament level (Sobieszek, 1977). In skeletal muscle, calcium ions are bound by troponin, a thin-filament associated protein, which then undergoes a conformational change that promotes the displacement of tropomyosin, another thin-filament associated protein. This displacement exposes the binding sites on actin for myosin. In smooth muscle cells, calcium binds to calmodulin and together activates myosin light chain kinase (MLCK). The calmodulin-MLCK complex phosphorylates myosin light chains and thus activates myosin, enabling its interaction with actin filaments.

1.2 LITERATURE REVIEW

1.2.1. MUSCLE TYPE AND ROLE

As its name suggests, skeletal muscle attaches to the body skeleton and is responsible for body movement and posture. Cardiac muscle is the muscle of the heart and is responsible for pumping the blood through the entire body (and for the entire life !!!). Smooth muscle is found in all hollow organs of the body. It is responsible, for example, for peristalsis, the mechanism that propels the content of the digestive tract, or for tension maintenance as in the blood vessels.

1.2.2. MYOSIN

Myosin is the molecular motor that generates force and movement associated with muscle contraction. The term myosin was used for the first time to describe a viscous muscular extract by Kühne (Kühne, 1864) who used a concentrated salt solution to study the proteins responsible for muscle in the rigor state. Following the footsteps of Lohman (Lohman, 1934) who suggested that MgATP was the energy source for muscle contraction, Engelhardt and Lyubimova (W. A. Engelhardt, Liubimova, M. N., 1939) reported that the extract had indeed ATPase activity. In 1942, Banga and Szent-Gyorgyi (Banga, 1942) treated ground muscle with high salt solutions for 20 minutes which led to the extraction of a protein of low viscosity which they called myosin A. Alternatively, overnight exposure yielded a protein with high viscosity which they called myosin B. Upon addition of MgATP, the viscosity of myosin B was reduced, while the viscosity of myosin A remained basically unchanged. Independently, Needham (Needham, 1942) observed that MgATP treatment of Kühne's extract also reduced its viscosity. Significantly, after incubation of threads of the extracted myosin B with an ATP buffer activated by magnesium, Szent-Gyorgyi observed contraction. The conclusion of the experiments conducted in Szent-Gyorgyi's laboratory was that myosin A was a distinct protein that retained the name myosin, whereas myosin B was in fact acto-myosin, undissociated until MgATP was added. Following the discovery of the mammalian skeletal myosin, there were more than 2,200 myosin sequences determined. The diversity of this motor protein can be classified in 35 classes, with the mammalian myosin being part of class II. These myosins have very diverse functions. For example, myosin V works as a cargo transporter inside the cell, myosin II, participates in cytoskeletal contraction, whereas myosin I, acts as a signaling molecule. Despite their different

functions, all these myosins produce force by hydrolyzing MgATP, which leads to conformational changes due to the sequential release of hydrolysis products: inorganic phosphate and MgADP. Myosin molecules have developed different rates of release of these hydrolysis products in order to match the specific role that they play in the cellular environment.

The structure of myosin-II and the role of each of its segments were studied intensively in the 1950s to 1960s using proteolytic enzymes. Firstly, the tryptic digestion showed two components sedimenting differently in a 0.6 M salt solution that were named respectively heavy meromyosin (HMM) and light meromyosin (LMM). Only the HMM preserved the capability to hydrolyze MgATP and to bind actin. At lower salt ionic strength (0.2 M KCl), the LMM crystallized, with a repeating pattern of about 43 nm (Philpott & Szent-Gyorgyi, 1954). The similarity between this value and the one measured between the protrusions of intact myofibrils, as observed by electron microscopy studies, pointed to its role in filament formation. Further investigations (Mueller & Perry, 1962) revealed that the HMM can also be separated in two functional structures: a major component, the subfragment 1 (S-1), which was likely to be the protrusion structure, and a remaining more heterogeneous structure, that was rapidly sedimenting, and that was named subfragment 2 (S-2). There were different suggestions on how these meromyosins assemble to form the myosin molecule, but it was only after the conclusive electron microscopy study of Slayter and Lowey (Slayter & Lowey, 1967) that it was determined that myosin is a double-stranded structure, with the LMM and HMM aligned linearly (Fig. 1.3). S-1 was further shown to maintain the ATPase activity and the capability to bind actin. More sub-structures were also identified: the light chains (Tsao, 1953).

After removal of one set of light chains (17kDa) in the presence of LiCl, the ATPase activity was lost. Removal of LiCl and recombination of the purified light chains with the myosin heavy chains, led to partial recovery of the ATPase activity (Stracher, 1969) thus the name of essential light chain (ELC).

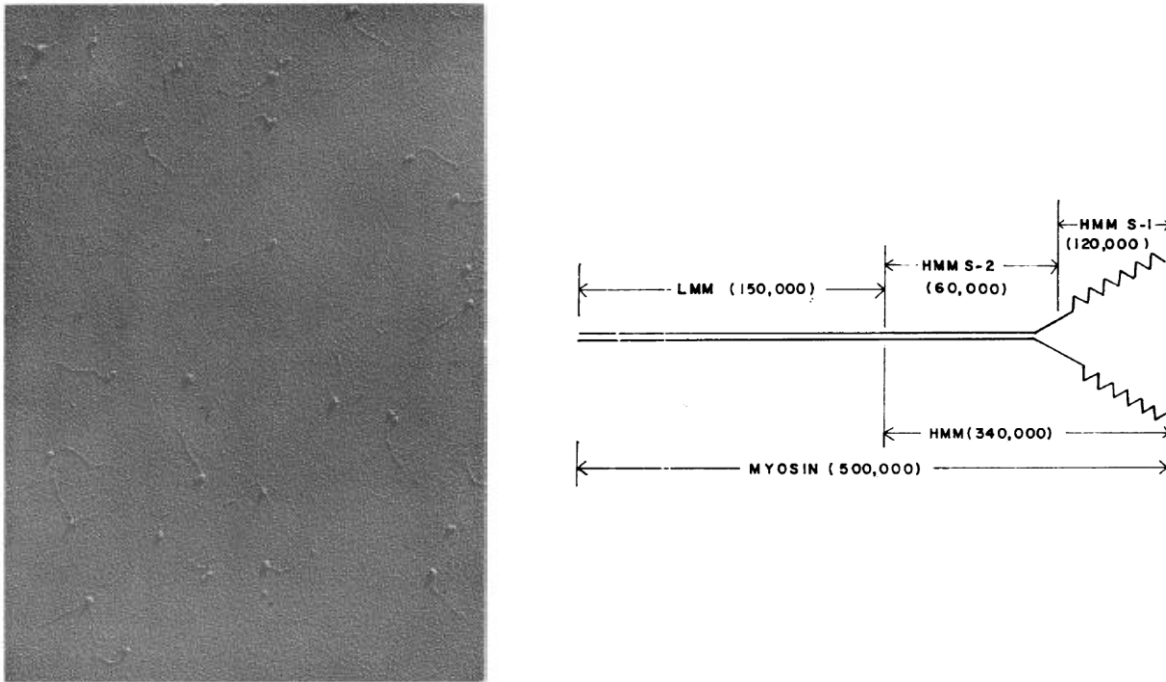


Fig. 1.3. Myosin molecules. *Left: Myosin molecules shadow-cast unidirectionally with platinum. Magnification 105,000 x; Right: Schematic of the meromyosins assembly. Adapted from (Slayter & Lowey, 1967)*

It was later shown that the ELC does not play an important role in the ATPase activity of myosin and its exact role remains unknown. It was suggested (Lowey & Trybus, 1995) that ELC may play a role in the modulation of the myosin kinetics, by strengthening the myosin neck region. The other light chain (20kDa) was shown to tightly regulate the ATPase activity of

smooth muscle (Sobieszek, 1977) and the molluscan muscle myosin and so was called the regulatory light chain (RLC). All light chains are bound in the neck region (Trotta, Dreizen, & Stracher, 1968) of the myosin heavy chains, in the S1 region.

This structural organization of myosin is well conserved for all classes so far studied. The N terminus of the protein has a globular structure, referred to as the “head” containing the nucleotide binding pocket and the actin binding site. The head is also called the motor domain of myosin because this is where the ATP hydrolysis takes place, leading to the actin translocation. The biochemical mechanism of ATP hydrolysis is similar for all the myosins studied but the reaction rates depend on their specific roles. The C terminus is also referred to as the tail region. The tail of the mammalian muscle myosin serves the function of filament assembly. Because the muscular class-II type myosin was the first to be characterized, the myosins that assemble into filaments are called “conventional” myosins. The roles of the myosin tail from other families include anchorage, cargo binding, and signaling. Between the myosin head and tail there is the neck region that acts as a lever arm during myosin-actin interactions.

1.2.3. ACTIN

Following his work on extracts from muscle tissue performed in the laboratory of Szent-Gyorgyi, Straub (1942) identified actin as the protein responsible for increasing the viscosity of myosin B. In intact muscle actin is present in filamentous form (F-actin). The actin cables have a crucial role in cellular motility and in cytoskeleton reconfiguration. Despite expressing multiple

isoforms, its sequence and structure and more importantly its property to assemble into filaments is highly conserved in all organisms.

In order to extract actin from muscle, myosin must be dissociated from F-actin using MgATP. Then, acetone denaturing is usually employed to remove the remaining actin bound myosin. To depolymerize actin, a low ionic strength alkaline solution is used. The resulting globular actin (G-actin) can be prevented from repolymerizing by keeping it in a solution without salt, with a pH above 6.0. MgATP also plays an important role in actin polymerization (Straub & Feuer, 1950), as it was shown that upon nucleotide removal, G-actin loses its capacity to polymerize. Even if polymerization is associated with MgATP hydrolysis, it is not essential for F-actin formation, as MgADP and a non-hydrolyzing form of MgATP can also induce a polymerization, although at a lower rate. Electron microscopy studies of the negatively stained F-actin revealed that actin forms a two-strand helix and the structure has a periodicity of 35 nm that contains approximately 13 globular actin monomers (Hanson & Lowy, 1964). The molecular mass of the protein is 42 kDa and six isoforms of actin were characterized based on their electrophoresis mobility and sequences. The electrophoresis showed three isoforms: α , β and γ . The isoforms are tissue specific but not species specific. The α isoforms are expressed in all three types of vertebrate muscle: skeletal, cardiac and smooth. The β isoform as well as one of the γ isoforms are associated with the cytoplasm, whereas the other γ isoform is specific to the gastrointestinal track. Despite their tissue specific expression, the purification of the skeletal actin isoforms has not yet revealed any functional difference. The actin activated ATPase activity and the actin propelling velocity in the in-vitro motility assay (see section 1.2.6) are identical (Harris & Warshaw, 1993) for a given myosin when using actin extracted from different types of

muscle (skeletal and smooth). The only noticeable difference is that smooth muscle actin in-vitro forms shorter filaments than the actin extracted from skeletal muscle (S. B. Marston & Smith, 1985). Thus, in the molecular studies skeletal actin is used for its ease of purification and polymerization. It is also possible that functional differences between different actin isoforms might come from their interactions with the various actin regulatory proteins.

1.2.3.1. Actin regulatory proteins

The regulation of smooth muscle contraction is not as well understood as that of striated muscle. The heterogeneous aspect of smooth muscle makes structural studies complex, so that associating a specific protein with a contractile mechanism is not straight forward. Furthermore, most theories elaborated to explain smooth muscle molecular mechanics are extrapolated from studies conducted at the tissue level. However, as the exact proportion of each contractile protein is hard to evaluate, the accurate interpretation rests on the investigator's shoulders. Most of the protein concentration estimates come from purification studies but the results are spoiled by the difficulty to accurately assess the cell compartment from which they came. Furthermore, the structure of the thin filament is not the same in all smooth muscle types so that the attribution of regulatory function of the decorating proteins is most of the time speculative, if not confirmed by molecular studies.

1.2.3.2. Tropomyosin

Tropomyosin is an actin regulatory protein, present in all types of mammalian muscle. The diversity of its isoforms comes from alternative gene splicing. Tropomyosin binds to actin in an end-to-end manner forming a continuous polymer along the long pitch of the actin strands (Phillips, Fillers, & Cohen, 1986). In skeletal and cardiac muscles, tropomyosin regulates actin-myosin interaction by a simple allosteric mechanism (Zot & Potter, 1982). It blocks the docking sites of the cross-bridges to prevent the myosin attachment and the power stroke. The on switch is provided by calcium binding to the troponin complex that leads to a change in tropomyosin conformation, freeing the binding sites. Skeletal muscle contains three isoforms of troponin. Troponin T is a long protein that binds tropomyosin at the connection between two tropomyosin monomers. The other two isoforms troponin C and troponin-I are globular proteins that bind to troponin T. After muscle stimulation, Ca^{2+} ions enter the cytoplasm and bind to troponin C imposing a structural change that further displaces the tropomyosin, uncovering the myosin docking site on actin. The efforts to demonstrate a similar steric hindering mechanism in smooth muscle were unsuccessful. The main role of tropomyosin is to stabilize the actin filaments so it is associated with all tasks requiring actin in the cellular environment: cell shape, cell adhesion and motility and vesicle transport. Also, tropomyosin has important contributions in regulating the cytoskeletal actin ensuring the cell viability. There are contradicting reports about tropomyosin effects on myosin actin-activated ATPase (Chacko & Eisenberg, 1990; Fanning, Wolenski, Mooseker, & Izant, 1994; Lehrer & Morris, 1982; Wever & Bremel, 1973). However, mechanical studies have shown that it enhances the actin filaments propelling velocity as measured in an in vitro motility assay (see section 1.2.6) (Fraser & Marston, 1995). It is hypothesized that the interaction of tropomyosin with actin changes the conformation of the actin

monomers interacting with the myosin heads (Fraser & Marston, 1995) Thus, tropomyosin plays a role in the co-operative attachment and synchronization of the power stroke of the cross-bridges (Fraser & Marston, 1995).

1.2.3.3. Caldesmon

Caldesmon is a smooth muscle actin binding protein with a molecular weight of about 90 kDa. On an SDS page gel it migrates as a 120-150 kDa protein. Caldesmon is a crosslinking protein that binds not only to actin, but also to calcium, calmodulin, tropomyosin and myosin. Following its first extraction (Sobue, Muramoto, Fujita, & Kakiuchi, 1981) from chicken gizzard in 1981, researchers thought that they had found the protein responsible for the steric block mechanism in smooth muscle, similar to troponin in the striated muscle. Indeed, Marston (Fraser & Marston, 1995; S. Marston, et al., 1998) proposed his model of smooth muscle regulation following the observation that caldesmon inhibits myosin's ATPase activity, and inhibits the myosin propelling velocity of actin, as measured in the in vitro motility assay (see section 1.2.6). This inhibition can be reversed either by calmodulin or through phosphorylation (Shirinsky, Biryukov, Hettasch, & Sellers, 1992). Interestingly, tropomyosin potentiates caldesmon's inhibitory effect on the ATPase (Makuch, Birukov, Shirinsky, & Dabrowska, 1991) and propelling actin velocity of myosin (Shirinsky, et al., 1992), which is opposite to what tropomyosin does on its own. Thus, caldesmon was hypothesized to be an allosteric effector that controls the actin-myosin interaction by acting on tropomyosin's conformation through a calcium dependent mechanism. Furthermore, different caldesmon contents are found in phasic and tonic smooth muscle. Indeed, caldesmon is found to be five to eight fold higher in the phasic than in tonic smooth muscle (Haeberle, Hathaway, & Smith, 1992), which suggests a different

regulation mechanism for the two types of muscle and potentially another functional role for caldesmon.

1.2.3.4. Calponin

In 1986, Takahashi et al. (Takahashi, Hiwada, & Kokubu, 1986) isolated from chicken gizzards a new protein with a molecular weight of 34 kDa. Initially named p34k, it was shown to bind to smooth muscle F-actin and to calmodulin. Its specificity to smooth muscle was demonstrated by exposing proteins extracted from different bovine smooth muscle and non-muscle tissues to a rabbit polyclonal antibody raised against gizzard p34K (Takahashi, Hiwada, & Kokubu, 1987). Because of its similarity with cardiac troponin T, it was given the name calponin. It also binds to smooth muscle tropomyosin and its affinity for smooth muscle actin is seven to eight fold greater than for skeletal F-actin. Calponin inhibits, in a dose dependent manner, the ATPase activity of smooth muscle myosin (Winder & Walsh, 1990) and the velocity (v_{max}) of actin propulsion in the in vitro motility assay (Haeberle, 1994) (see section 1.2.6). This inhibitory effect can be suppressed by the addition of Ca^{2+} and calmodulin or by calponin phosphorylation (Shirinsky, et al., 1992). At the cellular level, it has also been shown that calponin is necessary to inhibit the slow cycling of unphosphorylated myosin, stopping the shortening and force production of resting smooth muscle (Malmqvist, Trybus, Yagi, Carmichael, & Fay, 1997). It is not clear which of calponin or caldesmon has a greater effect on the ATPase activity as reports have been contradictory (Makuch, et al., 1991; S. B. Marston, 1991; Winder, Sutherland, & Walsh, 1992). Furthermore, because they can also bind to myosin, it is not clear why two proteins with similar effects are required for smooth muscle regulation. However, when competing with caldesmon, calponin is more effective at binding to actin filaments (Makuch, et

al., 1991). Furthermore, the inhibitory effect of calponin on myosin ATPase activity is not affected by tropomyosin (Makuch, et al., 1991).

1.2.4. MUSCLE MOLECULAR MECHANICS

The biomechanical interaction between myosin and actin was and continues to be a puzzle. After rejection of the folding filaments theory based on H.E. Huxley's observation that the A-band remains at constant length during contraction, he proposed the sliding filament theory that states that the overlapping of actin and myosin filaments leads to muscle contraction. To prove this theory a few questions had first to be answered. Indeed, the observation that actin and myosin dissociate in the presence of MgATP could not be reconciled with the fact that addition of MgATP also leads to the contraction of muscle fibers. As muscle contraction occurs in the presence of different regulatory proteins, one of them could potentially be responsible for this property. However, the interaction between myosin and actin could not be ruled out, because the basal ATPase activity of myosin is increased a hundred fold in the presence of actin without additional regulatory proteins. As myosin MgATP hydrolysis was considered to be the main driving energy, it was counterintuitive to assume that force could be generated if the proteins were to dissociate after addition of MgATP. However, additional measurements in insect flight muscle using low-angle X-ray scattering and electron microscopy showed that the protuberances of the myosin filaments attach to actin filaments at an approximately 45 degree angle in rigor and at about 90 degrees in the presence of MgATP (Reedy, Holmes, & Tregear, 1965). These results confirmed, once and for all, that force generation is driven by a conformational change of myosin upon interaction with actin filaments. The myosin protuberances, named cross-bridges,

are therefore responsible for the ATPase activity, for binding to the actin filaments and for generating the force that drives muscle contraction.

All these observations also pointed to a cyclic interaction. Transient kinetics studies were then performed to assess how many ATP molecules have to be hydrolyzed to lead to a complete cycle. The initial studies on skeletal myosin (Takahashi, Mori, Nakamura, & Tonomura, 1965) where the MgATP hydrolysis was stopped by addition of trichloroacetic acid, showed an initial burst of inorganic phosphate (Pi) release followed by a steady-state phase of Pi release. In order to explain their results, Tonomura et al. (Tonomura, Nakamura, Kinoshita, Onishi, & Shigekawa, 1969), proposed that before interacting with actin, myosin has to first be activated (phosphorylated) and that the burst of phosphate could be attributed to this initial fast occurring stage. The steady state phase was supposed to be a consequence of the de-activation of myosin that led to the release of the hydrolysis products, MgADP and Pi. Furthermore, they proposed that the sliding of the filaments occurred due to the weak bonds between myosin and actin when the myosin is dephosphorylated. In 1971, Lymn and Taylor (Lymn & Taylor, 1971) proposed a slightly different explanation for the different Pi release rates. Using a quenched-flow apparatus, they observed that the MgATP hydrolysis occurs when myosin and actin are detached. Thus they attributed the initial burst of Pi release to a rapid hydrolysis of MgATP that occurs when the myosin nucleotide pockets are empty. They also concluded that the steady-state Pi release occurs because of the slow MgADP release, which itself slows down the intake of the next ATP molecule.

Despite long controversies between these groups in the 1970s and 1980s, the explanation proposed by the Taylor group, which implies a one-way ATP hydrolysis mechanism, is still the most popular explanation nowadays. It is important to note that smooth muscle contraction is different from that of striated in that it cannot occur without myosin activation through a phosphorylation mechanism. Nevertheless, the mechanism of the interaction between myosin and actin following myosin activation was adequately described by Lymn and Taylor in 1971. Their four-state model, presented in Fig. 1.4, predicted that upon binding of ATP, the acto-myosin system dissociates due to myosin abrupt decrease in affinity for actin. Then, myosin hydrolyzes MgATP, a rapid process with a rate that they could not measure. The newly formed myosin-ADP-Pi complex is assumed to have very high affinity for actin. The hydrolysis product release is accelerated by the conformational changes of myosin binding to actin. This explains also why myosin ATPase activity is a hundred fold greater in the presence of actin. The release of Pi leads to the myosin conformational change, called the power-stroke, which displaces the actin filaments. The release of MgADP empties the nucleotide binding pocket, allowing myosin to bind a new MgATP molecule and therefore the cycle to start over. Although they considered their model to be “provisional and oversimplified”, the general scheme, as well as their findings are still valid after 40 years of assiduous research. Nonetheless, the introduction of new single molecule techniques, such as the in-vitro motility (Sheetz & Spudich, 1983) and the laser trap assays (Finer, Simmons, & Spudich, 1994) (see section 1.2.6), coupled to increased spatial and temporal measurement resolution, refined and upgraded our knowledge of muscle physiology.

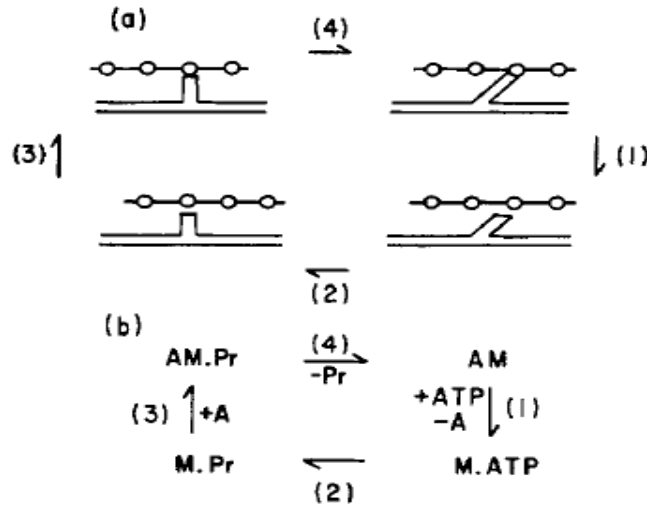


Fig 1.4. ATP hydrolysis cycle. *a)* Myosin (*M*) docking sites on actin (*A*) filaments are denoted by open circles; *b)* Steps in the ATP hydrolysis cycle : after binding to ATP, myosin hydrolyzes ATP in hydrolysis products (*Pr*). The release of *Pr* leads to conformational changes. Adapted from (Lymn & Taylor, 1971)

Using such techniques (Section 1.2.6), the unitary displacement of actin filament by myosin, called the unitary myosin step, as well as the force generated by a cross-bridge, were measured for both skeletal (Finer, et al., 1994) and smooth myosin (Lauzon, et al., 1998). Veigel et al. (Veigel, Molloy, Schmitz, & Kendrick-Jones, 2003) showed that smooth muscle cross-bridges displace actin in two stages and the duration of the first stage heavily depends on the external load applied on the cross-bridges, whereas the second stage depends on the ATP concentration (see table 1). Interestingly, the positive load (applied in the same direction as the myosin displaces actin) prolongs the binding time.

Table 1 Rate constants and mean lifetimes measured at different ATP concentrations			
	$t_{1/2}$ (ms) (s.e.m., *)	k_1 (s ⁻¹) (s.e.m., r)	k_2 (s ⁻¹) (s.e.m., r)
10 μ m ATP	122 (7)	23 (0.3, 0.9)	7 (0.3, 0.9)
50 μ m ATP	71 (6)	n.d.	n.d.
100 μ m ATP	64 (3)	21 (0.2, 0.8)	48 (0.2, 0.8)
20 μ m ATP: control	86 (6)	25 (0.2, 0.9)	13 (0.2, 0.9)
20 μ m ATP: push (1.6 pN)	39 (3)	55 (0.2, 0.9)	14 (0.2, 0.9)
20 μ m ATP: pull (1.6 pN)	138 (7)	12 (0.3, 0.9)	10 (0.3, 0.8)

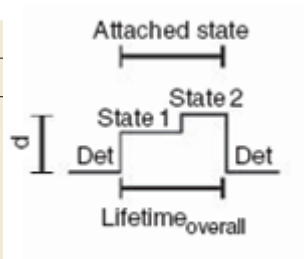


Table 1. Acto-myosin attachment time scale. Average smooth muscle myosin attachment time ($t_{1/2}$) and the rates of the two states of attached myosin at different ATP concentrations and force loadings as measured using the laser trap assay. (adapted from Veigel et al, 2003).

More recent data (Capitanio, et al., 2012), collected for skeletal muscle myosin and acquired with systems that allow a temporal resolution of close to 100 μ s, suggest that myosin attachment actually occurs in three phases, with an additional initial dwell phase during which the attached myosin does not displace the actin. The sensitivity of each of these phases on the nucleotide concentration and on the external force experienced by each individual myosin, coupled with the difficulty to extrapolate the results obtained from single molecule to ensembles of molecules (Hilbert, Cumarasamy, Zitouni, Mackey, & Lauzon, 2013; Walcott, Warshaw, & Debold, 2012) have made laborious the development of models to explain particular aspects of the acto-myosin interaction such as the latch state.

1.2.5. LATCH-STATE

AF Huxley suggested that the cross-bridges are the elements responsible for unitary force because the tension measured in skeletal muscle is proportional to the extent of the filaments overlap (A. F. Huxley, 1974). However, an observation made by Dillon et al. (Dillon, Aksoy, Driska, & Murphy, 1981) in muscle strips prepared from swine carotid artery led to the conclusion that smooth muscle contraction and regulation is more complex than was initially believed. In smooth muscle, cross-bridges can generate force only after activation. This activation is achieved by the phosphorylation of myosin's regulatory light chains, by MLCK as detailed in section 1.1. The deactivation of myosin is accomplished by dephosphorylation of the light chains by myosin light chain phosphatase (MLCP).

When measured in a smooth muscle stimulated to contract, the myosin light chain phosphorylation is observed to increase rapidly in the early stages of the contraction; it reaches a peak, and then decreases back to baseline levels. The velocity of shortening follows the same pattern as the activation level. Force, on the other hand, also increases rapidly, but then reaches a plateau that can be maintained for long periods of time. Dillon and co-workers termed this state the "latch-state" (Dillon, et al., 1981) . This observation that force is maintained and sometimes even increased while the cross-bridges are dephosphorylated suggests an additional regulation mechanism for smooth muscle force generation. To add to the mystery, force is maintained with a lower ATP consumption than would be required by skeletal muscle to generate a similar force. In order to explain their observation of force maintenance at low energy consumption, Dillon and coworkers suggested that smooth muscle myosin can modulate its cycling rate. They postulated

that if myosin gets dephosphorylated while attached to actin, its detachment rate decreases. The deactivated attached cross-bridges, or latch-bridges, were suggested to cycle very slowly if at all and to contribute to the general decreased cycling rate by imposing an internal load.

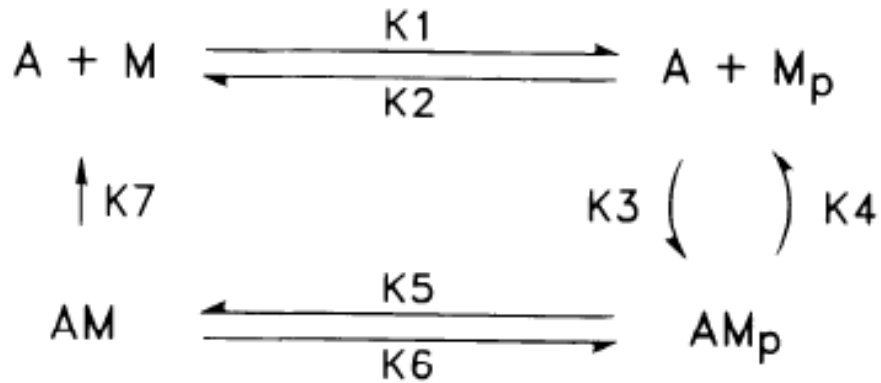


Fig 1.5. Latch-bridge cycle. Myosin (*M*), actin (*A*), phosphorylated myosin (*M_p*), phosphorylated myosin interacting with actin (*AM_p*), latch-state (*AM*). *K1-K7* represent reaction rate constants.

Hai and Murphy (Hai & Murphy, 1988), later on, proposed a mathematical model to explain their observations. This model is comprised of four possible states for the acto-myosin interactions, as in Fig. 1.5.: two not bound: *A+M* and *A+M_p*, and two bound: *AM_p* and *AM*, where *A* stands for actin, *M* for myosin and *p* for phosphorylation. The model quantitatively predicts the force (proportional to myosin being in the states *AM* and *AM_p*), the phosphorylation level (*A+M_p* and *AM_p*) and a linear relationship between the phosphorylation level and the shortening velocity.

There are still several questions and unresolved issues with the Hai and Murphy model of the latch-state. One criticism of the model is that it predicts that more than sixty percent of the

ATP is consumed for the phosphorylation of myosin (Hai & Murphy, 1988); this is counterintuitive for a low ATP consumption mechanism. Also, in order to resolve the issue of force maintenance while the phosphorylation levels decrease, the dephosphorylated cross-bridges were postulated to be capable of generating the same force as the phosphorylated cross-bridges; this has never been demonstrated. In addition, even if the model predicts a linear relationship between the phosphorylation level and the shortening velocity there are studies that indicate that the two are not correlated (Merkel, Gerthoffer, & Torphy, 1990; Mitchell, et al., 2001). Another particularity of their model is that the attachment of dephosphorylated myosin to actin is considered impossible. Thus, this model rests on several assumptions that were never validated at the molecular level. Furthermore, alternative views of the latch-state also exist. Dephosphorylated myosin may have the ability to attach to actin (Siegman, Butler, & Mooers, 1985). Also, co-operativity between phosphorylated and dephosphorylated myosin might promote the attachment of dephosphorylated myosin (Himpens, 1992). The role of the actin regulatory proteins in the latch-state has yet to be thoroughly assessed. For example, it is known that caldesmon and calponin decrease the ATPase activity and the actin propelling velocity in the *in vitro* motility assay (see section 1.2.6). Thus, could they be part of the regulatory system of the latch-state? These theories all need to be verified at the molecular level.

1.2.6. METHODS TO STUDY MUSCLE MOLECULAR MECHANICS

1.2.6.1. *In vitro* motility assay

The idea of designing *in vitro* assays to replicate the *in-vivo* interaction between myosin and actin materialized in 1983 (Sheetz & Spudich, 1983). Sheetz and Spudich used beads that

they attached to myosin molecular motors that travelled on actin cables. This assay gave the first insights into the kinetic properties of muscle proteins. After revisions in 1985 (Spudich, Kron, & Sheetz, 1985) and 1986 (Kron & Spudich, 1986), the in vitro motility assay is still today a major tool in the study of the acto-myosin interactions. After a first attempt at aligning actin filaments to the substrate by the Dictyostelium protein severing, the Spudich group used single actin filaments obtained by dissection of the plant *Nitella axillaris*. Assessing the velocity at which the beads moved, allowed the characterization of the acto-myosin interaction. Tampering with the experimental conditions allowed them to investigate the influence of various elements, such as pH, temperature, ionic strength or to assess the effect of the regulatory proteins. Following this first success, a new version of the in vitro motility assay was developed to avoid the contamination brought about by organisms such as the *Nitella* alga. The beads also needed to be removed as they were not moving continuously and only for short distances which made the velocities hard to assess. Thus, Yanagida reported in 1984 the movement of fluorescently labeled (using phalloidin-rhodamine) actin filaments propelled by myosin molecules (Yanagida, Nakase, Nishiyama, & Oosawa, 1984). In this version of the assay, a mixture containing actin filaments and myosin molecules was perfused into the volume created between a glass coverslip and a microscope slide. The fluorescent filaments were excited using a 100 W mercury lamp and the images were captured using a high sensitivity camera (Ikegami CTC-900) through the high numerical aperture objective ($N_A = 1.3$) of a NIKON VFD-TR microscope, equipped with epifluorescence optics. β -mercaptoethanol was used to prevent the photobleaching of the labeled filaments. However, a precise velocity measurement of actin propulsion still could not be reported, seemingly due to the low acquiring frequency of the camera used. A major

improvement of this assay was achieved in 1986 by the group of Spudich by immobilizing the myosin on a glass surface (Kron & Spudich, 1986).

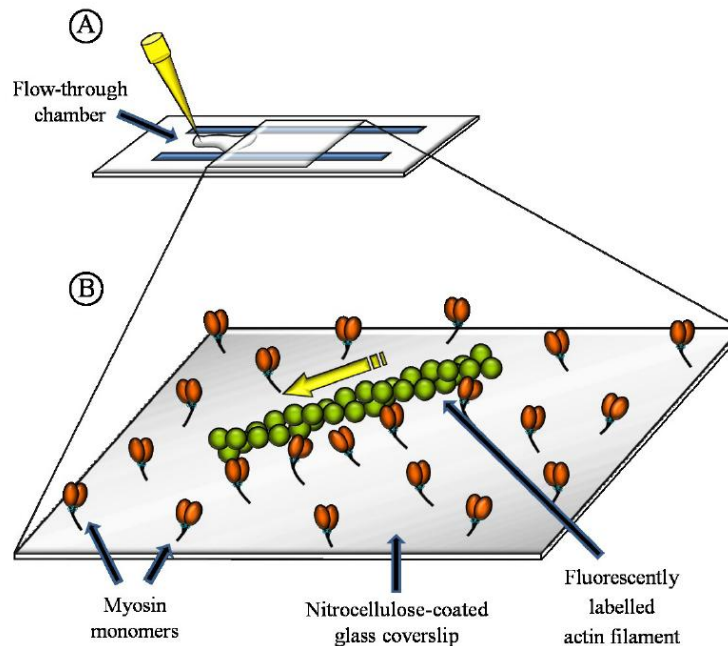


Fig 1.6. *In vitro* motility assay. The velocity of actin filaments propelled by myosin molecules randomly adhered to a microscope coverslip is assessed by dividing their total path by the elapsed time. See text for details. Figure kindly provided by Genevieve Bates.

Besides offering an anchorage for the acto-myosin interaction to take place, it also provided a surface for the movement to occur that respected the short focal distances of the objectives used. In addition, the use of image intensifiers contributed to a significant increase of the signal to noise ratio and of the image acquisition frequency. Since that time, the assay has been refined, but it retains basically the major steps mentioned above. That is, a flow through chamber (Fig. 1.6.) is created with a thin coverslip (50-200 μm) and a microscope slide separated by plastic shims (125 μm thick). The coverslip is coated with nitrocellulose or silicone to prevent

degradation of the myosin when in contact with glass. Monomeric myosin is perfused in the chamber and allowed to adhere to the coverslip. Bovine serum albumin (BSA) is then added to prevent the binding of actin filaments to the nitrocellulose surface. Fluorescently labeled actin filaments are then perfused, followed by the addition of a buffer containing MgATP and methylcellulose. While the role of MgATP in the fueling of myosin is obvious, the methylcellulose is used to limit the diffusion of the labeled actin filaments and promote the myosin-actin interaction. The assay has been well characterized by the Warshaw group (Warshaw, Desrosiers, Work, & Trybus, 1990). They reported that the actin velocity i) is independent of actin filament length ii) is maximum at a pH of 7.0 iii) increases with MgATP concentration up to 250 mM iv) increases slightly with ionic strength. However, above 60 mM KCl the binding of myosin to actin diminishes, so that the assay cannot be performed. The *in vitro* motility assay has been used to study several types of myosins, including skeletal, cardiac, smooth, and non-muscle myosin, as well as their regulatory mechanisms.

1.2.6.2. Laser trap assay

The forces of interaction between myosin and actin were hypothesized to be of the order of the piconewton. The conventional mechanics measurements methods could not measure such forces. However, Arthur Ashkin who was working for the Bell Laboratories, reported in 1969 the use of radiation pressure force of laser light to accelerate and manipulate small particles (Ashkin, 1970), which later on revolutionized the study of biological molecular motors. Trying to use the effect of conservation of light momentum, his group was interested in small particle motion. Using a laser with a power less than 1 W, they were able to observe particle motion in the

direction of the mildly focused Gaussian beam. An additional effect was also detected; the particles located in the fringes of the beam were constantly attracted towards the center of the beam, where the intensity was higher. When the beam was moved back and forth, the particle followed the laser movement, suggesting a possible particle guiding mechanism. The physics of the system shows that the effects observed are due to two forces exerted on the particle: the scattering force that pushes the particle in the direction of light propagation and the gradient force that acts like a three dimensional spring that brings the particle back toward the center of the laser trap. Using particles of diameter greater than the wavelength of the laser beam and objectives with high numerical apertures allows the gradient force to overcome the scattering force. Importantly, the refractive index of the trapped particle must be greater than that of surrounding milieu so that the light gets refracted when it hits the particle. Based on the Gaussian distribution of the focused light and on conservation of momentum, when the bead is displaced from the center of the laser trap, where the light is more intense, there is a net restoring force that pushes it back to the center of the trap. Offering a precise mean to control particles in solution, laser trapping has applications in fields as diverse as atomic physics and biology. In atomic physics, the laser trap is used to cool and trap atoms (Chu, Bjorkholm, Ashkin, Gordon, & Hollberg, 1986). Researchers from the Bell Laboratories were awarded a Nobel Prize for this discovery. In biology, the potential of optical trapping resides in the fact that the forces exerted by the optical tweezers closely match those occurring in the cellular environment. In addition, laser beams of wavelength of approximately 1000 nm (near infrared) are weakly absorbed by biological systems, making this tool quasi non-invasive. Ashkin (Ashkin & Dziedzic, 1987) was also the first to use the laser trap to study biological systems; he used it to capture and manipulate viruses (tobacco mosaic) and bacteria (E.coli). As the development of this tool

advanced further, researchers used the optical trap to capture polystyrene or silica microspheres because their regular shape allows for calibration, necessary for force measurements. Block (Block, Goldstein, & Schnapp, 1990) used a single bead system to estimate the number of kinesin molecules needed to coat a silica bead in order for the bead to be displaced out of the laser trap upon kinesin interaction with microtubules on a coverslip. This measurement allowed the estimation of the binding force of kinesin to the microtubule. Kuo and Sheets (Kuo & Sheetz, 1993) also used a single bead optical trap and reported the first active force value for a motor molecule (kinesin). They calibrated their system using the viscous drag force approach (Stokes, linear relationship between the drag force and the displacement of the trapped bead from its central position). Finer (Finer, et al., 1994) was the first to measure the displacement and force generated by a single myosin molecule. To achieve these measurements, the diffusion of the actin filament away from the myosin molecule was avoided using a three bead system (Fig. 1.7.). That is, two beads were captured in the optical traps. The surface of those beads was altered biochemically so that they could bind to actin.

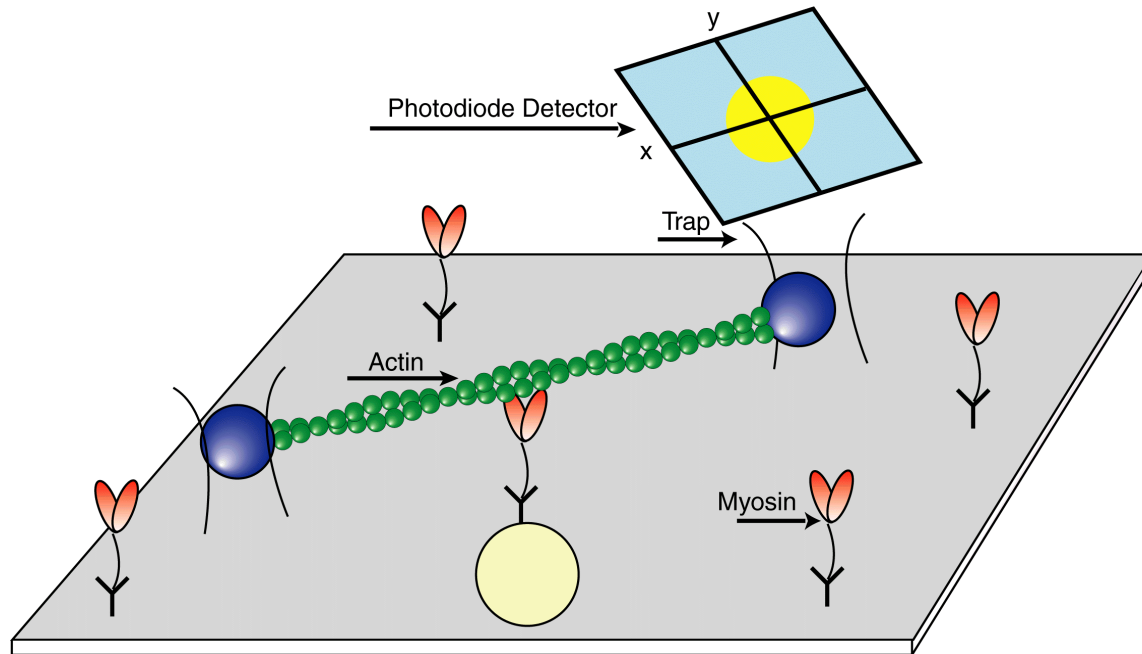


Fig 1.7. Three-bead laser trap assay. Low myosin density is used to ensure single interaction events between myosin molecule and the actin filament. See text for details. Adapted from (Guilford, et al., 1997)

Thus an actin filament was strung up between the two beads. By manipulating the traps, the filament was then brought in the vicinity of a third bead (larger in diameter) bound to the coverslip and used as a pedestal. This pedestal was coated with a low concentration of myosin molecules. As myosin interacted with the actin filament, a quadrant detector recorded the trapped bead's displacement, thus yielding the myosin unitary displacement. An acousto-optic modulator was later on used as a feedback system to keep that same bead stationary as the myosin pulled on the actin filament. By calibrating this feedback system the unitary force generated by myosin

was obtained because it is equal and opposite to the force needed to maintain the bead in place. Over time, the laser trap assay proved to be a reliable and conclusive technique because it allows for force assessment to be combined with high resolution light microscopy.

1.2.7. MICROFLUIDICS

The single molecule techniques like the in-vitro motility assay, the laser trap assay, the atomic force microscopy, the Förster resonance energy transfer (FRET) and quantum-dots have brought the necessity to control the molecular environment and to limit the contamination passed to the biological material. Thus, a good understanding of the theoretical aspects of the physical phenomena that occur at the microscopic level has to be acquired to advance the molecular level biological research. For example, several rules dictate the fundamentals of microfluidics which are not apparent from the macroscopic level. Factors such as viscosity, surface tension, energy dissipation, diffusion and fluidic resistance often dominate the systems. The Reynolds number reaches a low value which suggests a shift from inertial forces towards viscous forces (Brody, Yager, Goldstein, & Austin, 1996). While dimensions become smaller, the convective mass transport diminishes in importance and fast thermal transport and diffusion take over. Thus, the science of microfluidics has evolved to address these phenomena and to use them to our advantage to study, for example, biology at the molecular level. One advantage of using microfluidics for biological studies is the precise control over the transferred fluids. This property confers to the science of microfluidics the power of a new technology that is used more and more by researchers. The emergence of microfluidic devices is undeniably related to the introduction of polydimethylsiloxane (PDMS), a polymer that allows the engraving of micro

channels. Additionally, PDMS shows several advantages for biological research: it is biocompatible, inexpensive, transparent (in the range of 240nm-1100nm), it has a low autofluorescence and it can be molded with a resolution of a few nanometers. Furthermore, because PDMS binds covalently to glass following a simple plasma treatment, a readily sealed microfluidic device can easily be obtained following the carving of microchannels in PDMS.

1.3. THE GOAL OF THIS THESIS

The ultimate goal of this thesis was to verify at the molecular level the theories of the latch state. First, the contribution of the actin regulatory proteins to the binding of unphosphorylated myosin to actin was assessed. The role of calponin in the enhancement of the binding force of unphosphorylated myosin to actin via cross-linking was determined and is reported in chapter 2. The role of caldesmon in the enhancement of the binding force of unphosphorylated myosin to actin and its regulation of muscle relaxation via its phosphorylation by ERK are reported in chapter 3. Finally, to verify at the molecular level whether force maintenance does occur during myosin dephosphorylation, a microfluidic device was developed to allow the introduction of myosin light chain phosphatase in a flow-through chamber without perturbing the molecular mechanical measurements. The design and the proof of principle of this microfluidic chamber are reported in chapter 4.

1.4. REFERENCES

Ashkin, A. (1970). Acceleration and Trapping of Particles by Radiation Pressure. *Phys. Rev. Lett.* (24), 156–159

Ashkin, A., & Dziedzic, J. M. (1987). Optical trapping and manipulation of viruses and bacteria. *Science*, 235(4795), 1517-1520.

Astbury, W. T. (1945). The structural proteins of the cell. *Biochem J*, 39(5), lvi.

Astbury, W. T., & Bell, F. O. (1941). Nature of the Intramolecular Fold in Alpha-Keratin and Alpha-Myosin. *Nature*, 147, 696-699.

Banga, I., A. Szent-Györgyi. (1942). Preparation and properties of myosin A and B. *stud. Inst. Med. Chem. Univ. Szeged*, I, 5-15.

Block, S. M., Goldstein, L. S., & Schnapp, B. J. (1990). Bead movement by single kinesin molecules studied with optical tweezers. *Nature*, 348(6299), 348-352.

Brody, J. P., Yager, P., Goldstein, R. E., & Austin, R. H. (1996). Biotechnology at low Reynolds numbers. *Biophys J*, 71(6), 3430-3441.

- Capitanio, M., Canepari, M., Maffei, M., Beneventi, D., Monico, C., Vanzi, F., et al. (2012). Ultrafast force-clamp spectroscopy of single molecules reveals load dependence of myosin working stroke. *Nat Methods*, *9*(10), 1013-1019.
- Chacko, S., & Eisenberg, E. (1990). Cooperativity of actin-activated ATPase of gizzard heavy meromyosin in the presence of gizzard tropomyosin. *J Biol Chem*, *265*(4), 2105-2110.
- Chu, S., Bjorkholm, J. E., Ashkin, A., Gordon, J. P., & Hollberg, L. W. (1986). Proposal for optically cooling atoms to temperatures of the order of 10^{-6} K. *Opt Lett*, *11*(2), 73.
- Dillon, P. F., Aksoy, M. O., Driska, S. P., & Murphy, R. A. (1981). Myosin phosphorylation and the cross-bridge cycle in arterial smooth muscle. *Science*, *211*(4481), 495-497.
- Draeger, A., Amos, W. B., Ikebe, M., & Small, J. V. (1990). The cytoskeletal and contractile apparatus of smooth muscle: contraction bands and segmentation of the contractile elements. *J Cell Biol*, *111*(6 Pt 1), 2463-2473.
- Ebashi, S., Ebashi, F., Kodama, A. (1967). Troponin as the Ca^{++} -receptive protein in the contractile system. *J Biochem*, *62*(1), 137-138.
- Engelhardt, W. A. (1942). Enzymatic and Mechanical Properties of Muscle Proteins. *Yale J Biol Med*, *15*(1), 21-38.

- Engelhardt, W. A., Liubimova, M. N. (1939). Myosin and adenosine triphosphatase. *Nature*, 144(688, Oct. 14), 668–669.
- Fanning, A. S., Wolenski, J. S., Mooseker, M. S., & Izant, J. G. (1994). Differential regulation of skeletal muscle myosin-II and brush border myosin-I enzymology and mechanochemistry by bacterially produced tropomyosin isoforms. *Cell Motil Cytoskeleton*, 29(1), 29-45.
- Finer, J. T., Simmons, R. M., & Spudich, J. A. (1994). Single myosin molecule mechanics: piconewton forces and nanometre steps. *Nature*, 368(6467), 113-119.
- Fraser, I. D., & Marston, S. B. (1995). In vitro motility analysis of actin-tropomyosin regulation by troponin and calcium. The thin filament is switched as a single cooperative unit. *J Biol Chem*, 270(14), 7836-7841.
- Galpin, A. J., Raue, U., Jemiolo, B., Trappe, T. A., Harber, M. P., Minchev, K., et al. (2012). Human skeletal muscle fiber type specific protein content. *Anal Biochem*, 425(2), 175-182.
- Guilford, W. H., Dupuis, D. E., Kennedy, G., Wu, J., Patlak, J. B., & Warshaw, D. M. (1997). Smooth muscle and skeletal muscle myosins produce similar unitary forces and displacements in the laser trap. *Biophys J*, 72(3), 1006-1021.

- Haerberle, J. R. (1994). Calponin decreases the rate of cross-bridge cycling and increases maximum force production by smooth muscle myosin in an in vitro motility assay. *J Biol Chem*, 269(17), 12424-12431.
- Haerberle, J. R., Hathaway, D. R., & Smith, C. L. (1992). Caldesmon content of mammalian smooth muscles. *J Muscle Res Cell Motil*, 13(1), 81-89.
- Hai, C. M., & Murphy, R. A. (1988). Cross-bridge phosphorylation and regulation of latch state in smooth muscle. *Am J Physiol*, 254(1 Pt 1), C99-106.
- Hanson, J., & Lowy, J. (1964). The Structure of Actin Filaments and the Origin of the Axial Periodicity in the I-Substance of Vertebrate Striated Muscle. *Proc R Soc Lond B Biol Sci*, 160, 449-460.
- Harris, D. E., & Warshaw, D. M. (1993). Smooth and skeletal muscle actin are mechanically indistinguishable in the in vitro motility assay. *Circ Res*, 72(1), 219-224.
- Hilbert, L., Cumarasamy, S., Zitouni, N. B., Mackey, M. C., & Lauzon, A. M. (2013). The kinetics of mechanically coupled myosins exhibit group size-dependent regimes. *Biophys J*, 105(6), 1466-1474.
- Himpens, B. (1992). Modulation of the Ca(2+)-sensitivity in phasic and tonic smooth muscle. *Verh K Acad Geneesk Belg*, 54(3), 217-251.

Huxley, A. F. (1974). Muscular contraction. *J Physiol*, 243(1), 1-43.

Huxley, H. E. (1957). The double array of filaments in cross-striated muscle. *J Biophys Biochem Cytol*, 3(5), 631-648.

Huxley, H. E. (1963). Electron Microscope Studies on the Structure of Natural and Synthetic Protein Filaments from Striated Muscle. *J Mol Biol*, 7, 281-308.

Huxley, H. E. (2004). Fifty years of muscle and the sliding filament hypothesis. *Eur J Biochem*, 271(8), 1403-1415.

Kron, S. J., & Spudich, J. A. (1986). Fluorescent actin filaments move on myosin fixed to a glass surface. *Proc Natl Acad Sci U S A*, 83(17), 6272-6276.

Kühne, W. (1864). Untersuchungen über das Protoplasma und die Contractilität. *W. Engelmann, Leipzig*.

Kuo, S. C., & Sheetz, M. P. (1993). Force of single kinesin molecules measured with optical tweezers. *Science*, 260(5105), 232-234.

Lauzon, A. M., Tyska, M. J., Rovner, A. S., Freyzon, Y., Warshaw, D. M., & Trybus, K. M. (1998). A 7-amino-acid insert in the heavy chain nucleotide binding loop alters the kinetics of smooth muscle myosin in the laser trap. *J Muscle Res Cell Motil*, 19(8), 825-837.

- Lehrer, S. S., & Morris, E. P. (1982). Dual effects of tropomyosin and troponin-tropomyosin on actomyosin subfragment 1 ATPase. *J Biol Chem*, 257(14), 8073-8080.
- Lohman, K. (1934). Über die enzymatische aufspaltung der kreatin phosphorsaure; zugleich ein beitrag zum chemismus der muskel kontraktion. (On the enzymic cleavage of creatinephosphate; also a contribution to the chemistry of the muscle contraction). *Biochem Z*, 271, 264-277.
- Lowey, S., & Trybus, K. M. (1995). Role of skeletal and smooth muscle myosin light chains. *Biophys J*, 68(4 Suppl), 120S-126S; discussion 126S-127S.
- Lymn, R. W., & Taylor, E. W. (1971). Mechanism of adenosine triphosphate hydrolysis by actomyosin. *Biochemistry*, 10(25), 4617-4624.
- Makuch, R., Birukov, K., Shirinsky, V., & Dabrowska, R. (1991). Functional interrelationship between calponin and caldesmon. *Biochem J*, 280 (Pt 1), 33-38.
- Malmqvist, U., Trybus, K. M., Yagi, S., Carmichael, J., & Fay, F. S. (1997). Slow cycling of unphosphorylated myosin is inhibited by calponin, thus keeping smooth muscle relaxed. *Proc Natl Acad Sci U S A*, 94(14), 7655-7660.

- Marston, S., Burton, D., Copeland, O., Fraser, I., Gao, Y., Hodgkinson, J., et al. (1998). Structural interactions between actin, tropomyosin, caldesmon and calcium binding protein and the regulation of smooth muscle thin filaments. *Acta Physiol Scand*, 164(4), 401-414.
- Marston, S. B. (1991). Properties of calponin isolated from sheep aorta thin filaments. *FEBS Lett*, 292(1-2), 179-182.
- Marston, S. B., & Smith, C. W. (1985). The thin filaments of smooth muscles. *J Muscle Res Cell Motil*, 6(6), 669-708.
- Merkel, L., Gerthoffer, W. T., & Torphy, T. J. (1990). Dissociation between myosin phosphorylation and shortening velocity in canine trachea. *Am J Physiol*, 258(3 Pt 1), C524-532.
- Mitchell, R. W., Seow, C. Y., Burdyga, T., Maass-Moreno, R., Pratusевич, V. R., Ragozzino, J., et al. (2001). Relationship between myosin phosphorylation and contractile capability of canine airway smooth muscle. *J Appl Physiol (1985)*, 90(6), 2460-2465.
- Mueller, H., & Perry, S. V. (1962). The degradation of heavy meromyosin by trypsin. *Biochem J*, 85, 431-439.
- Needham, J., A. Kleinzeller, M. Miall, M. Dainty, D.M. Needham, A.S.C. Lawrence. (1942). Is muscle contraction essentially an enzyme-substrate combination? *Nature*, 150, 46-49.

- Phillips, G. N., Jr., Fillers, J. P., & Cohen, C. (1986). Tropomyosin crystal structure and muscle regulation. *J Mol Biol*, *192*(1), 111-131.
- Philpott, D. E., & Szent-Gyorgyi, A. G. (1954). The structure of light-meromyosin: an electron microscopic study. *Biochim Biophys Acta*, *15*(2), 165-173.
- Reedy, M. K., Holmes, K. C., & Tregear, R. T. (1965). Induced changes in orientation of the cross-bridges of glycerinated insect flight muscle. *Nature*, *207*(5003), 1276-1280.
- Sheetz, M. P., & Spudich, J. A. (1983). Movement of myosin-coated fluorescent beads on actin cables in vitro. *Nature*, *303*(5912), 31-35.
- Shirinsky, V. P., Biryukov, K. G., Hettasch, J. M., & Sellers, J. R. (1992). Inhibition of the relative movement of actin and myosin by caldesmon and calponin. *J Biol Chem*, *267*(22), 15886-15892.
- Siegman, M. J., Butler, T. M., & Mooers, S. U. (1985). Energetics and regulation of crossbridge states in mammalian smooth muscle. *Experientia*, *41*(8), 1020-1025.
- Slyter, H. S., & Lowey, S. (1967). Substructure of the myosin molecule as visualized by electron microscopy. *Proc Natl Acad Sci U S A*, *58*(4), 1611-1618.

- Sobieszek, A., Small, J. V. (1977). Regulation of the actin-myosin interaction in vertebrate smooth muscle: activation via a myosin light-chain kinase and the effect of tropomyosin. [In Vitro]. *J Mol Biol*, 112(4), 559-576.
- Sobue, K., Muramoto, Y., Fujita, M., & Kakiuchi, S. (1981). Purification of a calmodulin-binding protein from chicken gizzard that interacts with F-actin. *Proc Natl Acad Sci U S A*, 78(9), 5652-5655.
- Spudich, J. A., Kron, S. J., & Sheetz, M. P. (1985). Movement of myosin-coated beads on oriented filaments reconstituted from purified actin. *Nature*, 315(6020), 584-586.
- Stracher, A. (1969). Evidence for the involvement of light chains in the biological functioning of myosin. *Biochem Biophys Res Commun*, 35(4), 519-525.
- Straub, F. B., & Feuer, G. (1950). [Adenosine triphosphate, the functional group of actin]. *Kiserl Orvostud*, 2(2), 141-151.
- Takahashi, K., Hiwada, K., & Kokubu, T. (1986). Isolation and characterization of a 34,000-dalton calmodulin- and F-actin-binding protein from chicken gizzard smooth muscle. *Biochem Biophys Res Commun*, 141(1), 20-26.
- Takahashi, K., Hiwada, K., & Kokubu, T. (1987). Occurrence of anti-gizzard P34K antibody cross-reactive components in bovine smooth muscles and non-smooth muscle tissues. *Life Sci*, 41(3), 291-296.

- Takahashi, K., Mori, T., Nakamura, H., & Tonomura, Y. (1965). ATP-induced contraction of sarcomeres. *J Biochem*, *57*(5), 637-649.
- Tonomura, Y., Nakamura, H., Kinoshita, N., Onishi, H., & Shigekawa, M. (1969). The pre-steady state of the myosin-adenosine triphosphate system. X. The reaction mechanism of the myosin-ATP system and a molecular mechanism of muscle contraction. *J Biochem*, *66*(5), 599-618.
- Trotta, P. P., Dreizen, P., & Stracher, A. (1968). Studies on subfragment-I, a biologically active fragment of myosin. *Proc Natl Acad Sci U S A*, *61*(2), 659-666.
- Tsao, T. C. (1953). Fragmentation of the myosin molecule. *Biochim Biophys Acta*, *11*(3), 368-382.
- Varga, L. (1946). The relation of temperature and muscular contraction. *Hung Acta Physiol*, *1*(1), 1-8.
- Veigel, C., Molloy, J. E., Schmitz, S., & Kendrick-Jones, J. (2003). Load-dependent kinetics of force production by smooth muscle myosin measured with optical tweezers. *Nat Cell Biol*, *5*(11), 980-986.
- Walcott, S., Warshaw, D. M., & Debold, E. P. (2012). Mechanical coupling between myosin molecules causes differences between ensemble and single-molecule measurements. *Biophys J*, *103*(3), 501-510.

- Warshaw, D. M., Desrosiers, J. M., Work, S. S., & Trybus, K. M. (1990). Smooth muscle myosin cross-bridge interactions modulate actin filament sliding velocity in vitro. *J Cell Biol*, *111*(2), 453-463.
- Weber, A. (1959). On the role of calcium in the activity of adenosine 5'-triphosphate hydrolysis by actomyosin. *J Biol Chem*, *234*, 2764-2769.
- Wever, A., & Bremel, R. D. (1973). Does ATP cause relaxation by binding to actin or its regulatory proteins? *Biochim Biophys Acta*, *325*(2), 333-335.
- Winder, S. J., Sutherland, C., & Walsh, M. P. (1992). A comparison of the effects of calponin on smooth and skeletal muscle actomyosin systems in the presence and absence of caldesmon. *Biochem J*, *288* (Pt 3), 733-739.
- Winder, S. J., & Walsh, M. P. (1990). Smooth muscle calponin. Inhibition of actomyosin MgATPase and regulation by phosphorylation. *J Biol Chem*, *265*(17), 10148-10155.
- Yanagida, T., Nakase, M., Nishiyama, K., & Oosawa, F. (1984). Direct observation of motion of single F-actin filaments in the presence of myosin. *Nature*, *307*(5946), 58-60.
- Zhang, J., Herrera, A. M., Pare, P. D., & Seow, C. Y. (2010). Dense-body aggregates as plastic structures supporting tension in smooth muscle cells. *Am J Physiol Lung Cell Mol Physiol*, *299*(5), L631-638.

Zot, H. G., & Potter, J. D. (1982). A structural role for the Ca^{2+} - Mg^{2+} sites on troponin C in the regulation of muscle contraction. Preparation and properties of troponin C depleted myofibrils. *J Biol Chem*, 257(13), 7678-7683.

CHAPTER 2

UNPHOSPHORYLATED CALPONIN ENHANCES THE BINDING FORCE OF UNPHOSPHORYLATED MYOSIN TO ACTIN

Horia N. Roman, Nedjma B. Zitouni, Linda Kachmar, Gijs IJpma, Lennart Hilbert,
Oleg Matusovsky, Andrea Benedetti, Apolinary Sobieszek,

Anne-Marie Lauzon.

Article published in: *Biochimica et Biophysica Acta (BBA) General Subjects*. 2013 Oct;
1830(10):4634-41.

doi: 10.1016/j.bbagen.2013.05.042.

CHAPTER 2

2.1. PREFACE

The prevalent theory of the latch-state suggests that the force maintenance at low energy consumption is due to the dephosphorylation of myosin while attached to actin. This model rejects the possibility that dephosphorylated detached myosin could also reattach to actin and maintain force. However, recent studies have suggested that unphosphorylated myosin does indeed bind to actin and that actin regulatory proteins may also play a role in force maintenance. In chapter 2, the role of calponin in the binding of unphosphorylated myosin to actin was determined. The laser trap assay was used to measure the average force of unbinding of myosin from actin in the absence and presence of calponin.

2.2. ABSTRACT

Smooth muscle has the distinctive ability to maintain force for long periods of time and at low energy costs. While it is generally agreed that this property, called the latch-state, is due to the dephosphorylation of myosin while attached to actin, dephosphorylated-detached myosin can also attach to actin and may contribute to force maintenance. Thus, we investigated the role of calponin in regulating and enhancing the binding force of unphosphorylated tonic muscle myosin to actin. To measure the effect of calponin on the binding of unphosphorylated myosin to actin, we used the laser trap assay to quantify the average force of unbinding (F_{unb}) in the absence and presence of calponin or phosphorylated calponin. F_{unb} from F-actin alone (0.12 ± 0.01 pN; mean \pm SE) was significantly increased in the presence of calponin (0.20 ± 0.02 pN). This enhancement was lost when calponin was phosphorylated (0.12 ± 0.01 pN). To further verify that this enhancement of F_{unb} was due to the cross-linking of actin to myosin by calponin, we repeated the measurements at high ionic strength. Indeed, the F_{unb} obtained at a [KCl] of 25 mM (0.21 ± 0.02 pN; mean \pm SE) was significantly decreased at a [KCl] of 150 mM, (0.13 ± 0.01 pN). This study provides direct molecular level-evidence that calponin enhances the binding force of unphosphorylated myosin to actin by cross-linking them and that this is reversed upon calponin phosphorylation. Thus, calponin might play an important role in the latch-state. This study suggests a new mechanism that likely contributes to the latch-state, a fundamental and important property of smooth muscle that remains unresolved.

2.3. INTRODUCTION

Tonic smooth muscle is well known to maintain force for long periods of time at low energy levels. It is generally agreed that this property of smooth muscle, called the latch-state, is due to the dephosphorylation of myosin molecules while attached to actin filaments (Dillon, Aksoy, Driska, & Murphy, 1981). However, evidence is accumulating to suggest that calponin, a 35 kDa (Mezgueldi, Fattoum, Derancourt, & Kassab, 1992) actin binding protein (Kolakowski, Makuch, Stepkowski, & Dabrowska, 1995; Takahashi, Hiwada, & Kokubu, 1986) may also play a role in smooth muscle force maintenance, presumably through its effects on unphosphorylated myosin (Malmqvist, Trybus, Yagi, Carmichael, & Fay, 1997; Szymanski, 2004; Szymanski & Tao, 1993).

Calponin has an inhibitory effect on the ATPase activity of smooth muscle myosin (Winder & Walsh, 1990) and on the velocity (v_{max}) of actin propulsion in the in vitro motility assay (Haeberle, 1994; Kolakowski, et al., 1995). However, differently from caldesmon, the inhibitory effect of calponin is more of an all-or-none mechanism (Shirinsky, Biryukov, Hettasch, & Sellers, 1992), i.e. the filaments are either moving or they are stopped. At the cellular level, it has also been shown that calponin is necessary to inhibit the slow cycling of unphosphorylated myosin, stopping the shortening and force production of resting smooth muscle (Malmqvist, et al., 1997). The inhibitory action of calponin on the actomyosin ATPase rate is due to its binding to actin which can be suppressed by calponin phosphorylation (Winder & Walsh, 1990). However, calponin also binds to unphosphorylated myosin (Szymanski & Tao, 1993) so it presumably cross-links unphosphorylated myosin to actin. This interaction between calponin and

unphosphorylated myosin is dependent on ionic strength and it gets weaker at high [NaCl] (Szymanski & Tao, 1993).

We previously demonstrated, at the single molecule level, that unphosphorylated myosin purified from both tonic and phasic smooth muscles can bind to unregulated actin filaments with a binding force of approximately $1/10^{\text{th}}$ of the force generated by phosphorylated myosin (Leguillette, Zitouni, Govindaraju, Fong, & Lauzon, 2008). Unphosphorylated, and presumably dephosphorylated detached myosin, could therefore participate in force maintenance during the latch state. The actin regulatory proteins could possibly potentiate this binding force. Thus, in the current study, we investigated the role of calponin in the enhancement of this binding force as well as its regulation by phosphorylation.

2.4. MATERIALS AND METHODS

2.4.1. Proteins

Myosin was purified from pig stomach fundus following a previously published protocol (Sobieszek, 1994). For the protocols requiring myosin activation, myosin was thiophosphorylated (Trybus & Lowey, 1984). Actin was purified using the chicken pectoralis acetone powder protocol (Pardee & Spudich, 1982) and fluorescently labeled by incubation with tetramethylrhodamine isothiocyanate (TRITC)-phalloidin (P1951, Sigma-Aldrich Canada) (Warshaw, Desrosiers, Work, & Trybus, 1990). Turkey gizzard calponin was purified as a by-product of caldesmon purification (Sobieszek, Sarg, Lindner, & Seow). For the protocols requiring calponin activation, calponin was phosphorylated using Ca^{2+} /calmodulin-dependent

protein kinase II and MgATP (1 mol of Pi/mol of calponin) (Winder & Walsh, 1990). After 10 min, Ca²⁺ chelation was performed by adding 10mM EGTA to avoid contamination of the next assays with Ca²⁺.

2.4.2. Buffers

Myosin buffer (300 mM KCl, 25 mM imidazole, 1 mM EGTA, 4 mM MgCl₂, and 30 mM DTT; pH adjusted to 7.4); Actin buffer (25 mM KCl, 25 mM imidazole, 1 mM EGTA, 4 mM MgCl₂, and 30 mM DTT, with an oxygen scavenger system consisting of 0.25 mg/ml glucose oxidase, 0.045 mg/ml catalase, and 5.75 mg/ml glucose; pH adjusted to 7.4); Assay buffers: The in vitro motility assay buffer consisted of actin buffer to which methylcellulose (0.5%) was added, to favor binding of myosin to actin, and MgATP (2 mM). The laser trap assay buffer consisted of actin buffer to which methylcellulose (0.3%) and MgATP (200 μM) were added.

2.4.3. In vitro motility assay

The velocity (v_{max}) of actin filament propulsion by myosin was measured in the in vitro motility assay as previously described (Leguillette, et al., 2008) with minor changes. Briefly, a flow-through chamber (20 μl) was constructed from a nitrocellulose-coated coverslip and a glass microscope slide (Warshaw, et al., 1990). Non-functional myosin molecules were removed by ultracentrifugation (Optima ultracentrifuge L-90K and 42.2 Ti rotor, Beckman Coulter, Fullerton, CA) of myosin (500 μg/ml) with equimolar filamentous actin and 1 mM MgATP in myosin buffer. Myosin was then perfused in the flow through chamber at a concentration of 125 μg/ml and allowed to randomly attach to the nitrocellulose for 2 min. The following solutions were then

perfused sequentially in the flow through chamber (all in actin buffer): BSA (0.5 mg/ml), unlabeled G-actin (1.33 μ M) to bind to any remaining non-functional myosin and followed by MgATP (1 mM) to remove the unlabeled actin from the functional heads. Then two washes of actin buffer were followed by TRITC labeled actin (0.03 μ M), with or without calponin (0.3 μ M), incubated for 1 min, and finally, motility buffer. All molecular mechanics measurements were performed at 30°C. Motility was then assessed using an inverted microscope (IX70, Olympus, Melville, NY) equipped with a high numerical aperture objective (X100 magnification Ach 1.25 numerical aperture, Olympus, Melville, NY) and rhodamine epifluorescence. An image intensified video camera (KP-E500 CCD Camera, Hitachi Kokusai Electric, Woodbury, NY, 720 x 480 resolution, 68.6 μ m x 45.7 μ m real frame size, 29.94 frame/s, 8 bit grayscale) was used to visualize and record the actin filament movement on computer (Custom Built by Norbec Communication, Montreal, QC) using a frame grabber (Pinnacle Studio AV/DV V.9 PCI Card) and image capturing software (AMCap software V9.20) at 29.94 Hz. v_{max} was determined from the total path described by the filaments divided by the elapsed time using our automated version of the National Institutes of Health tracking software (NIH macro in Scion Image 4.02, Scion) coded in Matlab (R2009b). Only the filaments present for at least 20% of the recorded video time (~ 50 s) and describing a path of at least 3 μ m were considered. To calculate the percentage of stopped filaments, a threshold of 0.1 μ m/s was set below which, the filaments were considered immobile and moving only due to Brownian motion. This threshold was estimated by analyzing the frame-to-frame velocity of actin filaments in the absence of ATP (Homsher, Wang, & Sellers, 1992). Finally, filaments that were not moving continuously were eliminated from this analysis (Shirinsky, et al., 1992).

2.4.4. Laser trap assay

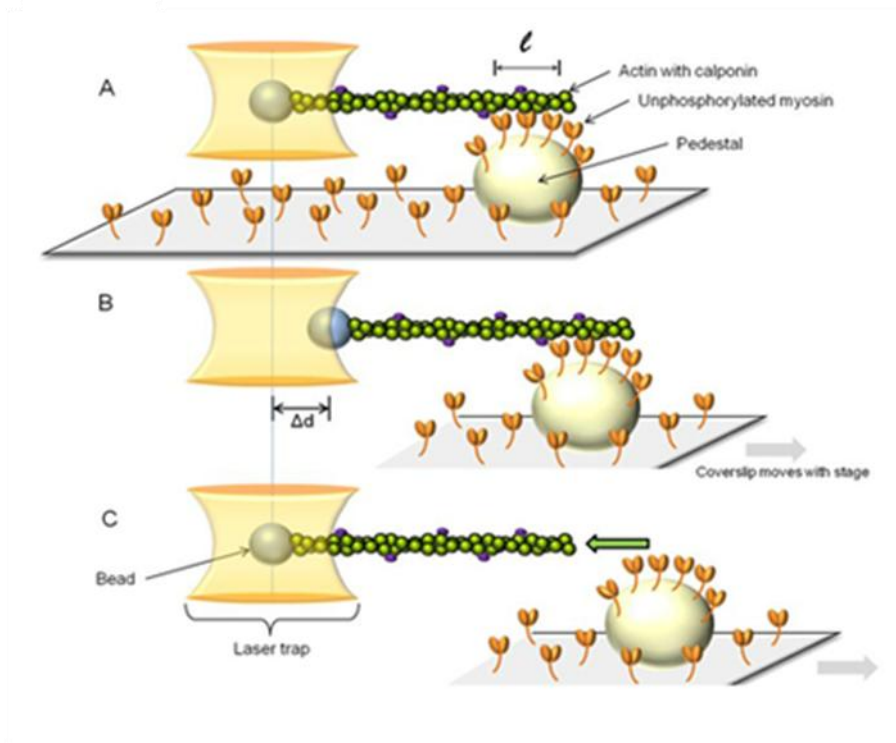


Fig. 2.1. A single beam laser trap assay. A polystyrene bead is used to capture a TRITC-labeled actin filament regulated by calponin. **A)** The regulated actin is brought in contact with unphosphorylated myosin that randomly coats a pedestal on a coverslip. ℓ : length of actin in contact with myosin. **B)** The pedestal/coverglass is then moved away from the laser trap at a constant and slow velocity, thereby dragging the trapped bead away from the trap center as a result of the attachment of unphosphorylated myosin to actin. **C)** When the force exerted by the trap on the bead is greater than the force of binding of unphosphorylated myosin to actin, the bead snaps back into the trap, its unloaded position. The unbinding force (F_{umb}) is then calculated as the maximal distance between the bead and the trap center ($\max \Delta d$) multiplied by the trap stiffness calculated by the Stokes force method. (See section 2.4.4. for details).

Our single beam laser trap assay was built around the Laser Tweezers Workstation (Cell Robotics, Albuquerque, NM) and the motility assay described above and was previously reported (Leguillette, et al., 2008). Briefly, pedestals were created by spraying 4.5 μm in diameter polystyrene microspheres (Polybead, Polysciences, Warrington, PA) on the coverslips before coating with nitrocellulose. 3 μm in diameter polystyrene microspheres (Polybead, Polysciences, Warrington, PA) coated by 30 min incubation at room temperature with N-ethylmaleimide-modified (NEM) skeletal myosin (Warshaw, et al., 1990) were used for trapping. The perfusion of proteins and solutions in the flow-through chamber followed the same sequence as for the motility assay except that the myosin was unphosphorylated and at a concentration of 16.7 $\mu\text{g}/\text{ml}$, TRITC-labeled actin was mixed with microspheres (13×10^3 microspheres/ μl) in a laser trap assay buffer, and there were no unlabeled G-actin and MgATP steps. A diode pumped Nd:YAG solid-state laser (TEM_{00} , 1.5 W, 1064 nm) was used to create the trap. To perform the assay, a microsphere visualized in bright field by a charge coupled device (CCD) camera (XC-75, Sony Corporation of America, New York, NY) was captured in the laser trap, and its position was recorded on computer as described above. An actin filament, visualized by fluorescence imaging (described above for the motility assay) was attached to the microsphere and brought in contact with unphosphorylated myosin molecules randomly adhered to a pedestal (Fig. 2.1. A). Contact between myosin and actin was allowed for approximately 10s. During that time, the microsphere baseline position in the trap was recorded. The pedestal was then displaced from the trap by moving the microscope stage at a slow and constant velocity of 0.5 $\mu\text{m}/\text{s}$. The microsphere initially followed the pedestal (Fig. 2.1. B) until the force exerted on it by the trap became greater than that exerted by the myosin molecules on the actin filament. At this point, the microsphere sprang back to its unloaded baseline position in the center of the trap (Fig. 2.1. C).

The total unbinding force ($Total F_{unb}$) of the myosin molecules was calculated as follows:

$$Total F_{unb} = k * \Delta d \quad (1)$$

where k is the trap stiffness and Δd is the maximal displacement of the trapped microsphere from its baseline position. k was calibrated using the Stokes force (F_f) approach, as previously reported (Leguillette, et al., 2008).

Briefly, a viscous drag was applied to a trapped microsphere by moving it at a constant velocity (v) in 0.3% methylcellulose while measurements of Δd were performed. According to Stokes' law, the frictional force exerted on spherical objects with very small Reynolds numbers is calculated as follows:

$$F_f = 6 \pi \eta r v \quad (2)$$

where η is the dynamic viscosity and r is the microsphere radius. The viscosity of 0.3% methylcellulose was measured with a viscometer (DV-I at 60 rpm, Brookfield, Middleboro, MA), using a UL (ultra low viscosity) adapter and was equal to 10.4 cP, at 30°C. Thus,

$$k = F_f / \Delta d \quad (3)$$

The value of k (0.013 pN/nm, $R^2=0.95$) was averaged from several measurements performed at different velocities and then used to perform the force measurements (see example of trap calibration in figure 3 from (Leguillette, et al., 2008)).

The average binding force per myosin head (F_{unb}) was obtained as follows: first, we measured the length of actin filament in contact with the pedestal (ℓ , Fig.2.1. A) by fluorescence imaging. That is, the portion of the pedestal where the actin filament was bound, was brought in

focus and the bound actin filament length (ℓ) was measured using the National Institutes of Health analysis software (NIH macro in Scion Image 4.02, Scion). Unbound actin was readily detected because it moved in and out of focus due to Brownian motion, so it was discarded from the length measurements. We then used the estimates of the number of active myosin heads on the motility surface previously obtained by Warshaw and co-workers (Harris & Warshaw, 1993; VanBuren, Work, & Warshaw, 1994) by performing $\text{NH}_4\text{-EDTA}$ ATPase assays directly on the cover slip. (Note that similar results have also been obtained by two other groups (Kishino & Yanagida, 1988; Uyeda, Kron, & Spudich, 1990). The density of active myosin heads was obtained by dividing this number by the surface area. The number of active myosin head per actin filament length was calculated by assuming that all myosins could interact with actin within a 26 nm wide band (Harris & Warshaw, 1993; Kishino & Yanagida, 1988; Uyeda, et al., 1990). For example, at a concentration of myosin of 20 $\mu\text{g/ml}$, a value of 26 heads/ μm of actin filament was estimated (Harris & Warshaw, 1993).

2.4.5. Microsphere displacement analysis software

Bead motion tracking was performed in Matlab using optimal fitting of a reference image. In short, in the first frame of the acquired video (720x480 resolution, 68.6 x 40.3 μm real frame size, 29.94 frame/s, 8 bit grayscale), the largest area of connected area pixels with a gray value above 90% of the highest pixel value in the image was identified (Fig. 2.2. A). A 60x60 pixel section of the frame, centered on the center of mass of the area of connected pixels, was defined as the reference image (Fig. 2.2. B). While this center of mass was not necessarily the center of mass of the bead, it was visually confirmed that the entire bead was always fully contained in the reference image. In each subsequent frame the reference image was matched to a section of the

frame of the same size by finding the location at which the summed absolute difference in pixel gray values (δz) between the current frame and the reference image was minimized (sample of

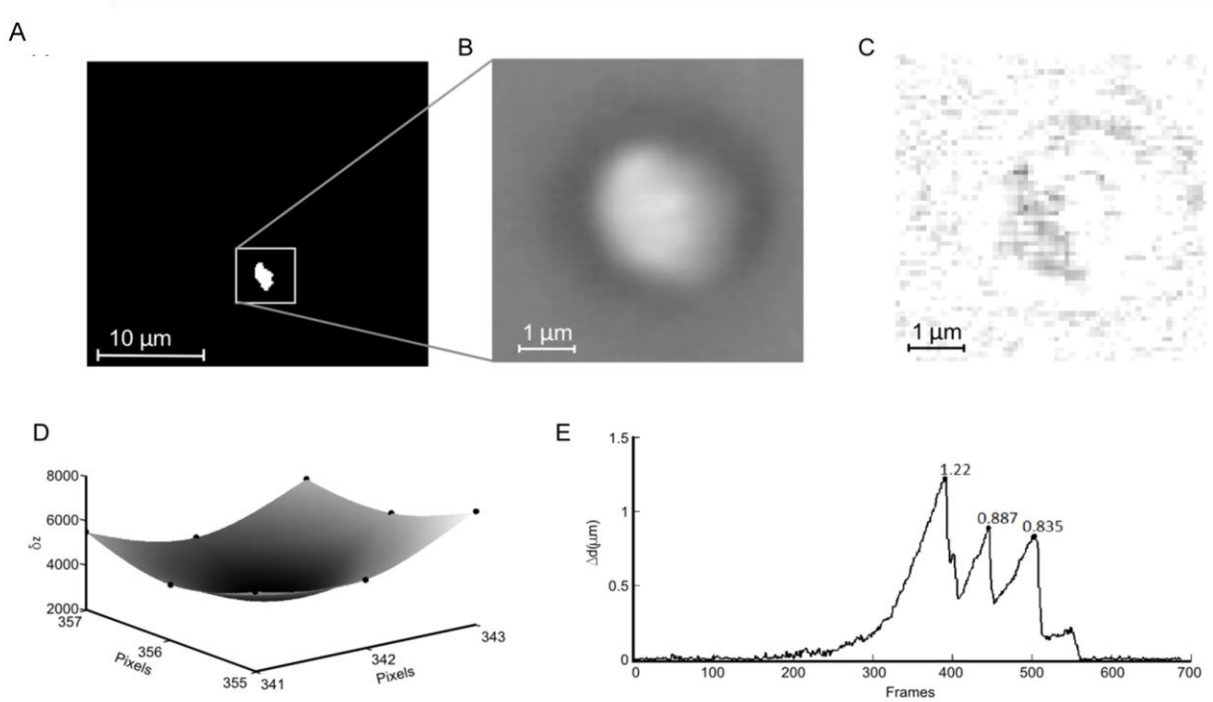


Fig. 2.2. Video analysis for the calculation of microsphere displacement. (see section 2.5 for detailed description). **A)** A threshold map of the first video frame. The white box indicates the reference region. **B)** The reference image as found from A. **C)** Example of the absolute difference image in optimal location (differences amplified 10x, white equals no difference). **D)** The summed pixel value differences (δz) in 9 points centered around the found optimal location were mapped (black dots) and interpolated with a cubic interpolation algorithm to find subpixel resolution of the coordinates of the bead (x and y are coordinates, δz equals the summed pixel value difference). **E)** The resulting displacement plot with marked local maxima (which correspond to the detachment of myosin from actin). In this sample the baseline position was calculated as the mean position over the first 100 frames.

difference image in Fig. 2.2. C). To achieve sub pixel resolution of the bead position, the δz values at the found location and the surrounding 8 pixels were interpolated with a cubic interpolation algorithm (Matlab, Fig. 2.2. D) and the coordinates of the global minimum point on this interpolation surface were stored as the position of the bead.

After analysis of the entire video a frame range where no movement occurs was manually chosen to calculate a baseline location of the bead and distances were plotted relative to this baseline location (Fig. 2.2. E). The relevant local maxima, which correspond to the detachment of myosin from actin, were found by searching for maxima in user defined regions. From these maxima the associated total F_{umb} were calculated.

2.4.6. Western Blot analysis of purified calponin

The phosphorylation of calponin was assessed by Western blot analysis. Proteins were separated by SDS-PAGE using a 4-15% ready gradient gel (Bio-Rad, Hercules, CA). Protein concentration was estimated by a standard Bradford assay, and 1.7 μg of calponin and phosphorylated calponin was loaded in each well. Proteins were transferred electrophoretically onto PVDF membranes (Bio-Rad, Hercules, CA). Membranes were blocked with 5% non-fat milk and probed with (inset of Fig. 2.3.) the monoclonal Ab65827 antibody that recognizes calponin (Abcam Inc, Cambridge, MA) or with the rabbit polyclonal SC16717R antibody that recognizes phosphorylated calponin (Santa Cruz Inc., Santa Cruz, CA). Antibody detection was done by Super Signal West Dura substrate (ThermoFisher, Waltham, MA).

2.4.7. Co-sedimentation assay

To confirm the effect of unphosphorylated calponin on the cross-linking of unphosphorylated myosin to actin, a co-sedimentation assay was performed. The proteins and calponin phosphorylation protocol were described in section 2.4.1. Combinations of actin (6 μM), myosin (1 μM) and calponin (2 μM) (phos- or unphosphorylated) were incubated in actin buffer (see section 2.4.2) for 1 h at 26°C with continuous mixing at 400 RPM. The samples were then centrifuged at low speed (13,300 rpm) for 20 min, at 4°C in order to sediment the myosin and cross-linked actin and calponin. The supernatants and re-suspended pellets were then separated by SDS-PAGE using a 4-20% ready gradient gel (Bio-Rad, Hercules, CA) and visualized by Comassie blue.

2.4.8. Statistical analysis

Differences in v_{max} and F_{unb} between multiple conditions were tested using one way ANOVAs, with a Bonferroni correction. Differences in v_{max} and F_{unb} with only two conditions were tested using the Student's t-test. In cases when the test for equal variance failed, a Mann-Whitney U test was performed. A value of $P < 0.05$ was considered significant. The Systat Software Inc., (San Jose, CA) was used. For the motility assay, N represents the number of flow-through chambers studied. A minimum of three locations in each flow-through chamber was analyzed; each location contained at least 10 filaments. Thus, a minimum of 30 filaments were analyzed per chamber to make up an N of 1. For the laser trap assay, N represents the number of actin filaments analyzed.

2.5. RESULTS

2.5.1. Maximal velocity of actin propulsion

To ascertain that our actin filaments are regulated by physiological levels of calponin, we measured v_{max} when propelled by pig stomach fundus myosin in the in vitro motility assay. As expected from the literature (Haeberle, 1994; Marston, Fraser, Bing, & Roper, 1996), v_{max} for actin ($0.54 \pm 0.01 \mu\text{m/s}$; mean \pm SE)

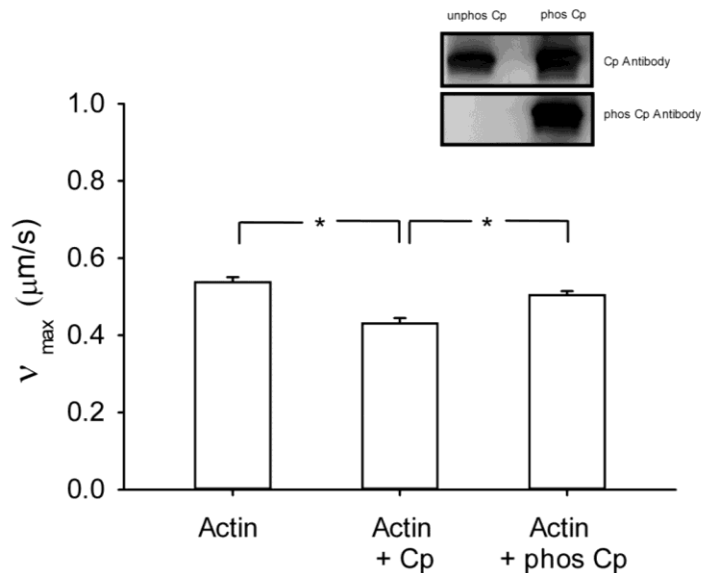


Fig. 2.3. Velocity of actin filaments. (v_{max}) when propelled by phosphorylated myosin as measured in the in vitro motility assay. The measurements were performed with naked actin ($N=4$) and in the presence of calponin ($N=6$) and phosphorylated calponin ($N=5$). Cp: calponin, phos Cp: phosphorylated calponin, and *: $p < 0.05$. Inset: Western blot analysis of calponin and phosphorylated calponin as assessed by probing with an antibody that recognizes top panel: calponin, and bottom panel: phosphorylated calponin.

was slightly but statistically significantly decreased in the presence of calponin ($0.43 \pm 0.01 \mu\text{m/s}$; $p < 0.001$), and this inhibitory effect was suppressed when calponin was phosphorylated ($0.50 \pm 0.01 \mu\text{m/s}$; $p = 0.04$), as shown in Fig. 2.3. The percentage of stopped filaments was also increased from 12.7 % for regular actin to 28.9 % in the presence of calponin and back to 12.5% in the presence of phosphorylated calponin. The phosphorylation of calponin was assessed by Western blot analysis as shown in the inset of Fig. 2.3.

2.5.2. Cross-linking of unphosphorylated myosin to actin

To verify if calponin alters the average binding force of unphosphorylated myosin to actin filaments, we measured F_{unb} using the laser trap assay. F_{unb} in the presence of actin only ($0.12 \pm 0.01 \text{ pN}$; mean \pm SE) was increased in the presence of calponin ($0.20 \pm 0.02 \text{ pN}$; $p = 0.009$). To investigate if this enhancement was due to the binding of calponin to actin, we repeated the F_{unb} measurements in the presence of phosphorylated calponin, i.e. detaching calponin from actin (Winder & Walsh, 1990). Indeed, this enhancement was lost when calponin was phosphorylated ($0.12 \pm 0.01 \text{ pN}$; $p = 0.006$), as shown in Fig. 2.4. A.

To confirm that calponin enhances F_{unb} by cross-linking unphosphorylated myosin to actin, we repeated the unbinding experiments at high ionic strength because the calponin-myosin interactions are known to be weak in such conditions in vitro. F_{unb} obtained at the regular [KCl] of 25mM ($0.21 \pm 0.02 \text{ pN}$; mean \pm SE) was significantly decreased at [KCl] of 150mM, ($0.13 \pm 0.01 \text{ pN}$; $p = 0.007$), as shown in Fig. 2.4. B. To control for the effect of high [KCl] on the F_{unb} measurements, we also measured F_{unb} at a [KCl] of 150mM but in the absence of calponin. The results were not significantly different from those obtained without calponin at a [KCl] of 25mM (Fig. 2.4. C).

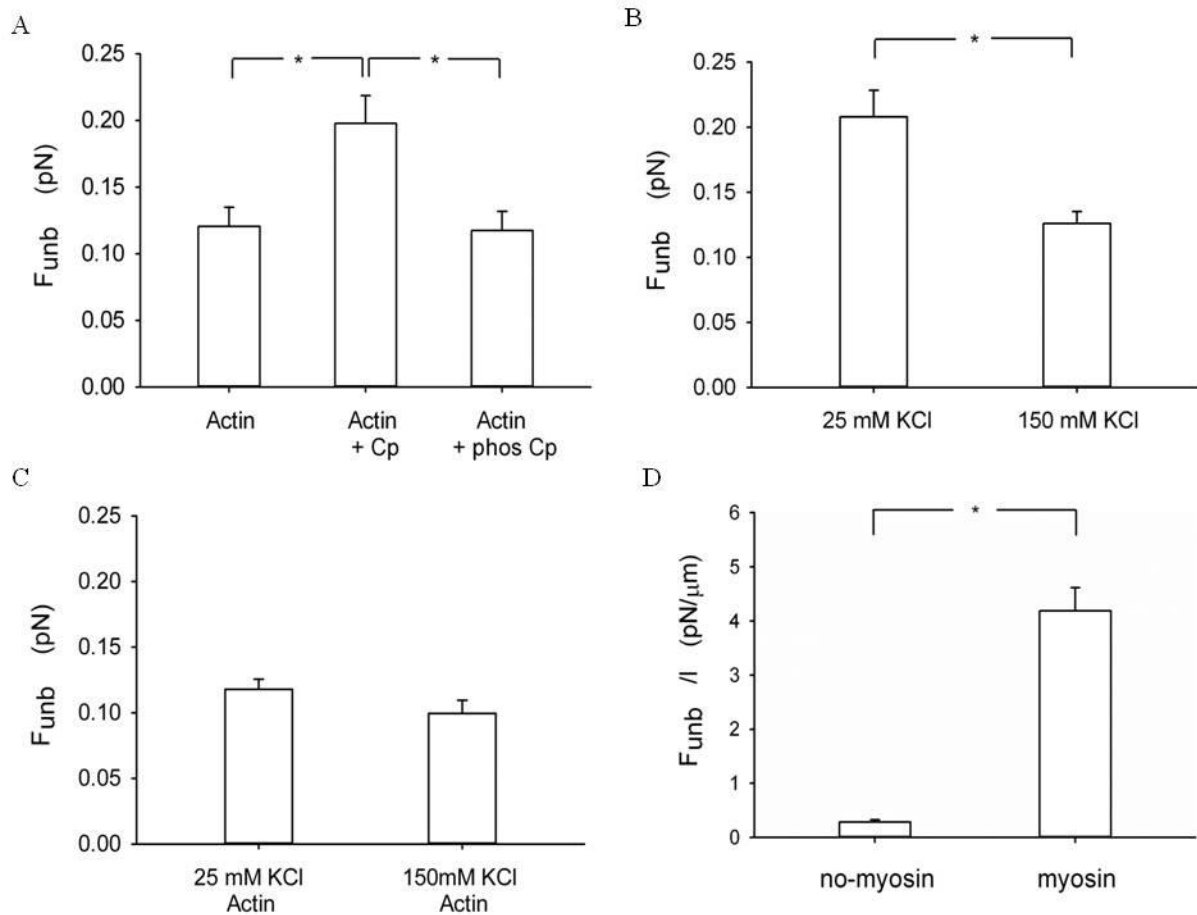


Fig. 2.4. Unbinding force (F_{unb}) of unphosphorylated myosin to actin.

F_{unb} was measured with the single beam laser trap assay. **A)** The measurements were performed with naked actin ($N=10$) and in the presence of calponin ($N=9$) and phosphorylated calponin ($N=10$). **B)** F_{unb} in the presence of calponin, at regular (25mM) and at high KCl (150mM); $N=11$ and 7, respectively. **C)** F_{unb} of unphosphorylated myosin to actin, in the absence of calponin, at regular (25mM) and at high KCl (150mM). $N= 17$ and 5, respectively.

F_{unb} is reported as the average force per myosin molecule (see section 2.4.4. for details).

D) Total unbinding force normalized per actin length (Total F_{unb}/l) in the absence ($N=12$) or presence ($N=12$) of unphosphorylated myosin but in the presence of calponin regulated actin.

*: $p < 0.05$.

2.5.3. Control measurements in the absence of myosin

To eliminate the possibility that calponin regulated actin was binding in an unspecific manner to the pedestal, the Total F_{umb} was also measured in the absence of myosin but in the presence of actin and calponin. The resulting force was normalized per length of actin in contact with the pedestal (Total F_{umb}/ℓ). In the absence of unphosphorylated myosin, a significantly smaller Total F_{umb}/ℓ (0.28 ± 0.04 pN/ μm ; mean \pm SE) was observed than in its presence (4.19 ± 0.42 pN/ μm ; $p < 0.001$), as shown in Fig. 2.4. D.

2.5.4. Co-sedimentation assay

As previously reported in the literature (Winder & Walsh, 1990), we confirmed that the phosphorylation of calponin by Ca^{2+} /calmodulin protein kinase II decreases its binding to actin, by performing a co-sedimentation assay in the presence of phosphorylated or unphosphorylated calponin. A low-speed centrifugation in actin buffer was used because under such conditions, actin and calponin are soluble but will pellet more when cross-linked together. Indeed, we found more calponin and actin in the supernatant (S) when the calponin was phosphorylated (Fig. 2.5. lanes 1 & 2) and more in the pellet (P) when calponin was unphosphorylated (Fig. 2.5. lanes 3 & 4). To then confirm the cross-linking of unphosphorylated myosin to actin by unphosphorylated calponin, a co-sedimentation assay was performed in the presence of phosphorylated or unphosphorylated calponin. The above centrifugation and buffer conditions were used again because they allow for myosin filaments to sediment whereas actin and calponin remain soluble. In the presence of phosphorylated calponin, less myosin-actin-calponin complex was found in the pellet (Fig. 2.5., lanes 5 & 6). (Note that the ATP used to phosphorylate the calponin made the myosin filaments more soluble so more myosin was also found in the supernatant than would

have been otherwise expected (Fig. 2.5. lane 5), as also observed in (Winder & Walsh, 1990)). To the contrary, in the presence of unphosphorylated calponin, more myosin-actin-calponin complex was found in the pellet (Fig. 2.5. lanes 7 & 8). These results demonstrate that the unphosphorylated calponin enhances the binding of unphosphorylated myosin to actin compared to phosphorylated calponin.

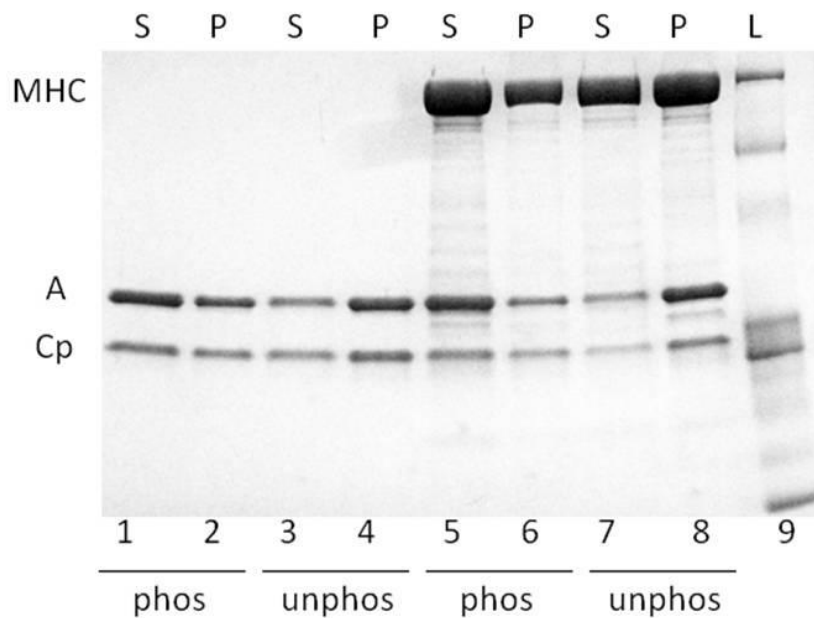


Fig. 2.5. Co-sedimentation assay. Results are shown after separation by SDS-PAGE. L: ladder, S: supernatant, P: pellet, MHC: myosin heavy chain, A: actin, Cp: calponin, phos: phosphorylated calponin, and unphos: unphosphorylated calponin.

2.6. DISCUSSION

In this study, we provided direct molecular level-evidence that calponin enhances the average force of binding of unphosphorylated myosin to actin and that this is reversed upon calponin phosphorylation. Furthermore, we showed that this enhancement in binding force is accomplished by the action of calponin cross-linking unphosphorylated myosin with actin. These findings suggest that calponin could be a key player in the force maintenance capacity of smooth muscle, known as the latch state.

Several studies have suggested a role for calponin in the binding of unphosphorylated myosin to actin (Malmqvist, et al., 1997; Szymanski, 2004; Szymanski & Tao, 1993). In a technically challenging study performed at the whole cell level, Malmqvist and co-workers (Malmqvist, et al., 1997) showed that when calponin is extracted from the smooth muscle cell and the myosin is exchanged for a non-phosphorylatable mutant, approximately 65% of the maximal cell force can still develop at approximately 30% of the maximal shortening velocity, following photolysis of caged ATP. Upon re-addition of calponin, the velocity and force development are prevented (Malmqvist, et al., 1997). Our results showed that this calponin-induced inhibition in movement and force production is not due to the lack of binding of unphosphorylated myosin to actin because, to the contrary, calponin enhances the binding. Thus, it is likely that calponin decreases the active cycling of the myosin heads (Haeberle, 1994; Marston, et al., 1996) promoting force maintenance. Indeed, Horiuchi and Chacko (Horiuchi, Samuel, & Chacko, 1991) reported that calponin inhibits the catalytic step in the actin-activated ATP hydrolysis. Furthermore, because calponin also binds to unphosphorylated myosin

(Szymanski & Tao, 1993), it most likely cross-links myosin to actin, thus explaining the enhancement of the binding force and the lack of cycling. We confirmed this possibility by measuring the F_{unb} at different ionic strengths because the binding of calponin to unphosphorylated myosin is known to be weak at high ionic strength (Szymanski & Tao, 1993). Indeed, we found that the calponin-induced enhancement of F_{unb} was lost at high [KCl]. These data support the concept that calponin cross-links unphosphorylated myosin to actin, thus enhancing their binding force and preventing active force generation.

One point worth noting is that the high [KCl] conditions in the in vitro motility and laser trap assays correspond to normal ionic strength conditions inside the cell. Indeed, these assays have always been performed at relatively low ionic strength. Several papers have reported best motility below 60 mM KCl and it is the standard procedure to perform molecular mechanics measurements at 25 mM KCl (Kron & Spudich, 1986; Kron, Toyoshima, Uyeda, & Spudich, 1991; Nagy, et al., 2013; Umemoto & Sellers, 1990; Wang, Ajtai, & Burghardt, 2013; Warshaw, et al., 1990). Whereas these conditions are not physiological, good quality molecular mechanics measurements are not possible otherwise. It is generally believed that the crowded cell environment provides conditions that are quite different from what can be obtained in the motility or laser trap assays, which leads to better protein binding conditions in vivo than in vitro. This has to be compensated for in vitro by working at lower ionic strengths. Nonetheless, the goal of working at high ionic strength was to change the conditions in such a way that calponin would detach from myosin in order to prove that this binding was indeed responsible for the increase in F_{unb} . Szymanski and Tao (Szymanski & Tao, 1993) demonstrated by a sedimentation assay that the calponin/myosin interaction was ionic strength dependent; they showed a strong

interaction at 50 mM NaCl which they said started to weaken at 100 mM NaCl and was abolished at 150 mM NaCl. Thus, using their approach in a molecular mechanics assay was the obvious procedure to follow. Because of such technical limitations, in vitro molecular mechanics studies cannot prove theories unequivocally but can suggest mechanisms that remain to be confirmed in vivo.

Calponin can be phosphorylated by protein kinase C and Ca^{2+} /calmodulin-dependant protein kinase II (Winder, Walsh, Vasulka, & Johnson, 1993). Furthermore, it has been shown from ATPase measurements that phosphorylation of calponin inhibits its binding to actin (Winder & Walsh, 1990). Thus, in the presence of phosphorylated calponin both phosphorylated or dephosphorylated myosin heads can cycle. Our data showed that upon phosphorylation of calponin, the binding force of unphosphorylated myosin to actin is reduced. Because calponin is likely to be phosphorylated during smooth muscle cell activation, it must detach from actin (Winder & Walsh, 1990) and not interfere with muscle shortening and force generation. Following calponin dephosphorylation, the binding of myosin to actin must be enhanced, due to their cross-linking by calponin, leading to force maintenance. The binding of unphosphorylated calponin to actin and the cross-linking of myosin to actin by unphosphorylated calponin were also demonstrated by our co-sedimentation results (Fig. 2.5.).

It is interesting to note that in intact tissue measurements, the phosphorylation of calponin has not been observed in the carotid artery (Adam, Haeberle, & Hathaway, 1995), a clearly tonic muscle, while it has been reported in the stomach and in airways (Pohl, et al., 1997; Winder,

Allen, et al., 1993). It is not clear why calponin would not be phosphorylated in the carotid artery but if as a general rule, calponin is less phosphorylated in the tonic than in the phasic muscles, it could certainly be a mechanism that contributes to the tonic muscle force maintenance. Furthermore, while the content of calponin is approximately the same in phasic and tonic smooth muscle, the effect of calponin is believed to be more prominent in tonic muscles because of the higher concentrations of caldesmon in phasic smooth muscle, and the fact that caldesmon and calponin compete for binding to actin (Szymanski, 2004).

Knocking-out calponin is an approach that has also been used to address its role in vivo (Babu, et al., 2006; Matthew, et al., 2000; Takahashi, et al., 2000). Although the results are not entirely clear due to concomitant alterations in α -actin and h-caldesmon expressions (Babu, et al., 2006; Matthew, et al., 2000), Takahashi and co-workers (Takahashi, et al., 2000) demonstrated that calponin inhibits shortening velocity during the tonic phase of contraction. They suggested that this was due to the direct regulation of the cross-bridge cycling rate, as can be seen in the in vitro motility assay (as we also reported in Fig. 2.3.). Our results suggest that in addition to the slowing effect of calponin on the phosphorylated and cycling cross-bridges, the decrease in shortening velocity may also be due to its enhancement of the binding force between dephosphorylated myosin and actin. Thus, instead of cycling, the dephosphorylated myosin molecules maintain the force that is actively generated by the few remaining phosphorylated myosin molecules.

We previously reported that the average binding force of unphosphorylated myosin to actin is approximately 10% of that generated by phosphorylated myosin (Lauzon, et al., 1998). This may seem low but our current data show that it is increased by approximately 40% in the presence of unphosphorylated calponin. In addition, the contribution of other actin regulatory proteins such as caldesmon and tropomyosin may also play a role in increasing this binding force further. However, it is also important to note that our measurements do not allow us to distinguish between stronger individual cross-bridges in the presence of calponin versus more cross-bridges of similar strength. This is why our data are reported in terms of average binding force per myosin molecule. The only way to distinguish between these two possibilities would be to perform molecular mechanics measurements on single myosin molecules in the presence of calponin, which is beyond the scope of the current study.

Another limitation of our study is that all experiments have been performed with unphosphorylated and not dephosphorylated myosin. Nonetheless, there are no data in the literature to suggest that dephosphorylated myosin is different from unphosphorylated myosin. However, if they were different structurally and functionally, we would have missed that effect. Because of the high sensitivity of our laser trap assay, if we were to work with dephosphorylated myosin, any remaining phosphorylated myosin heads would lead to overestimated force values.

Finally, although we believe that calponin plays an important role in force maintenance in the latch-state, it is not sufficient to explain the whole phenomenon. Instead we suggest that a combination of factors must be present to lead to force maintenance. For one, tonic muscle is

known to express a greater amount of the slower myosin heavy chain (Babij, 1993; White, Martin, & Periasamy, 1993). This myosin lacks the 7 amino acid insert found in the surface loop above the ATP binding pocket (Kelley, Takahashi, Yu, & Adelstein, 1993; White, et al., 1993) and thus is referred to as the (-)insert or SMA myosin isoform. Lacking the insert increases its time of attachment to actin (Lauzon, et al., 1998) by increasing its affinity for ADP (Fuglsang, Khromov, Torok, Somlyo, & Somlyo, 1993; Khromov, Somlyo, Trentham, Zimmermann, & Somlyo, 1995). The fact that the (-)insert isoform remains attached longer to actin presumably increases its chances of getting dephosphorylated while attached. This is likely to contribute to the greater propensity of tonic muscle to get into the latch state. Then, along with the few remaining phosphorylated cross-bridges that still generate active force, the attached and potentially reattaching dephosphorylated myosin molecules, cross-linked by calponin and most likely by other actin regulatory proteins, cooperate to lead to force maintenance. The fact that calponin does not appear to get phosphorylated in tonic muscle (Adam, et al., 1995) may also promote its cross-linking action.

2.7. CONCLUSION

In conclusion, the dephosphorylation of calponin provides a mechanism to enhance the binding of unphosphorylated myosin, and presumably dephosphorylated myosin, to actin. This enhanced binding is likely to contribute to the force maintenance observed in tonic smooth muscle.

2.8. ACKNOWLEDGEMENTS

We thank Professor John M. Dealy, from the department of Chemical Engineering, McGill University, for performing the methylcellulose viscosity measurements, Genevieve Bates for the art work of Fig. 2.1. and Michel Alveis from Marvid Poultry for the procurement of the chicken breasts for the purification of skeletal muscle actin and myosin for NEM preparation.

2.9. REFERENCES

- Adam, L. P., Haeberle, J. R., & Hathaway, D. R. (1995). Calponin is not phosphorylated during contractions of porcine carotid arteries. *Am J Physiol*, 268(4 Pt 1), C903-909.
- Babij, P. (1993). Tissue-specific and developmentally regulated alternative splicing of a visceral isoform of smooth muscle myosin heavy chain. *Nucleic Acids Res*, 21(6), 1467-1471.
- Babu, G. J., Celia, G., Rhee, A. Y., Yamamura, H., Takahashi, K., Brozovich, F. V., et al. (2006). Effects of h1-calponin ablation on the contractile properties of bladder versus vascular smooth muscle in mice lacking SM-B myosin. *J Physiol*, 577(Pt 3), 1033-1042.
- Dillon, P. F., Aksoy, M. O., Driska, S. P., & Murphy, R. A. (1981). Myosin phosphorylation and the cross-bridge cycle in arterial smooth muscle. *Science*, 211(4481), 495-497.
- Fuglsang, A., Khromov, A., Torok, K., Somlyo, A. V., & Somlyo, A. P. (1993). Flash photolysis studies of relaxation and cross-bridge detachment: higher sensitivity of tonic than phasic smooth muscle to MgADP. *J Muscle Res Cell Motil*, 14(6), 666-677.
- Haeberle, J. R. (1994). Calponin decreases the rate of cross-bridge cycling and increases maximum force production by smooth muscle myosin in an in vitro motility assay. *J Biol Chem*, 269(17), 12424-12431.

- Harris, D. E., & Warshaw, D. M. (1993). Smooth and skeletal muscle myosin both exhibit low duty cycles at zero load in vitro. *J Biol Chem*, 268(20), 14764-14768.
- Homsher, E., Wang, F., & Sellers, J. R. (1992). Factors affecting movement of F-actin filaments propelled by skeletal muscle heavy meromyosin. *Am J Physiol*, 262(3 Pt 1), C714-723.
- Horiuchi, K. Y., Samuel, M., & Chacko, S. (1991). Mechanism for the inhibition of acto-heavy meromyosin ATPase by the actin/calmodulin binding domain of caldesmon. *Biochemistry*, 30(3), 712-717.
- Kelley, C. A., Takahashi, M., Yu, J. H., & Adelstein, R. S. (1993). An insert of seven amino acids confers functional differences between smooth muscle myosins from the intestines and vasculature. *J Biol Chem*, 268(17), 12848-12854.
- Khromov, A., Somlyo, A. V., Trentham, D. R., Zimmermann, B., & Somlyo, A. P. (1995). The role of MgADP in force maintenance by dephosphorylated cross-bridges in smooth muscle: a flash photolysis study. *Biophys J*, 69(6), 2611-2622.
- Kishino, A., & Yanagida, T. (1988). Force measurements by micromanipulation of a single actin filament by glass needles. *Nature*, 334(6177), 74-76.
- Kolakowski, J., Makuch, R., Stepkowski, D., & Dabrowska, R. (1995). Interaction of calponin with actin and its functional implications. *Biochem J*, 306 199-204.

- Kron, S. J., & Spudich, J. A. (1986). Fluorescent actin filaments move on myosin fixed to a glass surface. *Proc Natl Acad Sci U S A*, 83(17), 6272-6276.
- Kron, S. J., Toyoshima, Y. Y., Uyeda, T. Q., & Spudich, J. A. (1991). Assays for actin sliding movement over myosin-coated surfaces. *Methods Enzymol*, 196, 399-416.
- Lauzon, A. M., Tyska, M. J., Rovner, A. S., Freyzo, Y., Warshaw, D. M., & Trybus, K. M. (1998). A 7-amino-acid insert in the heavy chain nucleotide binding loop alters the kinetics of smooth muscle myosin in the laser trap. *J Muscle Res Cell Motil*, 19(8), 825-837.
- Leguillette, R., Zitouni, N. B., Govindaraju, K., Fong, L. M., & Lauzon, A. M. (2008). Affinity for MgADP and force of unbinding from actin of myosin purified from tonic and phasic smooth muscle. *Am J Physiol Cell Physiol*, 295(3), C653-660.
- Malmqvist, U., Trybus, K. M., Yagi, S., Carmichael, J., & Fay, F. S. (1997). Slow cycling of unphosphorylated myosin is inhibited by calponin, thus keeping smooth muscle relaxed. *Proc Natl Acad Sci U S A*, 94(14), 7655-7660.
- Marston, S. B., Fraser, I. D., Bing, W., & Roper, G. (1996). A simple method for automatic tracking of actin filaments in the motility assay. *J Muscle Res Cell Motil*, 17(4), 497-506.

- Matthew, J. D., Khromov, A. S., McDuffie, M. J., Somlyo, A. V., Somlyo, A. P., Taniguchi, S., et al. (2000). Contractile properties and proteins of smooth muscles of a calponin knockout mouse. *J Physiol*, 529 Pt 3, 811-824.
- Mezgueldi, M., Fattoum, A., Derancourt, J., & Kassab, R. (1992). Mapping of the functional domains in the amino-terminal region of calponin. *J Biol Chem*, 267(22), 15943-15951.
- Nagy, A., Takagi, Y., Billington, N., Sun, S. A., Hong, D. K., Homsher, E., et al. (2013). Kinetic characterization of nonmuscle myosin IIb at the single molecule level. *J Biol Chem*, 288(1), 709-722.
- Pardee, J. D., & Spudich, J. A. (1982). Purification of muscle actin. *Methods Cell Biol*, 24, 271-289.
- Pohl, J., Winder, S. J., Allen, B. G., Walsh, M. P., Sellers, J. R., & Gerthoffer, W. T. (1997). Phosphorylation of calponin in airway smooth muscle. *Am J Physiol*, 272(1 Pt 1), L115-123.
- Shirinsky, V. P., Biryukov, K. G., Hettasch, J. M., & Sellers, J. R. (1992). Inhibition of the relative movement of actin and myosin by caldesmon and calponin. *J Biol Chem*, 267(22), 15886-15892.

- Sobieszek, A. (1994). Smooth muscle myosin. Molecule conformation, filament assembly and association of regulatory enzymes. In D. R. a. M. A. Giembycz (Ed.), *Airways smooth muscle: Biochemical Control of Contraction and Relaxation* (pp. 1-29). Bassel: Birkhauser.
- Sobieszek, A., Sarg, B., Lindner, H., & Seow, C. Y. Phosphorylation of caldesmon by myosin light chain kinase increases its binding affinity for phosphorylated myosin filaments. *Biol Chem*, 391(9), 1091-1104.
- Szymanski, P. T. (2004). Calponin (CaP) as a latch-bridge protein--a new concept in regulation of contractility in smooth muscles. *J Muscle Res Cell Motil*, 25(1), 7-19.
- Szymanski, P. T., & Tao, T. (1993). Interaction between calponin and smooth muscle myosin. *FEBS Lett*, 334(3), 379-382.
- Takahashi, K., Hiwada, K., & Kokubu, T. (1986). Isolation and characterization of a 34,000-dalton calmodulin- and F-actin-binding protein from chicken gizzard smooth muscle. *Biochem Biophys Res Commun*, 141(1), 20-26.
- Takahashi, K., Yoshimoto, R., Fuchibe, K., Fujishige, A., Mitsui-Saito, M., Hori, M., et al. (2000). Regulation of shortening velocity by calponin in intact contracting smooth muscles. *Biochem Biophys Res Commun*, 279(1), 150-157.

- Trybus, K. M., & Lowey, S. (1984). Conformational states of smooth muscle myosin. Effects of light chain phosphorylation and ionic strength. *J Biol Chem*, 259(13), 8564-8571.
- Umemoto, S., & Sellers, J. R. (1990). Characterization of in vitro motility assays using smooth muscle and cytoplasmic myosins. *J Biol Chem*, 265(25), 14864-14869.
- Uyeda, T. Q., Kron, S. J., & Spudich, J. A. (1990). Myosin step size. Estimation from slow sliding movement of actin over low densities of heavy meromyosin. *J Mol Biol*, 214(3), 699-710.
- VanBuren, P., Work, S. S., & Warshaw, D. M. (1994). Enhanced force generation by smooth muscle myosin in vitro. *Proc Natl Acad Sci U S A*, 91(1), 202-205.
- Wang, Y., Ajtai, K., & Burghardt, T. P. (2013). Qdot Labeled Actin Super-Resolution Motility Assay Measures Low Duty Cycle Muscle Myosin Step-Size. *Biochemistry*.
- Warshaw, D. M., Desrosiers, J. M., Work, S. S., & Trybus, K. M. (1990). Smooth muscle myosin cross-bridge interactions modulate actin filament sliding velocity in vitro. *J Cell Biol*, 111(2), 453-463.
- White, S., Martin, A. F., & Periasamy, M. (1993). Identification of a novel smooth muscle myosin heavy chain cDNA: isoform diversity in the S1 head region. *Am J Physiol*, 264(5 Pt 1), C1252-1258.

Winder, S. J., Allen, B. G., Fraser, E. D., Kang, H. M., Kargacin, G. J., & Walsh, M. P. (1993).
Calponin phosphorylation in vitro and in intact muscle. *Biochem J*, 296 (Pt 3), 827-836.

Winder, S. J., & Walsh, M. P. (1990). Smooth muscle calponin. Inhibition of actomyosin
MgATPase and regulation by phosphorylation. *J Biol Chem*, 265(17), 10148-10155.

Winder, S. J., Walsh, M. P., Vasulka, C., & Johnson, J. D. (1993). Calponin-calmodulin
interaction: properties and effects on smooth and skeletal muscle actin binding and
actomyosin ATPases. *Biochemistry*, 32(48), 13327-13333.

CHAPTER 3

THE ROLE OF CALDESMON AND ITS PHOSPHORYLATION BY ERK ON THE BINDING FORCE OF UNPHOSPHORYLATED MYOSIN TO ACTIN

CHAPTER 3

3.1. PREFACE

In chapter 2, the binding force of unphosphorylated myosin to actin was shown to increase in the presence of unphosphorylated calponin, demonstrating that the actin regulatory proteins may indeed contribute to the latch-state. Furthermore, the phosphorylation of calponin by Ca^{2+} -calmodulin dependant protein kinase II was shown to regulate this action. In chapter 3, the influence of another actin regulatory protein present in smooth muscle, caldesmon, was studied, as well as its interaction with tropomyosin. The laser trap assay was again used to measure the average force of unbinding of myosin from actin in the absence and presence of caldesmon. The effect of the regulation of caldesmon by ERK phosphorylation on the binding force of unphosphorylated myosin to actin was also studied.

3.2. ABSTRACT

Studies conducted at the whole muscle level have previously shown that smooth muscle can maintain tension with low ATP consumption. Whereas it is generally accepted that this property, called the latch-state, is a consequence of the dephosphorylation of myosin during its attachment to actin, detached dephosphorylated myosin can also bind to actin and contribute to force maintenance. In this study we investigated the role of caldesmon in regulating the binding force of unphosphorylated tonic smooth muscle myosin to actin. To measure the effect of caldesmon on the binding of unphosphorylated myosin to actin, we used a single beam laser trap assay to quantify the average unbinding force (F_{unb}) in the absence or presence of caldesmon, ERK phosphorylated caldesmon, or caldesmon plus tropomyosin. F_{unb} from unregulated actin (0.09 ± 0.01 pN) was significantly increased in the presence of caldesmon (0.17 ± 0.02 pN), tropomyosin (0.17 ± 0.02 pN) or both regulatory proteins (0.18 ± 0.02 pN). ERK phosphorylation of caldesmon significantly reduced the F_{unb} (0.06 ± 0.01 pN). Inspection of the traces of the F_{unb} as a function of time suggests that ERK phosphorylation of caldesmon either prevents the binding of myosin to actin or accelerates its detachment. Caldesmon enhances the binding force of unphosphorylated myosin to actin potentially contributing to the latch-state. ERK phosphorylation of caldesmon decreases this binding force to very low levels, thus suggesting a mechanism for muscle relaxation from the latch-state. This study suggests a role for caldesmon in the latch-state and in smooth muscle relaxation.

3.3. INTRODUCTION

Tonic smooth muscle exhibits the unique ability of maintaining force for long periods of time, with low energy consumption. A formal description of this property was elaborated by Dillon and coworkers in 1981 in which they termed this state of force maintenance the latch-state (Dillon, Aksoy, Driska, & Murphy, 1981). They suggested that the deactivation (dephosphorylation) of attached cross-bridges transforms them into non or slowly cycling latch-bridges, capable of maintaining force. Hai and Murphy (Hai & Murphy, 1988) subsequently adapted Huxley's model (Huxley, 1957) of cross-bridge cycling to include the regulation of shortening velocity by myosin light chain phosphorylation and the latch-state. One assumption of this model was that myosin must first be phosphorylated in order to attach to actin (Hai & Murphy, 1988). However, we and others have shown that unphosphorylated myosin can bind to actin (Haeberle, 1999; Leguillette, Zitouni, Govindaraju, Fong, & Lauzon, 2008; Roman, et al., 2013; Warshaw, Desrosiers, Work, & Trybus, 1990) and while it may not be actively cycling, it likely contributes to force maintenance.

In their initial description of the latch-state, Murphy and co-workers implied that phosphorylation and dephosphorylation of the myosin light chain was the only regulatory mechanism needed for smooth muscle myosin function (Dillon, et al., 1981; Hai & Murphy, 1988). However, several studies since then have suggested a role for the actin regulatory proteins in the latch-state (Hai & Kim, 2005; Hemric & Chalovich, 1988; Horiuchi & Chacko, 1995; Sobieszek, Sarg, Lindner, & Seow, 2010; Sutherland & Walsh, 1989). In particular, caldesmon

is known to have both actin and myosin binding sites (Huang, Li, Guo, & Wang, 2003; Morgan & Gangopadhyay, 2001) and could potentially act as a cross-linker and contribute to force maintenance. Its binding to actin and myosin is also regulated by various phosphorylation mechanisms (Huang, et al., 2003; Ngai & Walsh, 1984; Sobieszek, et al., 2010) allowing fine tuning of its function at various steps of the cross-bridge cycle.

The structure and function of caldesmon have been reviewed before (Morgan & Gangopadhyay, 2001; C. L. Wang, 2008). Briefly, the carboxyl terminus of caldesmon is responsible for its binding to actin whereas the amino-terminus binds to myosin (Morgan & Gangopadhyay, 2001; C. L. Wang, 2008). Caldesmon inhibits the actin activated myosin ATPase activity (Ngai & Walsh, 1984, 1987). This inhibition is also known to be amplified by tropomyosin (Dabrowska, Goch, Galazkiewicz, & Osinska, 1985; Horiuchi, Miyata, & Chacko, 1986; Sobue, Takahashi, & Wakabayashi, 1985). Caldesmon also decreases the velocity of actin propulsion in the in vitro motility assay (Okagaki, Higashi-Fujime, Ishikawa, Takano-Ohmuro, & Kohama, 1991; Shirinsky, Biryukov, Hettasch, & Sellers, 1992) and this inhibition is again facilitated by tropomyosin (Fraser & Marston, 1995; Shirinsky, et al., 1992). Caldesmon can be phosphorylated at several sites but each of their functions has yet to be identified (Fraser & Marston, 1995; Hedges, et al., 2000; Huang, et al., 2003; Morgan & Gangopadhyay, 2001; Shirinsky, et al., 1992; Sobieszek, et al., 2010). Phosphorylation by calmodulin dependant protein kinase II (PK2) in the amino-terminal region weakens the binding of caldesmon to myosin (Hemric, Lu, Shrager, Carey, & Chalovich, 1993) whereas phosphorylation in the carboxyl terminus by myosin light chain kinase (MLCK) increases its binding affinity for phosphorylated myosin filaments (Sobieszek, et al., 2010). Extracellular signal-regulated kinase

(ERK) phosphorylation of caldesmon, however, has been shown to remove the inhibition of movement in the in vitro motility assay (Gerthoffer, et al., 1996). ERK is also known to co-localize with caldesmon during contraction (Khalil, Menice, Wang, & Morgan, 1995).

At the whole muscle level, the role of caldesmon in smooth muscle relaxation has been studied by exogenous addition to permeabilized fibers (Albrecht, Schneider, Liebetrau, Ruegg, & Pfitzer, 1997) or more recently by studying muscle strips from caldesmon knockout mice (Guo, et al., 2013). Both studies reported that caldesmon accelerates the rate of smooth muscle relaxation and suggested that this is accomplished by inhibiting the cooperative reattachment of dephosphorylated myosin (Albrecht, et al., 1997; Guo, et al., 2013). In the current study, we investigated at the molecular level, the role of caldesmon in the binding of unphosphorylated myosin to actin. We report that caldesmon enhances the force of binding of unphosphorylated myosin to actin. Furthermore, this force of binding decreases to very low levels upon ERK phosphorylation of caldesmon, thus promoting relaxation.

3.4. MATERIALS AND METHODS

3.4.1. Proteins

Myosin was purified from pig stomach fundus (Sobieszek, 1994). For the protocols requiring myosin activation, myosin was thiophosphorylated (Trybus & Lowey, 1984). Actin was purified using the chicken pectoralis acetone powder protocol (Pardee & Spudich, 1982) and fluorescently labeled by incubation with tetramethylrhodamine isothiocyanate (TRITC)-

phalloidin (P1951, Sigma-Aldrich Canada) (Warshaw, Desrosiers, Work, & Trybus, 1990). Caldesmon was purified from pig stomach (Sobieszek, et al., 2010). For the protocols requiring caldesmon activation, caldesmon was phosphorylated according to Hedges and coworkers (Hedges, et al., 2000) with slight modifications. Briefly, caldesmon (0.1 mg/ml) was phosphorylated by active ERK (32.6 µg/ml; MAP kinase 2, active, phosphorylated by MEK1; Millipore Billerica, MA) in a buffer containing 25mM Tris, 10 mM magnesium acetate, 0.1 mM EGTA, 1mM DTT, pH 7.5), followed by a 60 min incubation at 30°C. Tropomyosin was purified from chicken gizzard (Sobieszek & Small, 1977).

3.4.2. Buffers

Myosin buffer (300 mM KCl, 25 mM imidazole, 1 mM EGTA, 4 mM MgCl₂, and 30 mM DTT; pH adjusted to 7.4); Actin buffer (25 mM KCl, 25 mM imidazole, 1 mM EGTA, 4 mM MgCl₂, and 30 mM DTT, with an oxygen scavenger system consisting of 0.25 mg/ml glucose oxidase, 0.045 mg/ml catalase, and 5.75 mg/ml glucose; pH adjusted to 7.4); Assay buffers: The in vitro motility assay buffer consisted of actin buffer to which methylcellulose (0.5%) was added, to favor binding of myosin to actin, and MgATP (2 mM). The laser trap assay buffer consisted of actin buffer to which methylcellulose (0.3%) and MgATP (200 µM) were added.

3.4.3. In vitro motility assay

The velocity (v_{max}) of actin filament propulsion by myosin was measured in the in vitro motility assay as previously described (Leguillette, Zitouni, Govindaraju, Fong, & Lauzon, 2008) with minor changes. Briefly, a flow-through chamber (20 µl) was constructed from a

nitrocellulose-coated coverslip and a glass microscope slide (Warshaw, et al., 1990). Non-functional myosin molecules were removed by ultracentrifugation (Optima ultracentrifuge L-90K and 42.2 Ti rotor, Beckman Coulter, Fullerton, CA) of myosin (500 $\mu\text{g/ml}$) with equimolar filamentous actin and 1 mM MgATP in myosin buffer. Myosin was then perfused in the flow through chamber at a concentration of 125 $\mu\text{g/ml}$ and allowed to randomly attach to the nitrocellulose for 2 min. The following solutions were then perfused sequentially in the flow through chamber (all in actin buffer): BSA (0.5 mg/ml), unlabeled G-actin (1.33 μM) to bind to any remaining non-functional myosin, followed by MgATP (1 mM) to remove the unlabeled actin from the functional heads. Then two washes of actin buffer were followed by TRITC labeled actin (30 nM), with or without caldesmon (10-500 nM), or tropomyosin (10-50 nM) or both, incubated for 1 min, and finally, assay buffer (for motility). All molecular mechanics measurements were performed at 30°C. Motility was then assessed using an inverted microscope (IX70, Olympus, Melville, NY) equipped with a high numerical aperture objective (X100 magnification Ach 1.25 numerical aperture, Olympus, Melville, NY) and rhodamine epifluorescence. An image intensified video camera (KP-E500 CCD Camera, Hitachi Kokusai Electric, Woodbury, NY, 720 x 480 resolution, 68.6 μm x 45.7 μm real frame size, 29.94 frame/s, 8 bit grayscale) was used to visualize and record the actin filament movement on computer (Custom Built by Norbec Communication, Montreal, QC) using a frame grabber (Pinnacle Studio AV/DV V.9 PCI Card) and image capturing software (AMCap software V9.20) at 29.94 Hz. v_{max} was determined from the total path described by the filaments divided by the elapsed time using our automated version of the National Institutes of Health tracking software (NIH macro in Scion Image 4.02, Scion) coded in Matlab (R2009b). Only filaments present for at least 20% of the recorded video time (~ 50 s) and describing a path of at least 3 μm were considered.

3.4.4. Laser trap assay

Our single beam laser trap assay was built around the Laser Tweezers Workstation (Cell Robotics, Albuquerque, NM) and the motility assay described above and was previously described (Leguillette, et al., 2008; Roman, et al., 2013). Briefly, pedestals were created by spraying 4.5 μm in diameter polystyrene microspheres (Polybead, Polysciences, Warrington, PA) on the coverslips before coating with nitrocellulose. 3 μm in diameter polystyrene microspheres (Polybead, Poly-sciences, Warrington, PA) coated by 30 min incubation at room temperature with N-ethylmaleimide-modified (NEM) skeletal myosin (Warshaw, et al., 1990) were used for trapping. The perfusion of proteins and solutions in the flow-through chamber followed the same sequence as for the motility assay except that the myosin was unphosphorylated and at a concentration of 16.7 $\mu\text{g/ml}$, TRITC-labeled actin (with and without caldesmon and/or tropomyosin) was mixed with microspheres (13×10^3 microspheres/ μl) in laser trap assay buffer, and there were no unlabeled G-actin and MgATP steps. A diode pumped Nd:YAG solid-state laser (TEM₀₀, 1.5 W, 1064nm) was used to create the trap. To perform the assay, a microsphere visualized in bright field by a charge coupled device (CCD) camera (XC-75, Sony Corporation of America, New York, NY) was captured in the laser trap, and its position was recorded on computer as described above. An actin filament (with or without the actin regulatory proteins), visualized by fluorescence imaging (described above for the motility assay) was attached to the microsphere and brought in contact with unphosphorylated myosin molecules randomly adhered to a pedestal. Contact between myosin and actin was allowed for approximately 10s. During that time, the microsphere baseline position in the trap was recorded. The pedestal was then displaced from the trap by moving the microscope stage at a slow and constant velocity of 0.5 $\mu\text{m/s}$. The microsphere initially followed the pedestal until the force exerted on it by the trap became

greater than that exerted by the myosin molecules on the actin filament. At this point, the microsphere sprang back to its unloaded baseline position in the center of the trap. The total unbinding force ($Total F_{umb}$) of the myosin molecules was calculated as follows:

$$Total F_{umb} = k * \Delta d \quad (1)$$

where k is the trap stiffness and Δd is the maximal displacement of the trapped microsphere from its baseline position. k was calibrated using the Stokes force (F_f) approach, as previously reported (Leguillette, et al., 2008; Roman, et al., 2013). Briefly, a viscous drag was applied to a trapped microsphere by moving it at a constant velocity (v) in 0.3% methylcellulose while measurements of Δd were performed. According to Stokes' law, the frictional force exerted on spherical objects with very small Reynolds numbers is calculated as follows:

$$F_f = 6 \pi \eta r v \quad (2)$$

where η is the dynamic viscosity and r is the microsphere radius. The viscosity of 0.3% methylcellulose was measured with a viscometer (DV-I at 60 rpm, Brookfield, Middleboro, MA), using a UL (ultra low viscosity) adapter and was equal to 10.4 cP, at 30°C. Thus,

$$k = F_f / \Delta d \quad (3)$$

The value of k (0.013 pN/nm, $R^2=0.95$) was averaged from several measurements performed at different velocities and then used to perform the force measurements.

The average binding force per myosin head (F_{umb}) was obtained as follows: first, we measured the length of actin filament in contact with the pedestal (ℓ) by fluorescence imaging. That is, the portion of the pedestal where the actin filament was bound, was brought in focus and

the bound actin filament length (ℓ) was measured using the National Institutes of Health analysis software (NIH macro in Scion Image 4.02, Scion). Unbound actin was readily detected because it moved in and out of focus due to Brownian motion, so it was discarded from the length measurements. We then used the estimates of the number of active myosin heads on the motility surface previously obtained by Warshaw and co-workers (Harris & Warshaw, 1993; VanBuren, Work, & Warshaw, 1994) by performing NH_4 -EDTA ATPase assays directly on the cover slip. (Note that similar results have also been obtained by two other groups (Kishino & Yanagida, 1988; Uyeda, Kron, & Spudich, 1990)). The density of active myosin heads was obtained by dividing this number by the surface area. The number of active myosin head per actin filament length was calculated by assuming that all myosins could interact with actin within a 26 nm wide band (Harris & Warshaw, 1993; Kishino & Yanagida, 1988; Uyeda, et al., 1990). For example, at a concentration of myosin of 20 $\mu\text{g}/\text{ml}$, a value of 26 heads/ μm of actin filament was estimated (Harris & Warshaw, 1993).

3.4.5. Microsphere displacement analysis software

Bead motion tracking was performed in Matlab using optimal fitting of a reference image as previously described in detail (Roman, et al., 2013). Briefly, in the first frame of the acquired video (720x480 resolution, 68.6x40.3 μm real frame size, 29.94 frame/s, 8 bit grayscale), the largest area of connected pixels with a gray value above 90% of the highest pixel value in the image was identified. A 60x60 pixel section of the frame, centered on the center of mass of the area of connected pixels, was defined as the reference image. While this center of mass was not necessarily the center of mass of the bead, it was visually confirmed that the entire bead was

always fully contained in the reference image. In each subsequent frame the reference image was matched to a section of the frame of the same size by finding the location at which the summed absolute difference in pixel grey values (δz) between the current frame and the reference image was minimized. To achieve sub pixel resolution of the bead position, the δz values at the found location and the surrounding 8 pixels were interpolated with a cubic interpolation algorithm (Matlab) and the coordinates of the global minimum point on this interpolation surface were stored as the position of the bead. After analysis of the entire video a frame range where no movement occurs was manually chosen to calculate a baseline location of the bead and distances were plotted relative to this baseline location. The relevant local maxima, which correspond to the detachment of myosin from actin, were found by searching for maxima in user defined regions. From these maxima the associated total F_{unb} were calculated.

3.4.6. Statistical analysis

Differences in v_{max} and F_{unb} between multiple conditions were tested using one way ANOVAs. Post-hoc comparisons between conditions were adjusted with a Bonferroni correction. Differences in v_{max} and F_{unb} with only two conditions were tested using the Student's t-test, with t-tests for unequal variance when it applied. A value of $p < 0.05$ was considered significant. The Systat Software Inc., (San Jose, CA) was used to compute the exact p values of ANOVAs or Student's t-tests. For the motility assay, N represents the number of flow-through chambers studied. A minimum of three locations in each flow through chambers were analyzed; each location contained at least 10 filaments. Thus, a minimum of 30 filaments were analyzed per

chamber to make up an N of 1. For the laser trap assay, N represents the number of actin filaments analyzed.

3.5. RESULTS

To assess whether caldesmon alters the average binding force of unphosphorylated myosin to actin filaments, we measured the F_{unb} using the laser trap assay. A significant increase in the F_{unb} was observed in the presence of a physiological caldesmon concentration of 10 nM (0.17 ± 0.02 pN; mean \pm SE) as compared to control, i.e. unregulated actin (0.09 ± 0.01 pN; $p < 0.001$, Fig. 3.1.). Raising the caldesmon concentration further did not significantly increase the F_{unb} above the value obtained at 10 nM (0.14 ± 0.02 pN at 50nM, $p = 0.120$; 0.17 ± 0.02 pN at 250nM, $p = 0.716$; 0.14 ± 0.03 pN at 500nM, $p = 0.160$). Because tropomyosin has been reported to mechanically potentiate the effect of caldesmon (Fraser & Marston, 1995; Shirinsky, et al., 1992), we tested their combined effect on the F_{unb} . The F_{unb} in the presence of both caldesmon (10nM) and tropomyosin (10nM) (0.18 ± 0.02 pN) was not significantly greater than in the presence of caldesmon alone ($p = 0.457$, Fig. 3.1.). The concentration of tropomyosin was also chosen to be within the physiological range and its effect on the F_{unb} was tested independently of caldesmon.

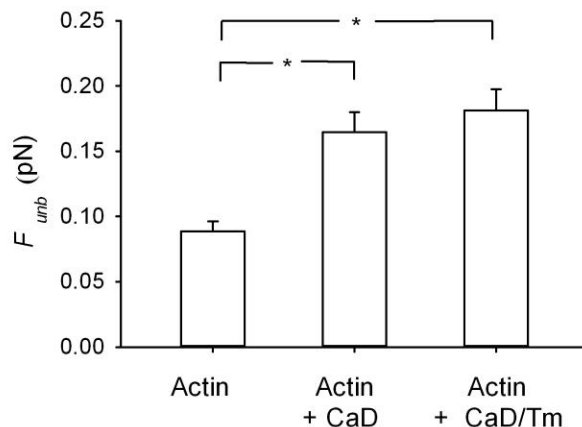


Fig. 3.1. F_{unb} in the presence of caldesmon and tropomyosin. Unbinding force (F_{unb}) of unphosphorylated myosin from actin measured using the laser trap assay. The measurements were performed with unregulated actin filaments ($N=14$) and actin filaments regulated by caldesmon ($N=14$), or by caldesmon and tropomyosin ($N=14$). The results are reported as average force per myosin molecule. CaD: caldesmon, Tm: tropomyosin and *: $p < 0.05$.

A significant increase in the F_{unb} was observed with a tropomyosin concentration as low as 5nM (0.17 ± 0.02 pN; mean \pm SE) as compared to control, i.e. unregulated actin (0.12 ± 0.01 pN, $p=0.005$). Raising the tropomyosin concentration further did not significantly increase the F_{unb} above the value obtained at 5nM (0.16 ± 0.02 pN; $p=0.632$, at 25nM; 0.17 ± 0.05 pN; $p=0.928$, at 50nM). Thus, both caldesmon and tropomyosin enhance the F_{unb} of unphosphorylated myosin to actin but their effects are not synergistic.

A series of control experiments were then performed to ascertain that the enhancement of the F_{unb} obtained in the presence of the actin regulatory proteins was not due to unspecific binding (Fig. 3.2. A-C). This was accomplished by skipping the myosin incubation on the coverslip and incubating directly with BSA (see methods of the *in vitro* motility assay).

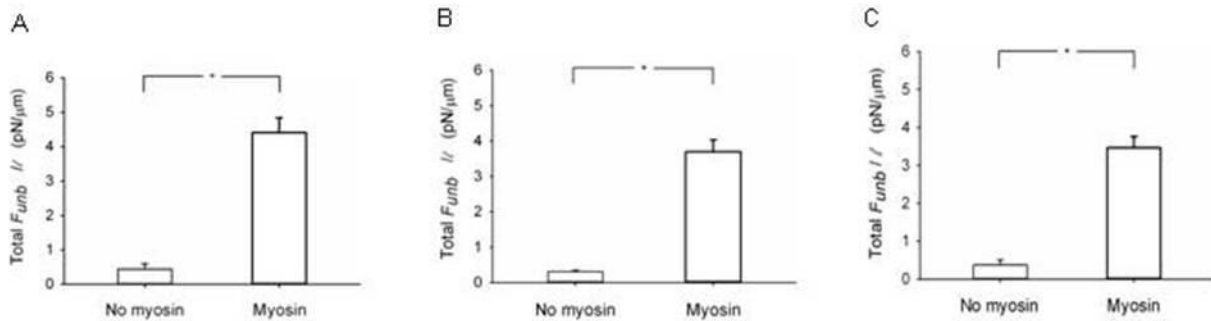


Fig. 3.2. Total F_{unb}/l in the absence or presence of unphosphorylated myosin. The measurements were performed in the presence of **A**) caldesmon ($N=5$ without and $N=5$ with unphosphorylated myosin), **B**) tropomyosin ($N=4$ without and $N=6$ with unphosphorylated myosin) or **C**) both caldesmon and tropomyosin ($N=5$ without and $N=5$ with unphosphorylated myosin). *: $p < 0.05$.

These results were reported in terms of pN per length of actin filament because there was no myosin to normalize to, unlike the results presented in Fig. 3.1.. In the presence of caldesmon, the F_{unb} was negligible (0.44 ± 0.16 pN/ μ m) in the absence of myosin as compared to its value in the presence of myosin (4.42 ± 0.43 pN/ μ m; $p < 0.001$). Similarly, in the presence of tropomyosin, the F_{unb} was negligible (0.31 ± 0.08 pN/ μ m) in the absence of myosin as compared to its value (3.7 ± 0.34 pN/ μ m; $p < 0.001$) in the presence of myosin. Finally, the F_{unb} was also found to be

negligible in the presence of both caldesmon and tropomyosin (0.37 ± 0.13 pN/ μm) in the absence of myosin as compared to its value in the presence of myosin (3.47 ± 0.3 pN/ μm ; $p < 0.001$).

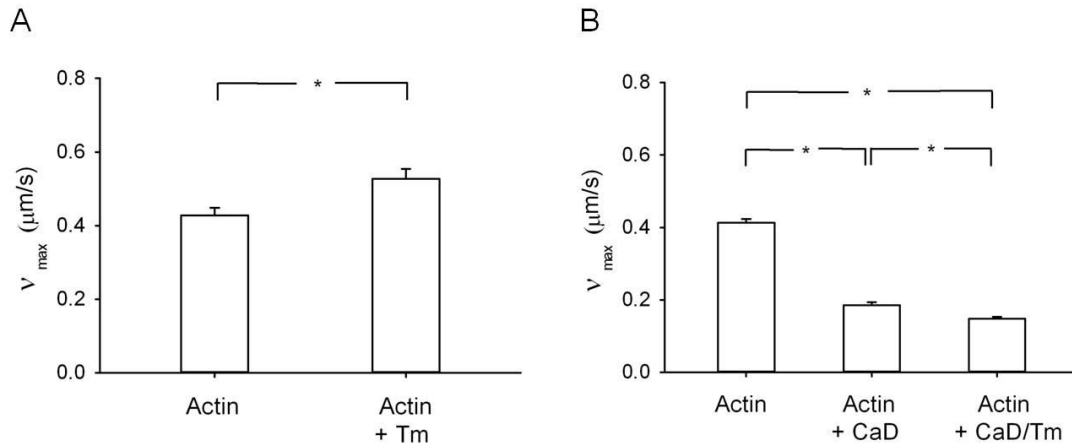


Fig. 3.3. v_{max} in the presence of caldesmon and tropomyosin. Velocity of actin filaments (v_{max}) when propelled by phosphorylated myosin as measured using the *in vitro* motility assay. **A)** The measurements were performed with unregulated actin filaments ($N = 8$) and actin filaments regulated by tropomyosin ($N = 8$). **B)** The measurements were performed with unregulated actin filaments ($N = 6$), actin filaments regulated by caldesmon ($N = 10$) and actin filaments regulated by caldesmon and tropomyosin ($N = 8$). *: $p < 0.05$.

Thus, the enhancement effect of caldesmon and tropomyosin on the F_{unb} is not due to unspecific binding to the pedestal or coverslip but to a direct action on the acto-myosin interaction.

Because caldesmon and tropomyosin have been more extensively studied for their effects on phosphorylated than on non-phosphorylated myosin, we verified using the *in vitro* motility

assay that the concentrations of these actin regulatory proteins that we worked at were producing results expected from the literature (Fig. 3.3.). Indeed, as previously reported (Fraser & Marston, 1995; Okagaki, et al., 1991), v_{max} for unregulated actin ($0.43 \pm 0.02 \mu\text{m/s}$; mean \pm SE) was significantly increased in the presence of tropomyosin ($0.53 \pm 0.03 \mu\text{m/s}$, $p = 0.011$, Fig. 3.3. A). Also, as expected from the literature (Okagaki, et al., 1991; Shirinsky, et al., 1992), v_{max} for unregulated actin ($0.41 \pm 0.01 \mu\text{m/s}$; mean \pm SE) was significantly decreased in the presence of caldesmon ($0.19 \pm 0.01 \mu\text{m/s}$; $p < 0.001$, Fig. 3.3. B). Furthermore, the combination of tropomyosin and caldesmon had a slight synergistic effect on v_{max} and significantly decreased it further ($0.15 \pm 0.01 \mu\text{m/s}$) from its value with caldesmon alone ($p = 0.009$, Fig. 3.3. B). Interestingly, this synergistic effect was not observed for the F_{umb} of unphosphorylated myosin (Fig. 3.1.).

To assess the role of the phosphorylation of caldesmon on the average binding force of unphosphorylated myosin to actin filaments, we measured the F_{umb} in the presence of ERK phosphorylated caldesmon. The phosphorylation of caldesmon by ERK significantly decreased the F_{umb} ($0.06 \pm 0.01 \text{ pN}$; mean \pm SE) as compared to non-phosphorylated caldesmon ($0.2 \pm 0.02 \text{ pN}$; $p < 0.001$) and to unregulated actin ($0.12 \pm 0.01 \text{ pN}$; $p < 0.001$; Fig. 3.4.).

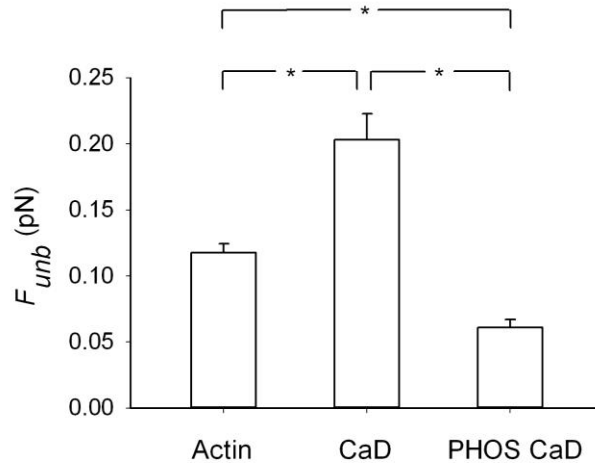


Fig. 3.4. F_{umb} in the presence of phosphorylated caldesmon. Unbinding force (F_{umb}) of unphosphorylated myosin from actin. The measurements were performed with unregulated actin filaments ($N = 10$), actin filaments regulated by caldesmon ($N = 14$) or actin filaments regulated by ERK phosphorylated caldesmon ($N = 8$). The results are reported as average force per myosin molecule. CaD: caldesmon, PHOS CaD: phosphorylated caldesmon. *: $p < 0.05$.

Sample traces of the unbinding maneuvers are shown in Fig. 3.5.. The F_{umb} observed in the presence of actin only (Fig. 3.5. A) is seen to be increased in amplitude in the presence of caldesmon (Fig. 3.5. B). Interestingly, the phosphorylation of caldesmon appears to either prevent the binding of myosin to actin or to accelerate its detachment, leading to a visco-elastic behavior, i.e. constant force as a function of constant pulling velocity of the pedestal myosin (Fig. 3.5. C). Fig. 3.5. D shows again that the F_{umb} is insignificant in the absence of myosin.

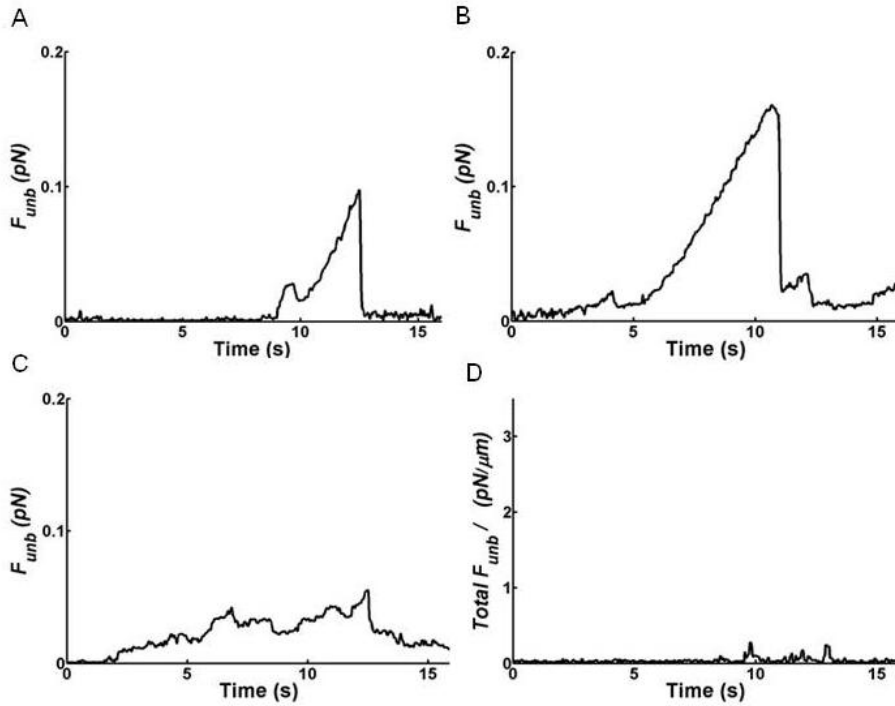


Fig. 3.5. Sample traces of the unbinding force (F_{umb}) from: A) unregulated actin filaments, B) actin filaments regulated by caldesmon, C) actin filaments regulated by phosphorylated caldesmon. These forces are reported as average per myosin head. D) Total F_{umb} normalized per actin filament length ($Total F_{umb}/\ell$) in the absence of unphosphorylated myosin but in the presence of unregulated actin filaments. The maxima correspond to filament detachment from myosin

To dissect out further the effect of ERK phosphorylation of caldesmon on the actomyosin interactions, we measured v_{max} of phosphorylated myosin in the in vitro motility assay. We found that the phosphorylation of caldesmon significantly increased v_{max} ($0.36 \pm 0.02 \mu m/s$; mean \pm SE) as compared to unphosphorylated caldesmon ($0.27 \pm 0.02 \mu m/s$; $p < 0.001$) but that this v_{max} was still significantly slower than in the absence of caldesmon ($0.48 \pm 0.01 \mu m/s$; $p < 0.001$; Fig. 3.6).

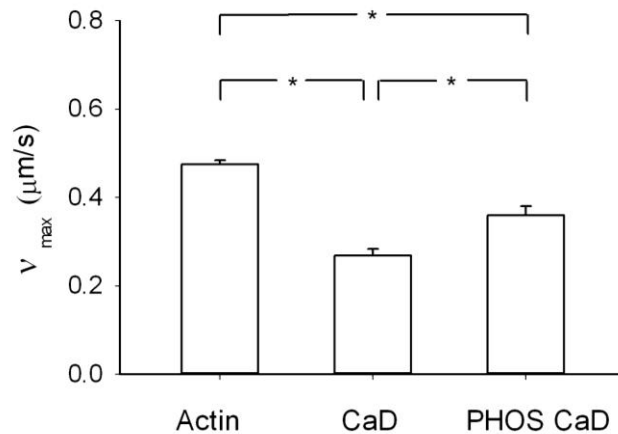


Fig. 3.6. v_{max} in the presence of phosphorylated caldesmon. Velocity of actin filaments (v_{max}) when propelled by phosphorylated myosin as measured using the *in vitro* motility assay. The measurements were performed with unregulated actin filaments ($N = 21$), actin filaments regulated by caldesmon ($N = 17$) and actin filaments regulated by phosphorylated caldesmon ($N = 15$). *: $p < 0.05$.

3.6. DISCUSSION

The major findings of this study are: 1) caldesmon increases the average force of binding of unphosphorylated myosin to actin thereby promoting force maintenance; 2) upon ERK phosphorylation of caldesmon, the average force of binding of unphosphorylated myosin to actin decreases to very low levels, thus promoting relaxation.

It is generally believed that caldesmon promotes relaxation. Albrecht *et al* (Albrecht, et al., 1997; Guo, et al., 2013) 1997 demonstrated that exogenous addition of caldesmon to

permeabilized tissues accelerates their rate of relaxation. They suggested that caldesmon inhibits cooperative attachment of dephosphorylated crossbridges in the latch-state phase (Albrecht, et al., 1997). More recently, Guo and coworkers (Guo, et al., 2013) knocked out h-caldesmon in arterial muscle and reported a slower rate of relaxation. They suggested that h-CaD facilitates the detachment of ATP-bound dephosphorylated cross-bridges rather than preventing phosphorylated cross-bridge formation. Although our results initially appear contradictory to those two previous studies, our molecular mechanics measurements suggest a mechanism by which caldesmon accomplishes this relaxation as our data demonstrate that one additional step is required for muscle relaxation. That is, caldesmon must be phosphorylated to lead to smooth muscle relaxation. Indeed, the data that we present in figures 3.1., 3.4. and 3.5. demonstrate that caldesmon enhances the average force of binding of unphosphorylated myosin to actin which is contrary to what both Albrecht *et al.* (Albrecht, et al., 1997) and Guo *et al.* (Guo, et al., 2013) suggested from data obtained at the whole tissue level. However, once caldesmon gets phosphorylated by ERK, its F_{unb} becomes lower than in the presence of unphosphorylated caldesmon, and even lower than in the absence of caldesmon. Thus, ERK phosphorylated caldesmon favors relaxation.

The mechanism that we propose for the contribution of ERK phosphorylation of caldesmon to smooth muscle relaxation becomes even more appealing when we consider the data previously reported in the literature on the timing of ERK activation. Ratz (Ratz, 2001) showed that upon stimulation of rabbit arterial smooth muscle with phenylephrine, the peak in ERK phosphorylation was delayed with respect to the maximum active force. Thus, this time course in conjunction with our data suggest that before its activation, caldesmon favors force

maintenance (latch state/cooperative reattachment) by increasing unphosphorylated/dephosphorylated myosin average binding force to actin (Figs. 3.1., 3.4. and 3.5.). Later in the contraction, once caldesmon becomes phosphorylated by ERK, this binding force is decreased to very low levels (Figs. 3.4. & 3.5.), thereby allowing the muscle to relax.

How does caldesmon accomplish these functions becomes the next question. To address this point, it is informative to look more closely at caldesmon's binding sites. Caldesmon binds via its N-terminus to the S2 region of myosin (Hemric & Chalovich, 1990; Ikebe & Reardon, 1988; Li, et al., 2000; Z. Wang, Jiang, Yang, & Chacko, 1997). The C-terminal region of caldesmon (Gao, et al., 1999; C. L. Wang, et al., 1991; Z. Wang, Horiuchi, & Chacko, 1996; Zhuang, Mabuchi, & Wang, 1996) has two strong actin-binding clusters whereas the N-terminal region has only weak actin binding sites (Zhuang, et al., 1996). The cluster closest to the C-terminus has been reported to be responsible for the inhibitory action of caldesmon (C. L. Wang, et al., 1991; Z. Wang, Yang, & Chacko, 1997). It also contains the site that gets phosphorylated by ERK (Adam & Hathaway, 1993). The ERK phosphorylation of CaD has been reported to "alleviate" the inhibitory effect of CaD on the actomyosin ATPase activity (Huang, et al., 2003) and on the in vitro actin propulsion velocity (Gerthoffer, et al., 1996) by detaching CaD from actin (Huang, et al., 2003). Only the phosphorylated cluster detaches while the other one remains attached (Huang, et al., 2003). Huang and co-workers suggested that it may be kinetically advantageous to have caldesmon stay close to actin and not detach completely (Huang, et al., 2003). Our results demonstrate that indeed, when attached to actin via its 2 carboxyl sites, caldesmon enhances the average force of binding of unphosphorylated myosin to actin, presumably resulting from the cross-linking of myosin to actin by caldesmon (Donovan, et al.,

2010). Thus, caldesmon promotes force maintenance. Upon ERK phosphorylation of caldesmon, and thus partial detachment of caldesmon from actin, the average force of binding becomes lower than in the absence of caldesmon. Thus, ERK phosphorylated caldesmon promotes relaxation.

Other regulatory mechanisms of caldesmon have also previously been studied. For instance, phosphorylation at the carboxyl terminus of caldesmon by MLCK increases its binding affinity for phosphorylated myosin filaments (Sobieszek, et al., 2010). Phosphorylation of caldesmon by MLCK must take place early in the contraction favoring binding of myosin to actin and promoting contraction. Indeed, the actin activated ATPase rate is increased in the presence of MLCK phosphorylated caldesmon (Sobieszek, et al., 2010). This mechanism is not believed to be active once myosin is dephosphorylated because MLCK phosphorylated caldesmon does not bind with high affinity to unphosphorylated myosin (Sobieszek, et al., 2010). Thus, a series of mechanisms must be orchestrated for the smooth muscle cell to sequentially favor cross-bridge cycling, followed by force maintenance, and finally followed by relaxation. Fine tuning seems to be possible due to the involvement of several factors including the contractile proteins expressed, the signaling involved and its exact timing.

A closer look at the maneuvers used to produce the F_{umb} traces, i.e the pulling at constant velocity of the pedestal/myosin away from the laser trap center, allows us to speculate on the mechanisms by which caldesmon enhances or suppresses the binding of unphosphorylated myosin to actin. Caldesmon increases the amplitude of the F_{umb} and the duration of the

attachment (Figs 3.5. A & B). In the presence and in the absence of caldesmon, the binding seems to rupture more or less at once, reflective of an elastic material. In contrast, phosphorylated caldesmon appears to create a constant and low F_{umb} , suggesting a visco-elastic behavior (Fig. 3.5. C). These behaviors are true functions of myosin because they are completely abolished in its absence (Figs. 3.2. A-C and Fig. 3.5. D). This visco-elastic behavior, created by the partial detachment from actin of the carboxyl region of caldesmon leads to very low binding force of myosin to actin.

Another point that is worth noting is the fact that tropomyosin is usually believed to potentiate the effects of caldesmon. We (Fig. 3.3. A) and others (Fraser & Marston, 1995; Okagaki, et al., 1991; Zhuang, et al., 1996) have reported an increase in v_{max} as measured in the in vitro motility assay in the presence of tropomyosin (Fig. 3.3. A), a decrease in the presence of caldesmon (Fig. 3.3. B) and a further decrease in the presence of both tropomyosin and caldesmon (Fig. 3.3. B). As others have reported (Fraser & Marston, 1995; Okagaki, et al., 1991; Zhuang, et al., 1996), the potentiation of the effect of caldesmon by tropomyosin on v_{max} is very small but statistically significant. However, this potentiating effect of tropomyosin on caldesmon does not seem to play a role in the presence of unphosphorylated myosin as can be seen in Fig. 3.1.. Taking that into consideration, we chose not to pursue the mechanics measurements on unphosphorylated myosin in the presence of tropomyosin.

A limitation of our study is that unphosphorylated and not dephosphorylated myosin was used in our measurements. Although there is no information in the literature to support this idea,

there is a possibility that dephosphorylated myosin is functionally different from unphosphorylated myosin. Unfortunately, it is not possible for us to work with dephosphorylated myosin because of the high probability that there would be some remaining phosphorylated myosin that would greatly overestimate our force measurements due to the sensitivity of our equipment.

It is interesting to note that there is more caldesmon in phasic than in tonic muscle. Furthermore, Guo and co-workers reported that, in their caldesmon knock-out animal, the non-muscle isoform of caldesmon was over-expressed in phasic but not in tonic muscle (Guo, et al., 2013). Taken together these observations suggest that caldesmon should play an essential role in phasic muscle. As suggested by Guo *et al.* (Guo, et al., 2013), caldesmon might be important in the rapid relaxation observed in the phasic but not seen in tonic smooth muscle.

3.7. CONCLUSION

In conclusion, caldesmon enhances the force of binding of unphosphorylated, and presumably dephosphorylated, myosin to actin. Furthermore, ERK phosphorylation of caldesmon decreases this force of binding to very low levels, thus promoting relaxation.

3.8. ACKNOWLEDGEMENTS

We thank Professor John M. Dealy, from the department of Chemical Engineering, McGill University, for performing the methylcellulose viscosity measurements and Michel Alveis from Marvid Poultry for the procurement of the chicken breasts for the purification of skeletal muscle actin and myosin for NEM preparation.

3.9. REFERENCES

- Adam, L. P., & Hathaway, D. R. (1993). Identification of mitogen-activated protein kinase phosphorylation sequences in mammalian h-Caldesmon. *FEBS Lett*, 322(1), 56-60.
- Albrecht, K., Schneider, A., Liebetrau, C., Ruegg, J. C., & Pfister, G. (1997). Exogenous caldesmon promotes relaxation of guinea-pig skinned taenia coli smooth muscles: inhibition of cooperative reattachment of latch bridges? *Pflugers Arch*, 434(5), 534-542.
- Dabrowska, R., Goch, A., Galazkiewicz, B., & Osinska, H. (1985). The influence of caldesmon on ATPase activity of the skeletal muscle actomyosin and bundling of actin filaments. *Biochim Biophys Acta*, 842(1), 70-75.
- Dillon, P. F., Aksoy, M. O., Driska, S. P., & Murphy, R. A. (1981). Myosin phosphorylation and the cross-bridge cycle in arterial smooth muscle. *Science*, 211(4481), 495-497.
- Donovan, G. M., Bullimore, S. R., Elvin, A. J., Tawhai, M. H., Bates, J. H., Lauzon, A. M., et al. (2010). A continuous-binding cross-linker model for passive airway smooth muscle. *Biophys J*, 99(10), 3164-3171.
- Fraser, I. D., & Marston, S. B. (1995). In vitro motility analysis of smooth muscle caldesmon control of actin-tropomyosin filament movement. *J Biol Chem*, 270(34), 19688-19693.

- Gao, Y., Patchell, V. B., Huber, P. A., Copeland, O., El-Mezgueldi, M., Fattoum, A., et al. (1999). The interface between caldesmon domain 4b and subdomain 1 of actin studied by nuclear magnetic resonance spectroscopy. *Biochemistry*, 38(47), 15459-15469.
- Gerthoffer, W. T., Yamboliev, I. A., Shearer, M., Pohl, J., Haynes, R., Dang, S., et al. (1996). Activation of MAP kinases and phosphorylation of caldesmon in canine colonic smooth muscle. *J Physiol*, 495 (Pt 3), 597-609.
- Guo, H., Huang, R., Semba, S., Kordowska, J., Huh, Y. H., Khalina-Stackpole, Y., et al. (2013). Ablation of smooth muscle caldesmon affects the relaxation kinetics of arterial muscle. [Research Support, N.I.H., Extramural]. *Pflugers Arch*, 465(2), 283-294.
- Hai, C. M., & Kim, H. R. (2005). An expanded latch-bridge model of protein kinase C-mediated smooth muscle contraction. *J Appl Physiol*, 98(4), 1356-1365.
- Hai, C. M., & Murphy, R. A. (1988). Regulation of shortening velocity by cross-bridge phosphorylation in smooth muscle. *Am J Physiol*, 255(1 Pt 1), C86-94.
- Harris, D. E., & Warshaw, D. M. (1993). Smooth and skeletal muscle myosin both exhibit low duty cycles at zero load in vitro. *J Biol Chem*, 268(20), 14764-14768.
- Hedges, J. C., Oxhorn, B. C., Carty, M., Adam, L. P., Yamboliev, I. A., & Gerthoffer, W. T. (2000). Phosphorylation of caldesmon by ERK MAP kinases in smooth muscle. *Am J Physiol Cell Physiol*, 278(4), C718-726.

- Hemric, M. E., & Chalovich, J. M. (1988). Effect of caldesmon on the ATPase activity and the binding of smooth and skeletal myosin subfragments to actin. *J Biol Chem*, 263(4), 1878-1885.
- Hemric, M. E., & Chalovich, J. M. (1990). Characterization of caldesmon binding to myosin. *J Biol Chem*, 265(32), 19672-19678.
- Hemric, M. E., Lu, F. W., Shrager, R., Carey, J., & Chalovich, J. M. (1993). Reversal of caldesmon binding to myosin with calcium-calmodulin or by phosphorylating caldesmon. *J Biol Chem*, 268(20), 15305-15311.
- Horiuchi, K. Y., & Chacko, S. (1995). Effect of unphosphorylated smooth muscle myosin on caldesmon-mediated regulation of actin filament velocity. *J Muscle Res Cell Motil*, 16(1), 11-19.
- Horiuchi, K. Y., Miyata, H., & Chacko, S. (1986). Modulation of smooth muscle actomyosin ATPase by thin filament associated proteins. *Biochem Biophys Res Commun*, 136(3), 962-968.
- Huang, R., Li, L., Guo, H., & Wang, C. L. (2003). Caldesmon binding to actin is regulated by calmodulin and phosphorylation via different mechanisms. *Biochemistry*, 42(9), 2513-2523.
- Huxley, A. F. (1957). Muscle structure and theories of contraction. *Prog. Biophys.*, 7, 255-317.

- Ikebe, M., & Reardon, S. (1988). Binding of caldesmon to smooth muscle myosin. *J Biol Chem*, 263(7), 3055-3058.
- Khalil, R. A., Menice, C. B., Wang, C. L., & Morgan, K. G. (1995). Phosphotyrosine-dependent targeting of mitogen-activated protein kinase in differentiated contractile vascular cells. *Circ Res*, 76(6), 1101-1108.
- Kishino, A., & Yanagida, T. (1988). Force measurements by micromanipulation of a single actin filament by glass needles. *Nature*, 334(6177), 74-76.
- Leguillette, R., Zitouni, N. B., Govindaraju, K., Fong, L. M., & Lauzon, A. M. (2008). Affinity for MgADP and force of unbinding from actin of myosin purified from tonic and phasic smooth muscle. *Am J Physiol Cell Physiol*, 295(3), C653-660.
- Li, Y., Zhuang, S., Guo, H., Mabuchi, K., Lu, R. C., & Wang, C. A. (2000). The major myosin-binding site of caldesmon resides near its N-terminal extreme. *J Biol Chem*, 275(15), 10989-10994.
- Morgan, K. G., & Gangopadhyay, S. S. (2001). Invited review: cross-bridge regulation by thin filament-associated proteins. *J Appl Physiol*, 91(2), 953-962.
- Ngai, P. K., & Walsh, M. P. (1984). Inhibition of smooth muscle actin-activated myosin Mg²⁺-ATPase activity by caldesmon. *J Biol Chem*, 259(22), 13656-13659.

Ngai, P. K., & Walsh, M. P. (1987). The effects of phosphorylation of smooth-muscle caldesmon. *Biochem J*, 244(2), 417-425.

Okagaki, T., Higashi-Fujime, S., Ishikawa, R., Takano-Ohmuro, H., & Kohama, K. (1991). In vitro movement of actin filaments on gizzard smooth muscle myosin: requirement of phosphorylation of myosin light chain and effects of tropomyosin and caldesmon. *J Biochem*, 109(6), 858-866.

Pardee, J. D., & Spudich, J. A. (1982). Purification of muscle actin. *Methods Cell Biol*, 24, 271-289.

Ratz, P. H. (2001). Regulation of ERK phosphorylation in differentiated arterial muscle of rabbits. *Am J Physiol Heart Circ Physiol*, 281(1), H114-123.

Roman, H. N., Zitouni, N. B., Kachmar, L., Ijpma, G., Hilbert, L., Matusovskiy, O., et al. (2013). Unphosphorylated calponin enhances the binding force of unphosphorylated myosin to actin. *Biochim Biophys Acta*, 1830, 4634-4641.

Shirinsky, V. P., Biryukov, K. G., Hettasch, J. M., & Sellers, J. R. (1992). Inhibition of the relative movement of actin and myosin by caldesmon and calponin. *J Biol Chem*, 267(22), 15886-15892.

- Sobieszek, A. (1994). Smooth muscle myosin. Molecule conformation, filament assembly and association of regulatory enzymes. In D. R. a. M. A. Giembycz (Ed.), *Airways smooth muscle: Biochemical Control of Contraction and Relaxation* (pp. 1-29). Bassel: Birkhauser.
- Sobieszek, A., Sarg, B., Lindner, H., & Seow, C. Y. (2010). Phosphorylation of caldesmon by myosin light chain kinase increases its binding affinity for phosphorylated myosin filaments. *Biol Chem*, *391*(9), 1091-1104.
- Sobieszek, A., & Small, J. V. (1977). Regulation of the actin-myosin interaction in vertebrate smooth muscle: activation via a myosin light-chain kinase and the effect of tropomyosin. [In Vitro]. *J Mol Biol*, *112*(4), 559-576.
- Sobue, K., Takahashi, K., & Wakabayashi, I. (1985). Caldesmon150 regulates the tropomyosin-enhanced actin-myosin interaction in gizzard smooth muscle. *Biochem Biophys Res Commun*, *132*(2), 645-651.
- Sutherland, C., & Walsh, M. P. (1989). Phosphorylation of caldesmon prevents its interaction with smooth muscle myosin. *J Biol Chem*, *264*(1), 578-583.
- Trybus, K. M., & Lowey, S. (1984). Conformational states of smooth muscle myosin. Effects of light chain phosphorylation and ionic strength. *J Biol Chem*, *259*(13), 8564-8571.

- Uyeda, T. Q., Kron, S. J., & Spudich, J. A. (1990). Myosin step size. Estimation from slow sliding movement of actin over low densities of heavy meromyosin. *J Mol Biol*, 214(3), 699-710.
- VanBuren, P., Work, S. S., & Warshaw, D. M. (1994). Enhanced force generation by smooth muscle myosin in vitro. *Proc Natl Acad Sci U S A*, 91(1), 202-205.
- Wang, C. L. (2008). Caldesmon and the regulation of cytoskeletal functions. *Adv Exp Med Biol*, 644, 250-272.
- Wang, C. L., Wang, L. W., Xu, S. A., Lu, R. C., Saavedra-Alanis, V., & Bryan, J. (1991). Localization of the calmodulin- and the actin-binding sites of caldesmon. *J Biol Chem*, 266(14), 9166-9172.
- Wang, Z., Horiuchi, K. Y., & Chacko, S. (1996). Characterization of the functional domains on the C-terminal region of caldesmon using full-length and mutant caldesmon molecules. *J Biol Chem*, 271(4), 2234-2242.
- Wang, Z., Jiang, H., Yang, Z. Q., & Chacko, S. (1997). Both N-terminal myosin-binding and C-terminal actin-binding sites on smooth muscle caldesmon are required for caldesmon-mediated inhibition of actin filament velocity. *Proc Natl Acad Sci U S A*, 94(22), 11899-11904.

Wang, Z., Yang, Z. Q., & Chacko, S. (1997). Functional and structural relationship between the calmodulin-binding, actin-binding, and actomyosin-ATPase inhibitory domains on the C terminus of smooth muscle caldesmon. *J Biol Chem*, 272(27), 16896-16903.

Warshaw, D. M., Desrosiers, J. M., Work, S. S., & Trybus, K. M. (1990). Smooth muscle myosin cross-bridge interactions modulate actin filament sliding velocity in vitro. *J Cell Biol*, 111(2), 453-463.

Zhuang, S., Mabuchi, K., & Wang, C. A. (1996). Heat treatment could affect the biochemical properties of caldesmon. *J Biol Chem*, 271(47), 30242-30248.

CHAPTER 4

A MICROFLUIDIC DEVICE TO STUDY THE DYNAMICS OF MUSCLE CONTRACTION

CHAPTER 4

4.1. PREFACE

The long standing main theory to explain the latch-state suggests that if myosin gets deactivated (dephosphorylated) while attached to actin, it remains attached and maintains force. Other theories suggest that dephosphorylated detached myosin can reattach to actin to maintain force and that actin regulatory proteins participate in this force maintenance. These later theories were investigated in chapters 2 and 3 by measuring the binding force of unphosphorylated myosin to actin, using the laser trap, in the absence and presence of the actin regulatory proteins. The results demonstrate that indeed the binding of unphosphorylated myosin to actin is likely to contribute to force maintenance and, thus to the latch-state, and that the actin regulatory proteins potentiate and regulate this effect.

Verifying the main theory of the latch state is, however, a much more difficult task to accomplish. That is, it requires the addition of myosin light chain phosphatase during molecular level force measurements without creating any bulk flow. This type of experiments cannot be done with the current technology. Thus, a microfluidic device was designed and developed to investigate the main latch-state theory at the molecular level. The proof of principle of this micro-fluidic device is presented in chapter 4.

4.2. ABSTRACT

Smooth muscle can maintain force for long periods of time and at low energy cost. It has been hypothesized that if myosin gets deactivated (dephosphorylated) while attached to actin, it will remain attached and maintain force. To verify this theory at the molecular level, deactivating agents (myosin light chain phosphatase) need to be suddenly added to the buffer of a mechanics setup during molecular force measurements. A laser trap is commonly used for molecular force measurements but the addition of any buffer cannot be performed without disturbing the single molecule force measurements. Thus, in this study we designed and developed a microfluidic device that allows the addition of chemicals without perturbing the force measurements performed with the laser trap assay. A micro-channel chamber was created by standard photolithography on silicon wafers with the patterns transferred to polymethylsiloxane (PDMS). The chamber was then bound to a polycarbonate membrane which itself was bound to a molecular mechanics flow-through chamber. The micro-channels assured rapid distribution of the chemicals whereas the membrane assured efficient delivery but prevented bulk flow. The performance of the chamber was tested by measuring the velocity (v_{max}) of actin filaments propulsion by myosin in the molecular mechanics chamber. Several channel designs were created and tested but all showed very similar filling time. Thus, the pattern was chosen based on the best compromise between channel area for bulk flow and binding surface for the membrane. Then, the biocompatibility of the membrane adhesion promoter (3-Aminopropyl) triethoxysilane (APTES) and of the adhesives used for the chamber assembly were tested by comparing v_{max} in their presence with that obtained when using the traditional flow-through chamber. No significant difference in v_{max} was observed. Finally, the performance of the chamber was tested

when infusing MgATP in the inlet of the micro-channel chamber and recording v_{\max} in the molecular mechanics chamber; this v_{\max} was compared with that obtained when MgATP was injected directly from the side of the flow-through chamber. The v_{\max} obtained with MgATP coming through the micro-channels ($2.37 \pm 0.48 \mu\text{m/s}$) was not statistically different from that obtained when MgATP was delivered directly in the mechanics chamber ($2.52 \pm 0.42 \mu\text{m/s}$). The proof of concept prototype for this microfluidic device validates the design proposed. Further testing with the laser trap are now required. After further development, the microfluidic device tested in this study may allow us to verify at the molecular level, a fundamental property of smooth muscle, namely, the latch-state.

4.3. INTRODUCTION

At the molecular level, muscle contraction is driven by the interaction of two proteins: myosin, a molecular motor and actin. Myosin hydrolyzes adenosine triphosphate (ATP) and uses the chemical energy liberated to generate a power stroke, pulling on the actin filament. To study the molecular mechanics of these proteins, techniques such as the *in vitro* motility (Kron & J. Spudich, 1986) and the laser trap assays (Finer, Simmons, & Spudich, 1994) have been developed. The general setup of these molecular assays is identical; a flow-through chamber (Work & Warshaw, 1992) is used to sequentially perfuse buffers to establish the protein interactions. The *in vitro* motility assay (Fig. 4.1. A) allows observation of the movement of fluorescently labeled actin filaments as they get propelled by myosin molecules randomly adhered to a microscope coverslip. The velocity of the actin filaments is quantified by measuring

the total trajectory travelled by each filament for a given period of time (Root & Wang, 1994).

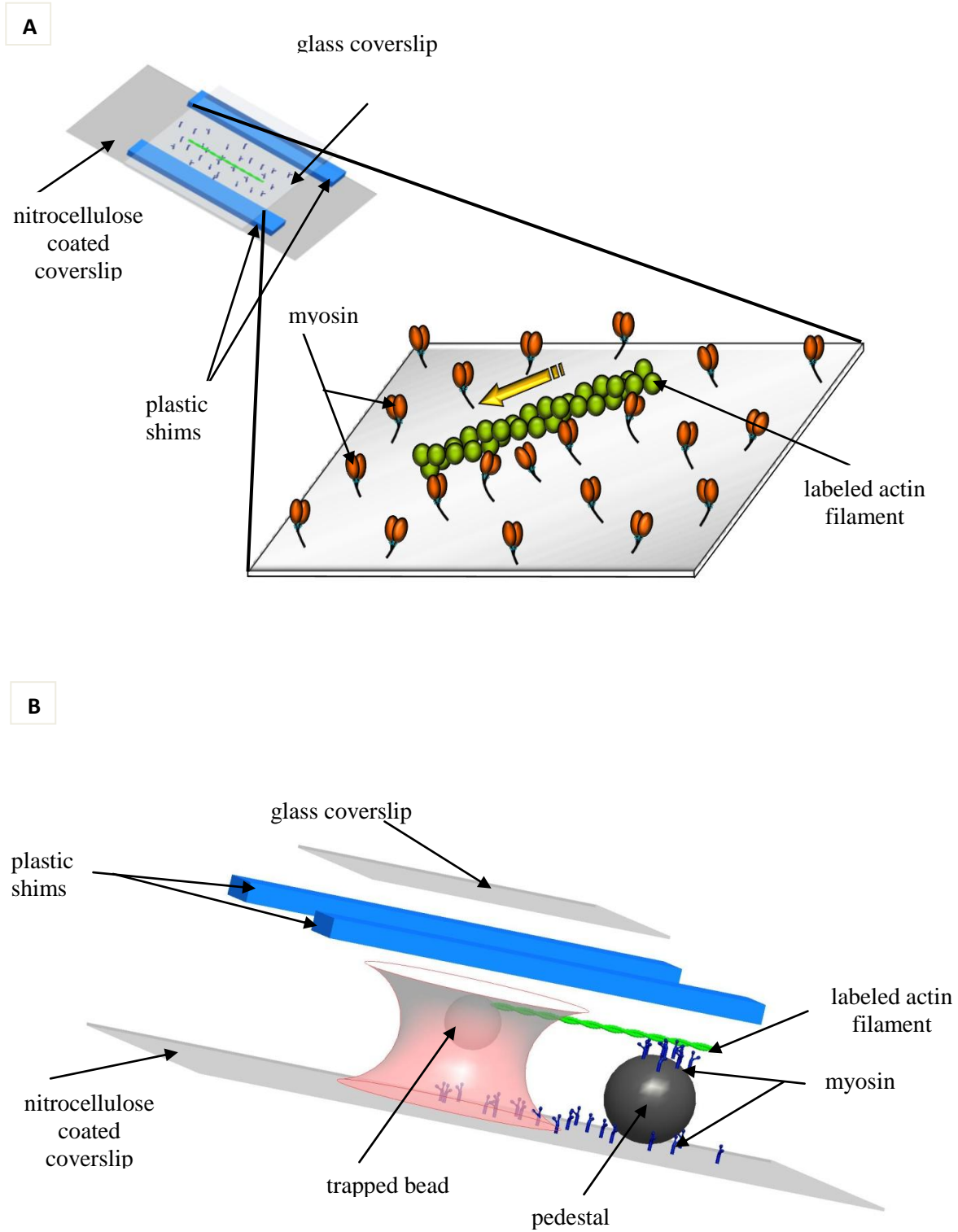


Fig. 4.1. See details on the next page

Fig. 4.1. Traditional molecular mechanics assays. **A)** *Molecular mechanics flow-through chamber made up of 2 coverslips (one coated with nitrocellulose to bind the myosin molecules) separated by plastic shims glued with a curable glue. Detailed view of the in vitro motility assay: the velocity (v_{max}) of fluorescently labeled actin filaments as they get propelled by myosin molecules randomly adhered to a microscope coverslip is obtained by dividing their total path described by the elapsed time.* **B)** *Exploded view of the laser trap assay. A polystyrene bead is captured in a laser trap. The surface of this bead is biochemically altered so that a fluorescently labeled actin filament can be bound to it and brought in the proximity of a pedestal coated with myosin molecules. The force generated by the myosin molecules is equal to the product of the trap stiffness by the displacement of the trapped bead from the trap center. (Dimensions are not to scale).*

The laser trap (Fig. 1.7.) uses the energy of laser light to create potential energy wells in which polystyrene beads are captured and between which a single actin filament is attached and made taut (Finer, et al., 1994). In another version of the laser trap assay (Block, Goldstein, & Schnapp, 1990; Leguillette, Zitouni, Govindaraju, Fong, & Lauzon, 2008) only one laser trap is used to capture a polystyrene bead (Fig. 4.1.B). The laser trap can be manipulated so that the trapped bead binds an actin filament. This filament is then brought in contact with single myosin molecules coating pedestals on a coverslip and the displacement and force generated by the myosin molecules can be determined by imaging (Roman, et al., 2013) or using quadrant detectors (Lauzon, et al., 1998).

Even though these molecular techniques are well established to study the mechanics of all sorts of molecular motors, there are still no possibilities of altering the buffers while the measurements are being performed. Indeed, these mechanical measurements are exquisitely sensitive to the addition of reagents because a single actin filament is interacting with very few or even just one myosin molecule. However, there are several situations where altering the buffer during the mechanics measurements would reveal very important information. One such example is the latch-state, which is a phase of force maintenance observed in the tonic smooth muscle (muscle found in all hollow organs of the body). It has been postulated for a long time that such force maintenance occurs when myosin gets deactivated (dephosphorylated) while it is attached to actin (Dillon, 1981). Such postulates cannot be verified at the molecular level unless we find a way of efficiently adding dephosphorylating enzymes while measuring force with a laser trap.

Thus, in the current study, we developed a microfluidic device (Fig. 4.2.) to allow the introduction of chemicals in a molecular mechanics flow-through chamber, without creating any bulk flow that would disturb the molecular mechanics measurements.

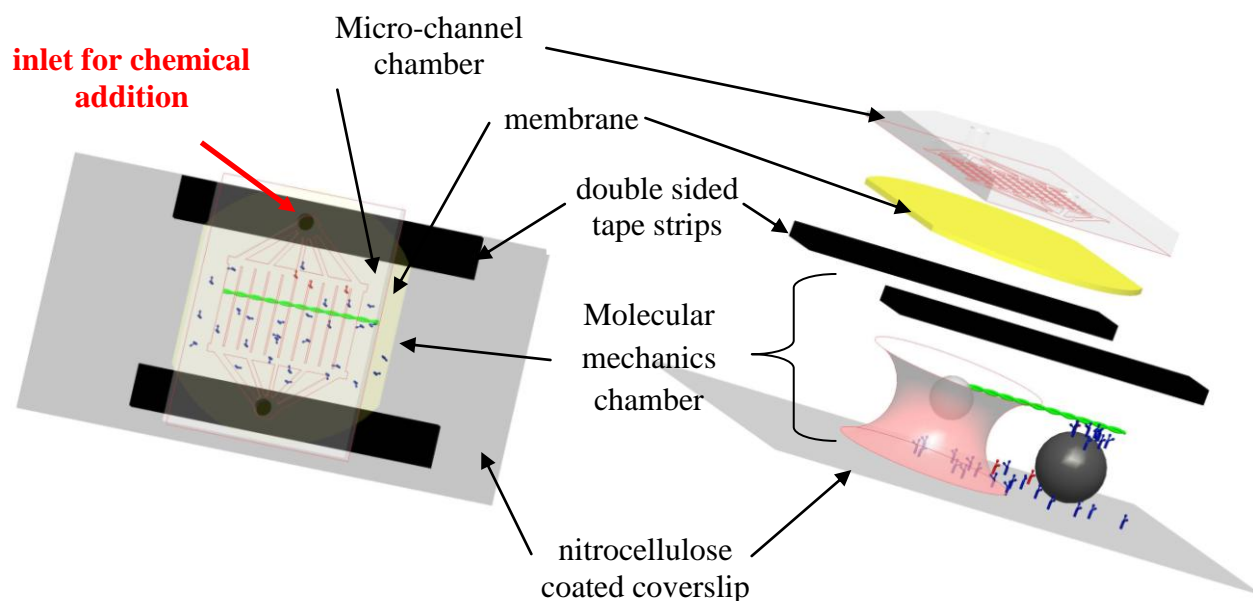


Fig. 4.2. Microfluidic chamber prototype Left: top view, right: side exploded view of the microfluidic device designed to infuse chemicals in a molecular mechanical chamber without creating any bulk flow that would perturb the mechanics measurements. The design includes a top chamber made up of horizontal micro-channels built in polydimethylsiloxane (PDMS) to distribute the chemicals rapidly and uniformly over a membrane and a membrane to allow the chemicals to reach the contractile proteins in the molecular mechanics chamber without creating any bulk flow. (Dimensions are not to scale)

This microfluidic device complements the traditional in vitro motility and laser trap setups (Figs.4.1. A and 4.1. B) by adding: 1) a chamber made up of horizontal micro-channels built in polydimethylsiloxane (PDMS) to distribute the chemicals rapidly and uniformly over a membrane; 2) a membrane that allows the chemicals to reach the contractile proteins in the molecular mechanics chamber without creating any bulk flow. The proof of principle of this microfluidic device is presented here. The final design was tested by injecting ATP in the micro-channel chamber to activate the motility in the molecular mechanics flow-through chamber. Actin propulsion by myosin was indeed observed, validating the design of this microfluidic device.

4.4. METHODS

4.4.1. Microfabrication of the micro-channel chamber

The micro-channel chamber was constructed by standard photolithography (Campo & Greiner, 2007) in the following way: a resin (SU-8 2050, Microchem) was spin-coated on a substrate (6 inch silicon wafer) at 1,600 rpm for 30s and then pre-baked at 65°C for 5 min and at 95°C for 15 min. Patterns were then created in the resin using a mask (chrome deposition on glass, Front Range Photomask, resolution 10 $\mu\text{m}/\text{feature}$) and exposing to ultraviolet (UV) light (35 mW/cm^2) for 34 s. The patterns were then fixed to the substrate by baking at 65°C for 5 minutes and at 95°C for 10 minute followed by an immersion in SU-8 developer for 10 min. To eliminate tensions in the structure, a final hard bake at 150°C for 5 min was performed. The patterns obtained were used as a mold to carve channels in PDMS (Sylgard 184, Dow Corning). The PDMS was prepared at a 10:1 ratio with the curing agent (Sylgard 184 Silicone Elastomer Curing Agent, Dow Corning) and cured overnight at 60°C.

4.4.2. Membrane

To allow diffusion of chemicals from the micro-channel chamber to the flow-through molecular mechanics chamber, a polycarbonate membrane (0.1 μm pore diameter, 4.18% porosity, Milipore) was bound between the two chambers, using a previously described procedure (Sunkara, et al., 2011). Briefly, the PDMS micro-channel chamber and the polycarbonate membrane were cleaned and dried and were then plasma treated (bombarding the surface of interest with ions to increase its adhesion properties) in a plasma chamber (PVA TePLA AG, Germany). After the plasma treatment (oxygen plasma, 60 W for 1 min.), the membrane was immersed in 1% v/v aqueous APTES (Sigma Aldrich) solution at room temperature for 20 min, washed with deionized water, dried under nitrogen jet and brought in conformal contact with the freshly plasma treated micro-channel device so that they were bound together.

4.4.3. Molecular mechanics chamber

The molecular mechanics chamber was created by adding a nitrocellulose coated glass microscope coverslip (50 x 22 x 0.15 mm, Premium Glass, Fisher Scientific) below the membrane. Molecular mechanics flow-through chambers (Warshaw, Desrosiers, Work, & Trybus, 1990) are traditionally made up of microscope coverslips spaced (5 mm) by plastic shims (40 x 3mm, 0.125 mm thickness). All parts are glued together using liquid adhesive (NOA, Norland Products) cured using ultra-violet light (Roman, et al., 2013). That type of gluing was not possible for binding our micro-mechanics chamber to the membrane because the liquid adhesive clogged the upper chamber channels and the membrane pores. To overcome this

problem, plastic shims were replaced by double coated carbon conductive tapes (Tedd Pella) of the same thickness.

4.4.4. Protein preparation

Actin was purified from chicken pectoralis as described by Pardee and Spudich (Pardee & Spudich, 1982) and fluorescently labeled by overnight incubation with tetramethylrhodamine isothiocyanate (TRITC)-phalloidin (P1951, Sigma-Aldrich Canada). Myosin was purified from chicken pectoralis following a previously published protocol (Sobieszek, 1994) but using a high ionic strength acto-myosin extraction buffer. Differently from the previous studies presented in this thesis, skeletal muscle myosin was used in this chapter because of its higher sensitivity to alterations in buffer conditions.

4.4.5. Buffers

Actin buffer (25 mM KCl, 25 mM imidazole, 1 mM EGTA, 4 mM MgCl₂, and 30 mM DTT, with an oxygen scavenger system consisting of 0.25 mg/ml glucose oxidase, 0.045 mg/ml catalase, and 5.75 mg/ml glucose; pH adjusted to 7.4); Myosin buffer (300 mM KCl, 25 mM imidazole, 1 mM EGTA, 4 mM MgCl₂, and 30 mM DTT; pH adjusted to 7.4); Assay buffer: The in vitro motility assay buffer consisted of actin buffer to which were added MgATP (2 mM) and methylcellulose (0.5%, viscous solution to favor the interactions between myosin and actin). Note that when the microfluidic chamber was tested by injecting MgATP from the micro-

channel chamber inlet, no methylcellulose was added to ensure a better diffusion and to reproduce better the laser trap assay conditions.

4.4.6. In vitro motility assay

To assess the performance of our microfluidic device at various steps of the construction, the velocity (v_{max}) of actin filament propulsion by myosin was measured and compared with that obtained with the regular in vitro motility assay (previously described (Roman, et al., 2013)).

Non-functional myosin molecules were removed by ultracentrifugation (Optima ultracentrifuge L-90K and 42.2 Ti rotor, Beckman Coulter, Fullerton, CA) of myosin (500 $\mu\text{g/ml}$) with equimolar filamentous actin and 1 mM MgATP in myosin buffer. Myosin was then perfused in the flow through chamber at a concentration of 200 $\mu\text{g/ml}$ and allowed to randomly attach to the nitrocellulose for 2 min. The following solutions were then perfused successively in the flow through chamber: BSA (0.5 mg/ml in actin buffer), unlabeled G-actin (1.33 μM in actin buffer) to bind to any remaining non-functional myosin, MgATP (1 mM in actin buffer) to release the unlabelled actin from the functional myosin, actin buffer (two washes), TRITC labeled actin (0.03 μM in actin buffer), incubated for 1 min, and assay buffer. Note that when the microfluidic chamber was tested by injecting MgATP from the micro-channel inlet, the unlabeled G-actin and MgATP steps were skipped to avoid the presence of MgATP in the assay before its diffusion through the membrane.

The motility was then assessed using an inverted microscope (IX70, Olympus, Melville, NY) equipped with a high numerical aperture objective (X100 magnification Ach 1.25 numerical aperture, Olympus, Melville, NY) and rhodamine epifluorescence. An image intensified video camera (KP-E500 CCD Camera, Hitachi Kokusai Electric, Woodbury, NY, 720 x 480 resolution, 68.6 μm x 45.7 μm real frame size, 29.94 frame/s, 8 bit grayscale) was used to visualize and record the actin filament movement on computer (Custom Built by Norbec Communication, Montreal, QC) using a frame grabber (Pinnacle Studio AV/DV V.9 PCI Card) and image capturing software (AMCap software V9.20) at 29.94 Hz. v_{max} was determined from the total path described by the filaments divided by the elapsed time using our automated version (Hilbert, Cumarasamy, Zitouni, Mackey, & Lauzon, 2013) of the National Institutes of Health tracking software (NIH macro in Scion Image 4.02, Scion) coded in Matlab (R2011a). Only filaments present for at least 20% of the recorded video time (~ 15 s) and describing a path of at least 3 μm were considered.

4.5. RESULTS

The performance of the microfluidic device was tested at several intermediate steps during the construction. First, the various designs for the channels (Fig. 4.3.) were compared by injecting a dye with a pipette in the channel inlet.

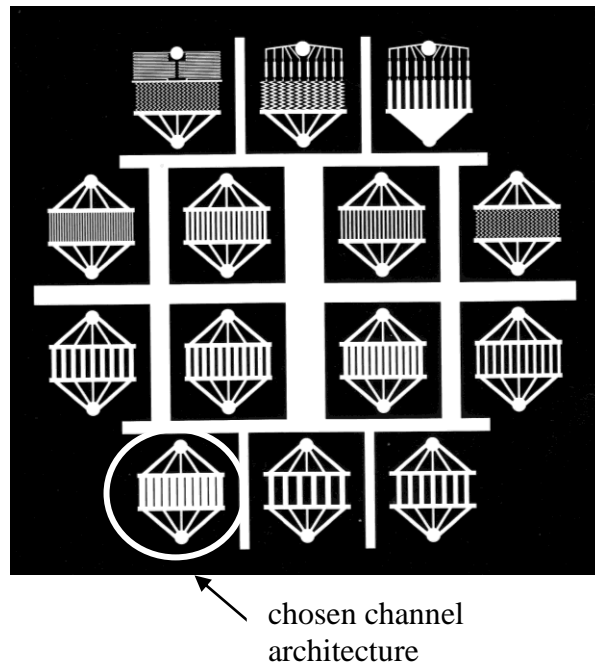


Fig. 4.3. Channel architecture design. Several channel patterns were tested to ensure uniform and efficient chemical distribution. The choice of the membrane was based on the best compromise between channel area for bulk flow and binding surface for the membrane. The circled pattern was chosen.

Because all patterns tested showed very similar filling time, the choice of the design was based on the highest surface available for diffusion without compromising the binding of the membrane to the walls of the micro-channel chamber. Thus the pattern circled in Fig. 4.3. was chosen. The membrane binding was tested manually by attempting to detach the membrane from the PDMS chamber. The maximal channel width was also chosen by considering the fact that membrane collapsing into the molecular mechanics chamber had to be prevented. Upon inspection, a ratio of 10: 1 with the flow-through chamber depth was chosen.

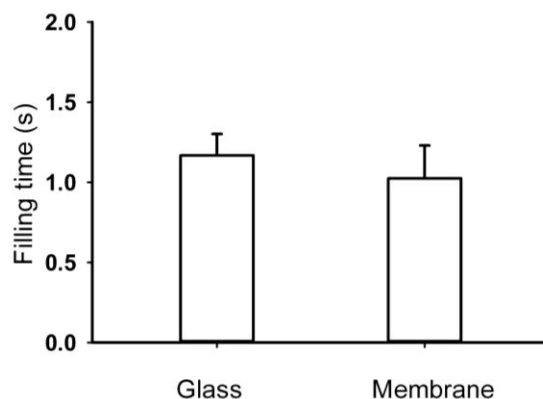


Fig. 4.4. Channel filling time. The time needed for uniform filling of the channels was measured using a dye for the micro-channel chamber sealed by plasma treated glass coverslips ($N = 4$) or by membranes ($N = 4$).

Next, the effect of the membrane on the filling time of the upper chamber channels was assessed. No significant difference in the filling time was observed if the bottom of the micro-channel chamber was made of plasma treated glass coverslips (1.12 ± 0.18 s, mean \pm SE) or plasma treated membranes (1.02 ± 0.15 s, $p = 0.765$; Fig. 4.4.).

The bio-compatibility of the material used to build the microfluidic device was assessed using the in vitro motility assay. Firstly, the biocompatibility of the double coated carbon conductive tape used to bind the lower chamber to the membrane was assessed. v_{\max} obtained from the flow-through chambers built using double coated carbon conductive tape (5.97 ± 0.31 $\mu\text{m/s}$, mean \pm SE) was not significantly different from that obtained with the conventional chambers (6.24 ± 0.36 $\mu\text{m/s}$, $p = 0.610$, Fig. 4.5. A). Secondly, the biocompatibility of the membrane treated with the adhesion promoters (APTES), used to bind it to the top chamber, was

also assessed. There was no significant difference in v_{\max} between the APTES binding agent ($3.41 \pm 0.32 \mu\text{m/s}$) and the non-treated (4.14 ± 0.51 ; $p = 0.287$, Fig. 4.5. B) membranes. However, the membrane per se decreased v_{\max} (compare Fig. 4.5. A and 4.5. B) and the filaments showed more of a stop and go movement.

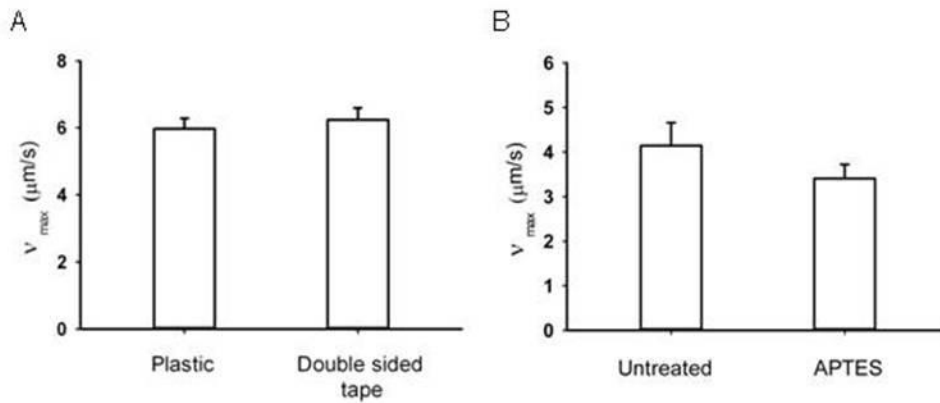


Fig. 4.5. Biocompatibility test. Velocity (v_{\max}) of fluorescently labeled actin filaments when propelled by myosin randomly adhered to the coverslip. **A)** The measurements were performed using the traditional assay in the presence of plastic shims ($N = 3$) or double sided carbon conductive tape strips ($N = 3$). **B)** The measurements were performed with untreated membranes ($N = 3$) or APTES treated membranes ($N = 3$) and bound to the micro-channel chambers.

The final performance test was done with the whole microfluidic device and consisted of infusing MgATP in the inlet of the micro-channel chamber and recording v_{\max} in the molecular mechanics chamber; this v_{\max} was compared with that obtained when MgATP was injected from

the side of the flow-through chamber (conventional assay (Warshaw, et al., 1990)). The v_{\max} obtained with ATP injected from the side of the flow-through chamber ($2.52 \pm 0.42 \mu\text{m/s}$) was not statistically different from that obtained with the ATP injected from the inlet of the micro-channel chamber ($2.37 \pm 0.48 \mu\text{m/s}$, $p = 0.822$, Fig. 4.6.). It is important to note that this later assay was not performed following the same conditions as for all the other motility measurements reported above (see methods for details, i.e. no unlabeled G-actin and MgATP steps and no methylcellulose) and so v_{\max} cannot be compared to the results reported above (Figs. 4.4.-4.5.).

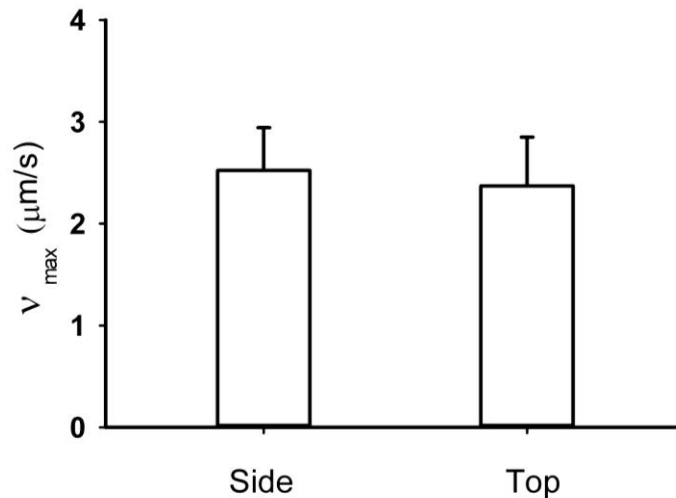


Fig. 4.6. Microfluidic device test. Velocity (v_{\max}) of fluorescently labeled actin filaments when propelled by myosin randomly adhered to the coverslip. v_{\max} was measured when MgATP was infused in the inlet of the micro-channel chamber (top, $N = 3$) or when MgATP was injected directly from the side of the flow-through chamber (side, $N=3$).

4.6. DISCUSSION

In this study, we provide a proof of concept prototype of a microfluidic device to efficiently introduce chemicals in a molecular mechanics flow-through chamber while minimizing any bulk flow that would otherwise disturb the single molecule assays.

The choice of the architecture of the channels was based on maximizing the surface available for diffusion of the chemicals while optimizing the surface area of the channel walls for the binding of the membrane (Fig.4.3.). The maximal channel width was also chosen to prevent the membrane from collapsing into the molecular mechanics chamber. The final design was obtained by trial and error as several solutions were possible. The flow rate through the channels was not affected significantly by the choice of the channel architecture whereas the binding of the membrane was more sensitive to the surface area optimization.

The biocompatibility of the materials used to construct the device was also demonstrated by comparing v_{\max} obtained with the new material with that obtained with the traditional chamber, as shown in Fig. 4.5. The v_{\max} recorded when the plastic shims were replaced by double sided carbon tape was similar to the one obtained with the conventional assay. The v_{\max} obtained when the membranes were treated with the binding promoter agent APTES was also similar to that obtained without the agent. However, a decrease in v_{\max} was observed when the glass coverslip was replaced by the membrane (compare Figs. 4.5. A and 4.5. B). This is most

likely due to the binding of myosin to the membrane, thus decreasing the myosin density on the motility surface. Such a decrease in myosin density would also explain the stop and go behavior observed for the actin filaments in the presence of the membrane. It is also possible that some back diffusion through the membrane occurred, thereby altering the conditions of the motility assay. Thus, further optimizations are still required for the conditions used for the in vitro motility or laser trap assays when performed within the microfluidic device environment.

The final test performed was aimed at verifying if a chemical could be injected in the micro-channel chamber to activate (or deactivate) a reaction in the molecular mechanics chamber. Thus, we chose to initiate the motility in the molecular mechanics chamber by injecting MgATP in the micro-channel chamber. However, the conditions that were used were those typically used for laser trap assays, i.e. no methylcellulose added. The unlabeled G- actin infusion followed by the MgATP wash was also skipped because of the risk of having MgATP left in the mechanics chamber which could have artificially activated the motility before the MgATP injected in the micro-channel chamber would have reached the mechanics chamber. These less than optimal conditions led to a further decrease in v_{\max} (compare Figs. 4.5. and 4.6.) because degraded myosin imposes a load on the actin filaments which slows them down. Such a load also leads to breakage of the filaments. Shorter filaments (less than 0.5 μm) are known to have lower propelling velocity (Hilbert, et al., 2013). In addition, the lack of methylcellulose favors the dispersion of filaments from the motility surface and thus decreases the actin-myosin interactions. Nonetheless, the design of the chamber was found to be successful because the v_{\max} obtained when the MgATP was injected in the micro-channel chamber was not significantly different from the one obtained when the MgATP was injected directly in the flow-through chamber. Thus,

these results provide the first proof of concept of this microfluidic device aimed at injecting chemicals in the top chamber to alter the conditions in the lower chamber without creating bulk flows that would affect the molecular mechanics measurements.

Several validation steps still have to be performed before finalizing the design. A proper measurement of disturbance of the molecular mechanics assay due to flow from the micro-channel chamber will have to be performed. This will require the use of the laser trap assay with an actin filament hooked up between trapped beads to measure if any movement is indeed induced by the injection of chemicals. The exact time required from injection in the micro-channel chamber for activation (deactivation) of the chemical reaction in the molecular mechanics chamber and the reproducibility of this timing will have to be measured. The successful completion of all these tests should lead to the optimal design of this microfluidic device which will allow us to perform key experiments to improve our understanding of molecular motors. Indeed, this chamber will allow us to test the long lasting latch-state theory, by dephosphorylating myosin molecules while attached to a single actin filament and measuring if force maintenance does occur.

4.7. CONCLUSION

In conclusion, this study provides a proof of concept prototype of a microfluidic chamber to deliver chemicals to a molecular mechanics chamber; speed and uniformity were provided by flow through micro-channels and a membrane assured delivery without bulk flow to the molecular mechanics chamber.

4.8. REFERENCES

- Block, S. M., Goldstein, L. S., & Schnapp, B. J. (1990). Bead movement by single kinesin molecules studied with optical tweezers. *Nature*, *348*(6299), 348-352.
- Campo, A. d., & Greiner, C. (2007). SU-8: a photoresist for high-aspect-ratio and 3D submicron lithography. *J. Micromech. Microeng*(17), R81-95.
- Dillon, P. F. A., M. O. Driska, S. P. Murphy, R. A. (1981). Myosin phosphorylation and the cross-bridge cycle in arterial smooth muscle. *Science*, *211*(4481), 495-497.
- Finer, J. T., Simmons, R. M., & Spudich, J. A. (1994). Single myosin molecule mechanics: piconewton forces and nanometre steps. *Nature*, *368*(6467), 113-119.
- Hilbert, L., Cumarasamy, S., Zitouni, N. B., Mackey, M. C., & Lauzon, A. M. (2013). The kinetics of mechanically coupled myosins exhibit group size-dependent regimes. *Biophys J*, *105*(6), 1466-1474.
- Kron, S., & J. Spudich, J. A. (1986). Fluorescent actin filaments move on myosin fixed to a glass surface. *Proc Natl Acad Sci U S A*, *83*(17), 6272-6276.
- Lauzon, A. M., Tyska, M. J., Rovner, A. S., Freyzon, Y., Warshaw, D. M., & Trybus, K. M. (1998). A 7-amino-acid insert in the heavy chain nucleotide binding loop alters the kinetics of smooth muscle myosin in the laser trap. *J Muscle Res Cell Motil*, *19*(8), 825-837.

- Leguillette, R., Zitouni, N. B., Govindaraju, K., Fong, L. M., & Lauzon, A. M. (2008). Affinity for MgADP and force of unbinding from actin of myosin purified from tonic and phasic smooth muscle. *Am J Physiol Cell Physiol*, 295(3), C653-660.
- Pardee, J. D., & Spudich, J. A. (1982). Purification of muscle actin. *Methods Cell Biol*, 24, 271-289.
- Roman, H. N., Zitouni, N. B., Kachmar, L., Ijpma, G., Hilbert, L., Matusovsky, O., et al. (2013). Unphosphorylated calponin enhances the binding force of unphosphorylated myosin to actin. *Biochim Biophys Acta*, 1830(10), 4634-4641.
- Root, D. D., & Wang, K. (1994). Calmodulin-sensitive interaction of human nebulin fragments with actin and myosin. *Biochemistry*, 33(42), 12581-12591.
- Sobieszek, A. (1994). Smooth muscle myosin. Molecule conformation, filament assembly and association of regulatory enzymes. In D. R. a. M. A. Giembycz (Ed.), *Airways smooth muscle: Biochemical Control of Contraction and Relaxation* (pp. 1-29). Bassel: Birkhauser.
- Sunkara, V., Park, D. K., Hwang, H., Chantiwas, R., Soper, S. A., & Cho, Y. K. (2011). Simple room temperature bonding of thermoplastics and poly(dimethylsiloxane). *Lab Chip*, 11(5), 962-965.
- Warshaw, D. M., Desrosiers, J. M., Work, S. S., & Trybus, K. M. (1990). Smooth muscle myosin cross-bridge interactions modulate actin filament sliding velocity in vitro. *J Cell Biol*, 111(2), 453-463.

Work, S. S., & Warshaw, D. M. (1992). Computer-assisted tracking of actin filament motility.
Anal Biochem, 202(2), 275-285.

CHAPTER 5

CONCLUSIONS

CHAPTER 5

5.1. CONCLUSIONS AND FUTURE DIRECTIONS

The effect of the actin regulatory proteins on the binding force of unphosphorylated myosin to actin was assessed at the molecular level. This was performed by measuring, with a laser trap, the force of unbinding (F_{unb}) from actin of unphosphorylated myosin, in the presence or absence of actin regulatory proteins. Calponin, caldesmon and tropomyosin increased the F_{unb} of unphosphorylated myosin to actin.

The mechanism by which calponin leads to this increase in the F_{unb} was further investigated by phosphorylating calponin with Ca^{2+} -calmodulin protein kinase II (which detaches calponin from actin) or by performing the measurements at high ionic strength (which detaches calponin from myosin). Both measurements reverted the F_{unb} to baseline level, thus demonstrating that calponin exerts its effect by cross-linking myosin to actin.

The phosphorylation of caldesmon by the extracellular signal-regulated kinase (ERK) demonstrated that the regulation of the actin regulatory proteins exerts another level of control over the F_{unb} of unphosphorylated myosin to actin. Indeed, ERK phosphorylation of caldesmon led to a further decrease in F_{unb} , below the level measured for unregulated actin. These data, in conjunction with the literature that reports that ERK phosphorylation of caldesmon occurs late in the contraction, strongly suggest that this mechanism is responsible for smooth muscle relaxation

from the latch-state. Furthermore, inspection of F_{umb} traces demonstrated a visco-elastic behavior in the presence of ERK phosphorylated caldesmon. This suggests that ERK phosphorylated caldesmon either prevents the attachment of unphosphorylated myosin to actin or favors its detachment.

Our data also show that various types of phosphorylation of the actin regulatory proteins lead to very different mechanics. Whereas the Ca^{2+} -calmodulin protein kinase II detached calponin from actin and thus abolished its mechanical function, the ERK phosphorylation of caldesmon led to a more subtle partial detachment with a potent mechanical inhibitory effect. Further investigation of these regulatory mechanisms promises to be interesting although challenging. For example, myosin light chain kinase phosphorylates myosin light chain during contraction and is also known to phosphorylate caldesmon. However, it was impossible for us to study this effect without risking to also phosphorylate myosin which would artificially increase the F_{umb} . Future studies addressing the simultaneous action of the actin regulatory proteins should also reveal important information. The fact that tropomyosin does not promote the effect of caldesmon on the F_{umb} as it does when it is in the presence of phosphorylated myosin was an unexpected result. This deserves further investigation. The combined effects of calponin and caldesmon should also be studied but this will be difficult because of their competing binding to actin. Nonetheless, our findings so far suggest the following potential mechanism for the contribution of unphosphorylated myosin to the latch-state: calponin gets phosphorylated at the same time as myosin, promoting force generation. Later during the contraction, calponin gets dephosphorylated and together with caldesmon contribute to the enhancement of the force maintenance by the dephosphorylated myosin molecules. Finally caldesmon gets phosphorylated

and decreases the force of binding of unphosphorylated myosin to actin to very low levels, thus promoting muscle relaxation.

In order to further verify the latch-state theories at the molecular level, a microfluidic device was designed and developed. The design included bulk flow through microfluidic channels to assure fast and uniform delivery of chemicals, and a membrane, to provide delivery without bulk flow to the molecular mechanics chamber. The design was tested by injecting MgATP in the inlet of the micro-channel chamber and the velocity v_{\max} of the actin propulsion by the resulting activation of myosin in the molecular mechanics chamber was measured as the output. The design and development of this chamber were successful; v_{\max} when injecting the MgATP through the microfluidic device was similar to that measured when activating myosin directly in the assay chamber. Further testing using the laser trap will be required to insure that the passage through the membrane does not induce any bulk flow, although unlikely. In addition, whereas the bio-compatibility of the materials was demonstrated, the motility could have been improved further by preventing proteins from sticking on the membrane, etc. Another feature that will be important to optimize is the accuracy and reproducibility of the time necessary for delivery of the chemicals. Thus, whereas the proof of principle of this microfluidic chamber is provided in this thesis, further development is still required to optimize it for future latch-state studies. Ultimately, this chamber will allow us to determine whether or not force is maintained if myosin dephosphorylation occurs while it is attached to actin. This will finally close a chapter that was started in the early 80s on the theories of the latch-state.

5.2. SUMMARY (ORIGINAL CONTRIBUTION TO THE FIELD)

The following results represent original contributions to the field:

(1) I measured, for the first time, the force of binding of unphosphorylated myosin to actin in the presence of actin regulatory proteins. I demonstrated that calponin, caldesmon and tropomyosin increase the force of binding of unphosphorylated myosin to actin.

(2) I showed that the mechanism by which calponin enhances the force of binding of unphosphorylated myosin to actin is by cross-linking them together.

(3) I demonstrated that, similarly to the binding of calponin to actin, the enhancement of the binding force of unphosphorylated myosin to actin by calponin is regulated by its phosphorylation by Ca^{2+} -calmodulin dependant protein kinase II.

(4) My data demonstrating the cross-linking of unphosphorylated myosin to actin offer a mechanism to explain data, from the literature and obtained at whole muscle level that suggested that calponin prevents active force generation.

(5) I showed that, contrary to their usual action on phosphorylated myosin, the effect of caldesmon and tropomyosin on the force of binding of unphosphorylated myosin to actin is not synergistic.

(6) My results demonstrated that the enhancement of the binding force of unphosphorylated myosin to actin by caldesmon is regulated by its phosphorylation by extracellular signal-regulated kinases (ERK).

(7) I showed that ERK phosphorylation of caldesmon decreases the force of binding of unphosphorylated myosin to actin to levels below those of unregulated actin, suggesting a relaxation mechanism from the latch state.

(8) I showed that the force of binding of unphosphorylated myosin to actin in the presence of ERK phosphorylated caldesmon exhibits a visco-elastic behavior; this suggests that ERK phosphorylated caldesmon either prevents attachment or enhances detachment of unphosphorylated myosin to actin.

(9) I showed that the phosphorylation of caldesmon also leads to a decrease in the velocity of actin filament propulsion by phosphorylated myosin as compared to unregulated actin; this demonstrates that ERK phosphorylation does not lead to a simple detachment of caldesmon from actin but to fine tuning of its action.

(10) My findings on the action of the actin regulatory proteins on the binding force of unphosphorylated myosin to actin strongly support that unphosphorylated (or dephosphorylated) myosin can contribute to force maintenance during the latch-state.

(11) I provided a proof of concept that a microfluidic chamber can be constructed to deliver chemicals to a molecular mechanics chamber; speed and uniformity were provided by flow through microfluidic channels and a membrane assured delivery without bulk flow to the molecular mechanics chamber.

(12) I demonstrated that the flow through a micro-channel polydimethylsiloxane chamber is not significantly affected by changing the bottom glass wall by a polycarbonate membrane.

(13) I demonstrated the biocompatibility of the double coated carbon conductive tapes (Tedd Pella) and of the adhesion promoters (APTES) for molecular mechanics measurements.